TECHNISCHE UNIVERSITÄT MÜNCHEN

Lehrstuhl für Strahlenbiologie

Fakultät für Medizin

Long-term developmental alterations in the mouse heart after low doses of ionizing radiation revealed by quantitative proteomic investigations

Mayur Bakshi

Vollständiger Abdruck der von der Fakultät für Medizin der Technischen Universität München zur Erlangung des akademischen Grades eines *Doktors rerum naturalium* (Dr.rer.nat.) genehmigten Dissertation.

Vorsitzender: Prof. Dr. Dr. Stefan Engelhardt

Prüfer der Dissertation:

1. Prof. Dr. Michael J. Atkinson

2. Prof. Dr. Gabriele Multhoff

Die Dissertation wurde am 22.01.2016 bei Technischen Universität München eingereicht und durch die Fakultät für Medizin am 03.08.2016 angenommen.

Doctoral thesis

TECHNISCHE UNIVERSITÄT MÜNCHEN

Faculty of Medicine

Chair of Radiation Biology

Long-term developmental alterations in the mouse heart after low doses of ionizing radiation revealed by quantitative proteomic investigations

Mayur Bakshi

4th October 2016

Dedicated to my parents

Summary

Exposure to ionizing radiation is a daily part of modern human life. In the form of therapeutic, diagnostic and environmental exposure people receive low to high doses of ionizing radiation. Cancerous and non-cancer diseases are the major classes of adverse effects that may results from exposure to ionizing radiation. Cardiovascular diseases are one of the major non-cancer consequences occurring after moderate to high doses of ionizing radiation. Epidemiological evidence show that both children and adults, for example atomic bomb survivors, childhood cancer survivors and nuclear workers have increased risk of developing cardiovascular disease even at low doses. The molecular mechanisms responsible for these adverse health effects are unknown. The heart is complex machinery in the circulatory system and is the primary component involved in the vascular radiation effect. The development of the heart can be divided in prenatal and postnatal growth period. Mechanical and chemical stress received during these developmental stages can adversely impact the normal heart growth. Ionizing radiation can also hinder the heart development and can lead to long-term postnatal damage.

For studies reported in this thesis, we have used the mouse as an experimental model. Mice were irradiated at either prenatal or early postnatal stage with gamma irradiation at low to moderate doses (0.02 to 1.0 Gy); the changes in the heart proteome were studied over different periods of time using Isotope Coded Protein Labeling (ICPL) and quantitative mass spectrometry analysis.

A range of bioinformatics platforms were used on the quantified proteome data to find the molecular pathways involved in the radiation damage. This is the first study to identify radiation-induced global molecular alterations in the developing heart after irradiation.

In the prenatal total body irradiation study we found radiation-induced deregulation of structural proteins normally controlled by MAPK signaling. The level of the kinase MAP4K4 was found to be decreased and less phosphorylated in the irradiated hearts compared to the sham-irradiated hearts even months after the exposure. Using postnatal total body irradiation we observed that the metabolic alterations in the heart were synchronized between those found in the liver and serum. These data suggest that early exposure to ionizing radiation leads to developmental alterations in the heart that are still present in the

adult heart. A key finding is the important role of the age at exposure for subsequent health effects. These data will be helpful in improving cardiovascular disease prognosis after irradiation and may indicate novel therapeutic approaches in order to prevent or treat early radiation-induced damage in the heart.

Zusammenfassung

Ionisierende Strahlung gehört zu dem modernen täglichen Leben. Menschen werden in Form von Therapie, Diagnose oder Umwelteinflüssen geringen bis hohen Dosen an ionisierender Strahlung ausgesetzt. Krebserkrankungen und Erkrankungen, die nicht mit Krebs zusammenhängen, zählen dabei zu den unerwünschten Auswirkungen, die ionisierende Strahlung haben kann. Im Wesentlichen treten hierbei Herz-Kreislauf-Erkrankungen nach moderaten bis hohen Strahlendosen auf. Epidemiologische Daten von sowohl Kindern als auch Erwachsenen, von Überlebenden der Atom-Bomben, Überlebenden von Krebserkrankungen im Kindesalter und strahlenexponierten Arbeitern, zeigen schon nach geringen Strahlendosen ein erhöhtes relatives Risiko eine Herz-Kreislauf-Erkrankung zu bekommen. Allerdings ist der molekulare Mechanismus, der diesen gesundheitsschädlichen Auswirkungen zu Grunde liegt, noch unbekannt. Das Herz ist ein komplexes Organ in der Maschinerie des Blutkreislaufs und ist primär involviert an den Auswirkungen ionisierender Strahlung. Die Entwicklung des Herzens lässt sich in eine pränatale und postnatale Wachstumsphase unterteilen; mechanischer und chemischer Stress während dieser Entwicklungsphasen können zu Auswirkungen auf das Herz führen. Ionisierende Strahlung kann die Entwicklung des Herzens beeinträchtigen und zu postnatalen Langzeitschäden des Herzens führen.

Für die Studien, die dieser Arbeit zu Grunde liegen, haben wir die Maus als experimentelles Model gewählt und diese in der pränatalen oder frühen postnatalen Phase mit niedrigen bis moderaten Dosen (0,02 bis 1,0 Gy) Gammastrahlung bestrahlt. Die zu verschiedenen Zeitpunkten isolierten Herzen dieser Tiere wurden für Isotope Coded Protein Labelling (ICPL) und quantitative Massenspektrometrie verwendet und die Veränderungen nach Bestrahlung im Proteom untersucht.

Die quantifizierten Proteom-Daten wurden anschließend mit Hilfe von Bioinformatik-Plattformen den entsprechenden molekularen Signalwegen zugeordnet. Dies ist die erste Studie dieser Art, um die molekularen Änderungen im sich entwickelnden Herzen nach Bestrahlung zu identifizieren.

In der pränatalen Ganzkörper-Bestrahlungsstudie haben wir herausgefunden, dass Strukturproteine, die normalerweise durch den MAPK-Signalweg kontrolliert werden,

dereguliert sind. Die MAP4K4 Kinase wurde selbst nach Monaten in deaktivierter und nicht-phosphorylierter Form vorgefunden. In der postnatalen Ganzkörper-Bestrahlungsstudie fanden wir heraus, dass Veränderungen im Stoffwechsel des Herzens synchron zu denen in Leber und Serum ablaufen. Diese Daten geben Einblicke in Veränderungen in der Entwicklung des Herzens, verursacht durch frühe Strahlenexposition. Eine Schlüsselentdeckung ist, dass das Alter zum Zeitpunkt der Exposition für die daraus resultierenden Gesundheitsschäden wichtig ist. Diese Erkenntnisse werden helfen, die Prognose zu verbessern und mögliche neue therapeutische Ansätze aufzuzeigen, um frühen Strahlenschäden am Herzen vorzubeugen oder diese zu behandeln.

Table of Contents

Chapter 1: Introduction

This cumulative thesis report aims to understand the effects of low acute doses of ionizing radiation (IR) on the embryonic and postnatal mouse heart. The first manuscript (chapter 2.1) gives an insight into the effects of low-dose ionizing radiation on the embryonic development of the heart. Publications II and III (chapter 2.2 and 2.3) summarize the effects of ionizing radiation on neonatal heart development, including the observation of metabolic maladaptation facilitated by possible cross talk between heart and liver.

Epidemiological studies suggest that an exposure to ionizing radiation in the developmental phase increases the risk of cardiovascular disease later in the life (Baker, Moulder et al. 2011). The molecular mechanisms behind the elevated risk for cardiovascular disease during different stages of the heart development are unknown. Undisturbed growth at prenatal and postnatal phases is important in order to achieve optimal cardiac function throughout the life (Sanford, Ormsby et al. 1997, Vallaster, Vallaster et al. 2012) To understand why people that received radiation exposure *in-utero* or at young age are more susceptible to cardiac disease, it is important to know which molecular pathways are affected in the heart during these different developmental stages.

1.1 The heart development

1.1.1 Prenatal (*in-utero*) heart development

The embryonic development of the mammalian heart involves the formation of a four-chambered contractile balloon from a small number of cardiac progenitor cells (Moorman, Webb et al. 2003) (Anderson, Webb et al. 2003). Figure 1 shows the major events in mammalian heart formation. In mice, the initial prenatal growth stage is the formation of a crescent of myocardial progenitor cells on embryonic day 8 (E8) (Buckingham, Meilhac et al. 2005) and then linearization of the crescent (E8 toE9). This is followed by folding and finally by the chamber formation (E10.5) and maturation of heart (E14) until birth (Anderson, Webb et al. 2003) (Figure 1). In human embryonic development, the heart formation follows a similar progression, but takes place over a considerably longer time of 50 days during the prenatal phase (Figure 1) until maturation (Srivastava 2006, Rose, Force et al. 2010).

In the embryonic phase, the early lineage specification of cardiac progenitor cells is followed by differentiation into new cell types, namely cardiomyocytes (Ieda, Fu et al. 2010), fibroblasts, and smooth muscle cells as the main populations (van Weerd, Koshiba-Takeuchi et al. 2011). For cardiomyocyte differentiation from progenitor cells the protein BRG1 plays a vital role (Takeuchi, Lou et al. 2011). The BAF complex protein BAF60C forms a molecular bridge to bring the BRG1 complex together with the transcription factors TBX5 and GATA4 to transcribe important target genes, including bone morphogenic proteins (BMP), and proteins involved in Wnt and ß-Catenin signaling (Klaus, Saga et al. 2007, van Weerd, Koshiba-Takeuchi et al. 2011)

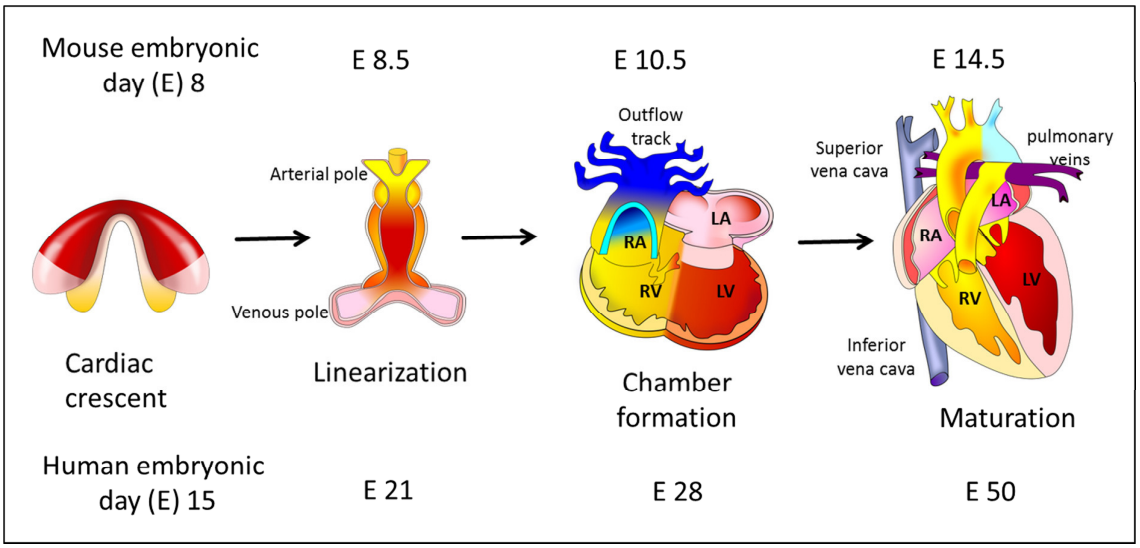

Figure 1: Key stages in the embryonic development of the mammalian heart *(modified from (Buckingham, Meilhac et al. 2005, Srivastava 2006). In mouse, myocardial progenitor cells come to lie under the head folds and form the cardiac crescent (E8), where differentiated myocardial cells can be observed. The early cardiac linearization of the crescent can be observed on E8.5. The linear heart tube undergoes looping to form distinguishable chambers on E10.5. The final maturation of the mouse fetal heart can be observed at E14.5, where the chambers are separated from the vascular structures, which in the immediate postnatal phase divide to create the systemic and pulmonary circulations. RA; right atrium, LA; left atrium, RV; right ventricle, LV; left ventricle*

The BMP and Wnt signaling pathways are important for determining the continued activity of *in-utero* development (Brand 2003). Multiple branches of the Wnt pathway such as

Wnt/ß-Catenin, Wnt/JNK, and Wnt/Ca^{2+} pathways are involved in the prenatal development of the mammalian heart (Gessert and Kuhl 2010). Wnt/ß-Catenin pathway is involved especially in the formation of the heart chambers (Figure 1) and the intermediate outflow track (OFT) responsible for the separation of pulmonary and systemic circulation in the mouse at E10 and E11 (Cai, Liang et al. 2003). The other (non-canonical) Wnt pathways have often been linked to cell polarity and cell migration caused by cytoskeletal rearrangements (Gessert and Kuhl 2010). Mitogen activated protein kinase (MAPK) cascade determines the formation of structural components of the heart by targeted phosphorylation of downstream targets, including Wnt, BMP-2 and EGFR signaling in embryonic heart development (Rose, Force et al. 2010). These signaling pathways are actively involved in the heart chamber formation. Environmental stresses, such as fetal hypoxia, can lead to disturbances in Wnt and BMP-2 signaling pathways, followed by cardiac growth restriction and myocardial thinning (Ream, Ray et al. 2008) by blocking transcriptional function of HIF-1. They participate in formation of the myocardium and control abnormal hypoxia in the fetal heart (Patterson and Zhang 2010).

1.1.2 Postnatal heart development

The postnatal mammalian heart development represents a transition from the prenatal hyperplasticity to postnatal physiological hypertrophy (increase in size) (Vakili, Okin et al. 2001) (Frey and Olson 2003) (Figure 2). In mouse, this rapid increase in the size of the heart occurs until postnatal day 21, in rat until 7 weeks and in human until 2 years of age (Dowell 1984, Wessels and Sedmera 2003, Porrello, Mahmoud et al. 2011).

1.1.2.1 Structural components of growth and regulation

The neonatal four-chambered heart consists of multiple differentiated cell types including cardiomyocytes, fibroblasts, endothelial cells, smooth muscle cells, and pacemaker cells (Xin, Olson et al. 2013). Proliferative myocytes of the prenatal stage mature to give rise to non-dividing cardiomyocytes during the neonatal developmental phase. Thus, the neonatal mouse heart only retains regenerative potential until around 7 days after birth (Figure 2B) (Porrello, Mahmoud et al. 2011). Although the adult heart can undergo some structural regeneration (Porrello, Mahmoud et al. 2011) damaged cardiomyocytes can only be replaced in a limited manner from the available stem cell pool (Kimura, Xiao et al. 2015).

The Wnt, Hippo, and mTOR signaling pathways are known to maintain the functionality of the adult cardiomyocyte (Figure 2C) (Rolfe, McLeod et al. 2005, Heallen, Morikawa et al. 2013, Ozhan and Weidinger 2015). The Hippo pathway, by the activation of STE20-like protein kinase 1 (MST1), influences the Wnt and IGF pathways that are necessary for growth regulation of cardiomyocytes and which determine the size of the heart the in postnatal development (Heallen, Zhang et al. 2011, Xin, Olson et al. 2013).

Cardiac fibroblasts contribute to the heart structural and functional composition. In the postnatal phase they are from multiple origins such as endothelial cell precursors, native fibroblasts and the bone marrow mesenchyme (Zeisberg and Kalluri 2010). They have essential functions in inflammatory cytokine signaling (Mann 2003) and in the regulation of myocardial regeneration through β1 integrin signaling for the damage control and tissue remodeling in case of myocardial injury (Ieda, Tsuchihashi et al. 2009).

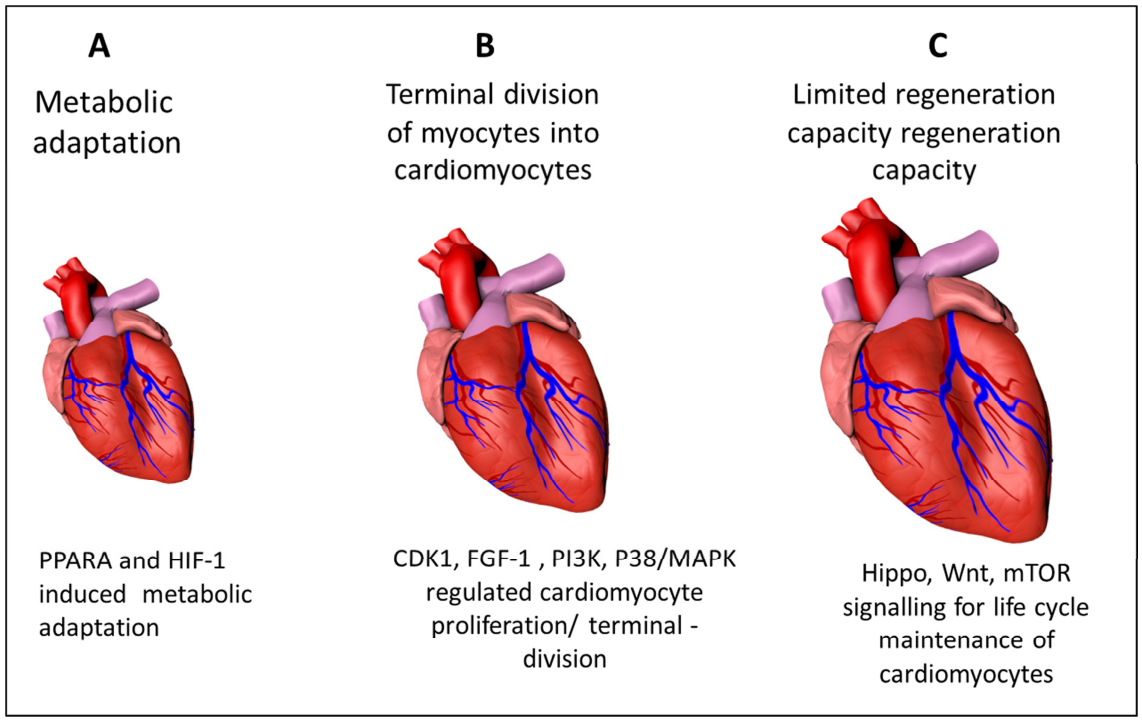

Figure 2: Postnatal development of the mammalian heart. *In the postnatal phase the heart undergoes (A) metabolic adaptation from glucose to lipids as an energy source. In the early developmental stage the myocytes either proliferate or terminally divide, a process driven by kinase signaling pathways including CDK-1, PI3K, and MAPK signaling (B). The cell cycle of terminally divided cardiomyocytes (C) is maintained by Hippo, Wnt and mTOR signaling.*

1.1.2.2 Metabolic adaptation

In the postnatal phase, the heart adapts to a new metabolic environment. Cardiomyocytes undergo a metabolic switch from glucose as an energy substrate to lipids (Makinde, Kantor et al. 1998). The activation of the nuclear transcription factor peroxisome proliferator-activated receptor alpha (PPAR-alpha) and hypoxia-inducible factors (HIF) plays an important role in regulation of this metabolic transition (Figure 2A) (Nau, Van Natta et al. 2002, Breckenridge 2014). The HIF-1 protein acts as an essential sensor of oxygen (O_2) for oxidative phosphorylation (Semenza, Agani et al. 1998, Semenza 2000). The stimulation of mitochondrial β-oxidation by activated PPAR alpha enables the energy substrate switch in cardiomyocytes to use fatty acids as an energy source in the postnatal period (Lehman and Kelly 2002, Breckenridge 2014). Throughout the life, PPAR alpha continues to play a role in controlling important pathways such as fatty acid oxidation and anti-inflammatory responses that are essential for energy production as well as controlling inflammation in the cardiovascular system (Burns and Vanden Heuvel 2007).

1.1.3 Metabolic cross talk between postnatal heart and liver

Postnatal use of fatty acid as an energy source requires ß-oxidation in the liver, as in the heart (Poirier, Antonenkov et al. 2006, Fillmore, Mori et al. 2014). The levels of PPAR alpha rapidly increase during the postnatal stages in the liver and activate fatty acid metabolism by mitochondrial ß-oxidation activation (Panadero, Herrera et al. 2000, Lehman and Kelly 2002). PPAR alpha in the liver also regulates the level of circulatory lipids such as triglycerides (TG) and frees fatty acids (FFA).These are known ligands of the PPAR alpha protein (Aoyama, Peters et al. 1998, Edvardsson, Ljungberg et al. 2006, Wierzbicki, Chabowski et al. 2009). This indicates that the systemic metabolism is coordinated by cross talk between heart and liver to adopt to the new metabolic challenges under environmental stress (Magida and Leinwand 2014).

1.2 Ionizing radiation

Ionizing radiation has a number of adverse effects on biological systems. Generally, these effects are classified as deterministic, when the level of damage is directly dependent on the absorbed radiation dose or as stochastic if the detriment is not correlated with the absorbed

dose (Little 2003). The probability of stochastic effects is increased with increased radiation doses. The development of cataracts and arrhythmias are considered to be deterministic whereas the pathogeneses of malignancies and genetic disorders represent stochastic events. The radiation dose is measured in the International System of Units (SI) as the Gray (Gy) or Sievert (Sv). Each unit has a different application in context of absorbed dose and health hazard. One Gray is defined as the absorption of one joule of energy, deposited in the form of ionizing radiation, per kilogram of living or non-living substance. The biological effects per unit of absorbed dose differ with the physical nature of the radiation or the tissue exposed (UNSCEAR 2000, Eric J. Hall 2006) (Bureau International des Poids et Measures; BIPM).

Classically, it was believed that radiation-induced cardiovascular disease (CVD) was of a deterministic nature where there is a threshold dose for damage induction (Kumar 1980, Baker, Moulder et al. 2011, Little 2013). This assumption has been challenged by more recent epidemiological studies of A-bomb survivors (Shimizu, Kodama et al. 2010) and breast cancer patients treated with radiotherapy (Darby, Doll et al. 1985, McGale, Darby et al. 2011). There are recent data indicating that the age at exposure may influence the development of radiation-induced CVD (Boerma and Hauer-Jensen 2010, Shimizu, Kodama et al. 2010, Wondergem, Boerma et al. 2013). Consequently, more research on the effects of low-dose ionizing radiation on the heart at different ages is needed to solve the question of risk at low dose (Wondergem, Boerma et al. 2013).

1.3 Ionizing radiation and CVD

Mortality due to CVD is a cause for concern in western as well as mid to low income countries (Cannon 2013). Ischemic heart disease (IHD) caused by blockage of the blood vessels supplying blood to heart itself (Weber and Noels 2011), failure of the heart as a pump (Parmley 1985, Kemp and Conte 2012) and cerebrovascular disease (Weischer, Juul et al. 2010, Sim, Shi et al. 2014, Ueda, Cnattingius et al. 2014) represent major classes of CVD. Reduced physical activity, smoking, high fat diet and excessive use of alcohol are major risk factors contributing to cardiac morbidity (Epstein 1996, Wong 2014). There are other factors such as age, gender and hereditary features that also influence the risk of CVD (Wilson, D'Agostino et al. 1998). A number of epidemiological studies show an increased risk of CVD

over a range of radiation doses. Several international agencies such as the International Commission for Radiation Protection (IRCP) and (Advisory Group on Ionizing Radiation) AGIR have compared the data from different epidemiological studies (Shimizu, Kodama et al. 2010) (Bhatti, Sigurdson et al. 2008) and have estimated that the radiation dose causing enhanced CVD risk may be as low as 0.5 Gy (Cousins, Miller et al. 2013).

1.4 Epidemiology

1.4.1 Occupational exposures

In the early 20th century medical staffs routinely using diagnostic and therapeutic radiation where both patients and professionals were exposed to significant cumulative doses. A study following 90,000 radiography technologists show the increased incidence of CVD above a 0.3 Sv dose (Hauptmann, Mohan et al. 2003). A later smaller study published by Berrington et al. of United Kingdom radiologists showed no clear increase in CVD at this dose range (Berrington, Darby et al. 2001).

Another population receiving occupational radiation exposure is nuclear industry workers. A study amongst the U.S. nuclear power plant workers showed a statistically significant increase in mortality from atherosclerosis and heart disease at cumulative doses as low as 30 mSv compared to non-exposed workers (Howe, Zablotska et al. 2004). A study on Mayak plutonium enrichment plant workers also showed an elevated risk of mortality due to CVD from external doses of gamma radiation (Azizova, Haylock et al. 2014). Here, doses equal to or higher than 1.0 Gy were associated with increased risk of ischemic heart disease (Azizova, Muirhead et al. 2012). The 15-country mortality study of nuclear industry workers who have received a dose of up to 500 mSv did not show increased excess relative risk per Sievert (ERR/Sv) from ischemic heart disease (IHD), but the majority of workers were relatively young and the follow up period was relatively short (Vrijheid, Cardis et al. 2007)

1.4.2 A- bomb survivors

Atomic bomb survivors are the best studied radiation exposed group. Here epidemiological data show an elevated risk of CVD even several decades after the initial acute exposure (Preston, Shimizu et al. 2003). Doses as low as 0.5 Gy have been shown to result in a significant increase in the risk of CVD, especially if the exposure occurred below 40 years of

age (Shimizu, Kodama et al. 2010). The *in-utero* exposed group of atomic bomb survivors did not show significant increase in the risk of elevated CVD. The study did not have strong statistical power and follow-up period was too short to allow a comparison with the sporadic incidence peak of CVD (Tatsukawa, Nakashima et al. 2008). However, Nakashima et al. found elevated systolic hypertension in atomic bomb survivors exposed *in utero* (Nakashima, Akahoshi et al. 2007).

1.4.3 Therapeutic exposures

The use of radiation therapy in the treatment of some thoracic malignancies such as breast cancer and Hodgin´s disease results in local exposure to the heart. Patients are typically treated with doses as high as 50 Gy, delivered in a fractionated manner (Rutqvist, Rose et al. 2003, Lin and Tripuraneni 2011, Yeoh and Mikhaeel 2011). Thus, in right sided breast cancer patients the mean local dose to the heart has been estimated to be around 1.3 to 1.7 Gy whereas the dose to the heart in left side breast cancer patient was higher with a mean of 3.7 Gy and a maximum dose up to 20 Gy (Hurkmans, Borger et al. 2000, Baker, Moulder et al. 2011, Johansen, Tjessem et al. 2013). Such high local doses (20 Gy) to the heart cause local fibrosis in the ventricles, cardiac tissue degeneration, and blockage of pericardial blood vessels and eventually lead to clinical CVD pathologies (Taylor, Povall et al. 2008, Baker, Fish et al. 2009). There are growing data on increased cardiac mortality after therapeutic application of irradiation at lower doses but molecular pathologies are unknown (Aleman, van den Belt-Dusebout et al. 2003, Henson, McGale et al. 2013).

Childhood cancer survivors who have received radiation therapy at an early age are also highly prone to increased risk of CVD later in life if the heart has received doses bigger or equal to 1.0 Gy (Armstrong, Liu et al. 2009, Wong, Bhatia et al. 2014). The relative risk of 12.5 % for the cardiovascular mortality was calculated in the childhood cancer survivor patients who received an average radiation dose to the heart that exceeded 5 Gy (Tukenova, Guibout et al. 2010).

1.4.4 Diagnostic exposures

Computed Tomography (CT), X-ray examinations, and mammography are all common diagnostic tools in the clinical practice use of ionizing radiation. No excess risk of CVD was

found in tuberculosis patients receiving chest X-rays (Davis, Boice et al. 1989). Children receiving multiple CTs at an early age show a modest increase in heart disease that was observed 30-40 years later in life (Laskey, Feinendegen et al. 2010).

1.5 Experimental background

1.51. Cellular experiments

In vitro models have been used to study the effects of ionizing radiation on the different compartments of the heart and vascular system. These studies can be divided into those investigating radiation effects on the endothelial cells and those on the cardiomyocytes. A study using acute 4 Gy irradiation has shown the activation of nuclear factor kappa-B (NF-κB) in human umbilical vascular endothelial cells (HUVECs) (Chou, Chen et al. 2009); this resulted in changes in the expression of a number of adhesion molecules including intracellular adhesion molecule 1 (ICAM-1), vascular cell adhesion molecule 1 (VCAM-1), E-selectin and platelet endothelial cell adhesion molecule (PECAM-1) (Wondergem, Wedekind et al. 2004, Baluna, Eng et al. 2006). Cytokines such as IL-4, and IL-11 were also observed to be elevated after high (10 Gy) acute doses of ionizing radiation in endothelial cells (Van der Meeren, Mouthon et al. 2004). TGF-ß which plays the crucial role in the regulation of inflammation in endothelial cells was also found to be induced after an acute dose of 20 Gy or five fractions of 9 Gy (Kruse, Bart et al. 1999, Boerma, Roberto et al. 2008).The above mentioned data at high doses show that increased vascular adhesiveness and inflammation are typical characteristics of radiation-induced endothelial dysfunction.

Low-dose studies involving doses ranging from 0.1 Gy to 1 Gy have shown an anti-inflammatory effect of reduced adhesion of monocytes to endothelial lining of blood vessels (Rodel, Frey et al. 2012). Primary human umbilical vein endothelial cells have shown the induction of premature senescence after chronic exposure to low dose rate of 4.1 mGy/h(Yentrapalli, Azimzadeh et al. 2013). The PI3K/Akt/mTOR pathway was found to be involved in the progression of radiation-induced premature senesce (Yentrapalli, Azimzadeh et al. 2013).

Compared to the studies using endothelial cells less data are available concerning direct effects of ionizing radiation on the cardiomyocyte cell population. The main limitation of the

cardiomyocyte studies is that the survival of cardiac cells in culture is limited so that long-term effects of irradiation are difficult to examine (Louch, Sheehan et al. 2011, Sander, Suñe et al. 2013). Recent studies using 3D cultures of cardiomyocytes that were irradiated with X-rays ranging between 0.5 to 7 Gy have shown significant changes in electrophysiology as well as reactive oxygen species(ROS) -induced apoptosis only at the highest dose (7 Gy) (Friess, Heselich et al. 2015).

1.5.2 Animal experiments

The majority of animal experiments on radiation exposure and CVD have been performed using mice. These studies can be divided into acute vs. chronic exposure or local heart vs. total body exposure to mimic the different clinical, occupational and environmental exposures in human.

A functional study using male C57BL/6J mice and high radiation doses of 2, 8 and 16 Gy has shown thickening of epicardium, modest alteration in systolic and diastolic function, and structural damage to the myocardium and microvasculature (Seemann, Gabriels et al. 2012). Another functional study using mast cell–deficient rats exposed to a local 18 Gy dose has shown a reduction in left ventricle (LV) diastolic area from 0.50 to 0.24 cm after irradiation and a greater increase in LV posterior wall thickness after irradiation (Boerma, Wang et al. 2005)

An increase in the atherosclerotic lesions in $ApoE^{-/-}$ mice was observed after a dose of 14 Gy given to adult mice (Stewart, Heeneman et al. 2006). A study using rats irradiated with local high doses of 15 Gy or 20 Gy showed deposition of von Willebrand factor (vWf) 6 months after irradiation (Boerma, Kruse et al. 2004). Mitochondrial permeability transition pore (mPTP) opening leading to ischemia was also found at local high doses (21 Gy) using the rat model (Sridharan, Aykin-Burns et al. 2014).A proteomic study of local high dose (8 and 16 Gy) irradiation on adult murine heart has shown changes in proteins involved in the metabolic activity of heart and mitochondria (Azimzadeh, Sievert et al. 2013). A total body irradiation study with a 10 Gy dose using 5-week old rats has shown sustained increase in the level of low density lipoprotein (LDL) in serum, a decrease in endothelial nitric oxide synthase (e-NOS) and an increase in fibrinogen and PAR-1 protein after 120 days (Baker, Fish et al. 2009).

A study on long-term effects of moderate heart doses (2 Gy) using C57BL/6 adult mice has shown increase in oxidative stress, and dysfunction in mitochondrial function (Barjaktarovic, Shyla et al. 2013). Histopathological studies suggest modulation of the TGF-β1 pathway and pro-inflammatory responses characterized by IL-6 regulation after 2 Gy irradiation (Monceau, Meziani et al. 2013). An inflammation profiling study using $ApoE^{-/-}$ mice and low to moderate total body doses (0.05 Gy to 2 Gy) has shown elevation of IL-6, ICAM-1, VCAM-1, fibrinogens, and MCP-1 in the heart. These markers have also shown to be more significantly increased if the irradiation was given at the age of 5 or 8 months compared to that at 2 months (Mathias, Mitchel et al. 2015), indicating a progressive inflammatory reaction after low to moderate doses.

1.5.3 The early radiation exposure

Recent animal studies using an NMRI mouse model show the effects of total body low-dose (0.02 Gy to 1 Gy) ionizing radiation. This study found adverse effects on the brain development indicated by altered phosphorylation in protein signaling cascades (Kempf, Casciati et al. 2014). However, no animal studies have been performed to challenge the epidemiological data on increased risk of CVD after neonatal irradiation. Consequently, the molecular mechanisms behind the cardiac effects of low to medium total body doses given early in life are unknown.

1.6 Working hypothesis

The importance of age at exposure and increased relative risk of CVD after low doses of ionizing radiation have been indicated. This work was conducted to elucidate the molecular targets in heart of early radiation exposure by using global proteome screening of the cardiac tissue. Our main hypothesis was that the biological effects of low dose ionizing radiation depend on the age at exposure. Distinct biological pathways are activated at different stages of the heart development. We suggested that those pathways being activated at the time of irradiation are more susceptible to damage than those already switched on or those not yet functioning. We also suggested that the alteration in these pathways would be seen in a persistent manner even in the adult hearts.

Apart from size, the anatomy and the development of the heart in mouse and human are quite similar, with few exceptions (Wessels and Sedmera 2003). A mouse model can thus serve as a good model system to evaluate radiation-induced changes in the heart development and to identify biological pathways involved in the radiation-induced alteration.

1.7 Analysis of the mouse heart proteome

The pre- and postnatal development of the heart highlights the significance of proteins as signaling molecules in the heart structural development, energy switch mechanism and cardiomyocyte maintenance. Detailed analysis of changes in the cardiac protein expression after radiation insult applied at different developmental stages is essential in order to elucidate molecular mechanisms of low dose ionizing radiation on the developing heart.

Proteins can be used as biomarkers in several pathophysiological conditions to diagnose bacterial and viral infections, status of cancer metastasis, organ functions etc. In this context, it becomes very important to be able to identify and quantify proteins in different biological systems. In 1994 Marc Wilkins invented the term proteome as “the total amount of proteins in the living system at a particular time and at a particular situation” (Wilkins 2009). There are several ways to identify and quantify the proteome starting from the classical two-dimensional SDS-PAGE electrophoresis (Weber and Osborn 1969) to recent hybrid mass spectrometer analysis (Kolkman, Dirksen et al. 2005, Bantscheff, Lemeer et al. 2012).

In this study, the effects of low-dose ionizing radiation on the heart were investigated by measuring the quantitative proteomic changes between sham-irradiated and irradiated tissue samples using Isotope-Coded Protein Label (ICPL) method combined with 1D gel based fractionation and LC-MS/MS analysis. The methods used for the proteomic analyses of heart and liver tissue are described below briefly.

1.7.1 Sample preparation

One of the crucial steps in proteomic analysis is the sample preparation. Different biological systems require customized sample preparation methods. The isolation of the cardiac proteome needs special consideration since heart is one of the most rigid tissues due to the

strong cardiac muscles. There are many mechanical ways to extract proteins from heart including sonication, homogenization, and pulverization in liquid nitrogen. The buffers used for solubilization of the proteins are normally chosen according to the intended method for downstream proteomic analysis. Commonly used strong ionic buffers to lyse the tissue for proteomic analysis include 2% SDS in Tris-hydroxymethyl aminomethane (Tris), 6 M urea, and 8 M guanidine hydrochloride.

1.7.2 Protein labeling

In quantitative mass spectrometry studies the labeling of proteins is a well-established method, especially when it comes to the relative quantification. Labeling can be categorized into two main classes i.e. chemical labeling (e.g. ICPL, iTRAQ, iCAT, O^{18}) and metabolic labeling (SILAC). The metabolic labeling is done *in vivo* while chemical labels are commonly used *in vitro* i.e. after protein isolation.

The ICPL quantification is based on the usage of heavy and light labels, which result in a mass shift to the corresponding labeled protein. This is used to determine the relative protein abundances in the mass spectrometric analysis. N-nicotinoyloxy-succinimide labels are introduced by the different compositions of C^{12}/C^{13} and hydrogen/deuterium isotopes. This method enables the relative quantification of up to four different protein samples in one experiment. The chemical N-nicotinoyloxy-succinimide reacts with free amine group of proteins (–NH2) that typically exist at the N-terminus and on lysine residues. In duplex ICPL technology the control samples are labeled with C^{12}-N-nicotinoyloxy-succinimide (light) and the irradiated protein samples with C^{13}--N-nicotinoyloxy-succinimide (heavy). Peptides labeled with the heavy label show a typical mass shift of 6 Da, compared to the light-labeled control (Lottspeich and Kellermann 2011). Figure 3 shows the typical labeling reaction using heavy and light N-nicotinoyloxy-succinimide. Once labelled the two sets of labelled proteins are mixed. After separation by 1D gel electrophoresis, the proteins are in-gel digested with proteases and after elution the peptide fragments are analyzed with mass spectrometry. The mass spectrometry data is further evaluated with various bioinformatics tools (Figure 4).

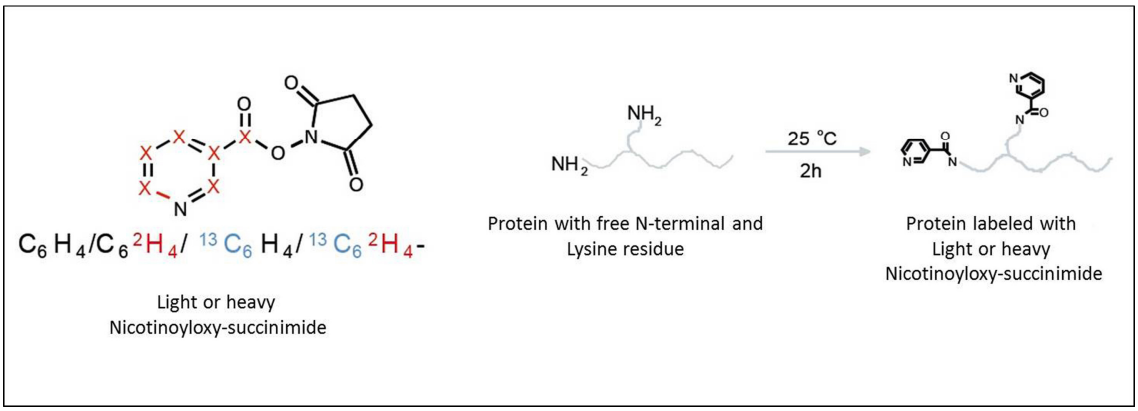

Figure 3: ICPL labeling reaction. *Heavy and light isotopes of N-nicotinoyloxy-succinimide react with free N-terminal and lysine residues of proteins.*

1.7.3 SDS-PAGE pre-fractionation

Electrophoresis is a classical method to separate proteins based on their molecular weight. Sodium dodecyl sulfate (SDS) is a strong anionic detergent; it unfolds the proteins from 3D structure to linearity (Shapiro, Vinuela et al. 1967). The Laemmli sample buffer is used to denature the proteins. It contains reducing agents like dithiothreitol (DTT), ß-mercaptoethanol (Laemmli 1970). This electrophoresis provides an additional fractionation step before the chromatographic resolution of proteins which enables to get good coverage of the total proteome in the mass spectrometry (MS) analysis.

1.7.4 Enzymatic digestion of proteins

To reduce the complexity of the proteome and determine the accurate molecular mass, the proteins are digested with proteases. In classical data dependent acquisition (DDA) experiment, proteins are digested directly in solution or they are separated on 1D or 2D gels and in-gel digested (Camerini and Mauri 2015). Chymotrypsin, trypsin, Lys-c, Arg-C, and pepsin are some of the common proteases used for digestion. Each of these proteases has selective cleavage sites allowing accurate mapping of peptides. The peptides generated by the proteolytic cleavage are mapped to the original proteins based on the databases such as EXPASY or MASCOT.

1.7.5 Liquid chromatography

Chromatographic methods are well established techniques in the individual protein and total proteome analysis. On the basis of physicochemical properties including size, charge, and hydrophobicity the complex peptide and protein mixtures are resolved on the analytical columns on liquid mobile phase (Horvath, Preiss et al. 1967).

Nowadays, high pressure/performance liquid chromatography (HPLC) is routinely used in proteomic workflow. In the case of protein separation for analytical purposes the reverse phase (RP) chromatography is the method of choice (Dauly, Perlman et al. 2006). In RP-HPLC proteins are separated on columns packed with porous particles with a typical diameter of 30 to 40 µm. These particles consist of silica, polystyrene-divinyl-benzene synthetic resin that is an alumina-like material. For the elution of peptides from the reverse phase columns polar solvents are required (Peterson, Hohmann et al. 2009). The column material consists of a C18 resin. The pore size of the column beads for peptide elution can be reduced to 2 µm which gives efficient peptide separation in very low concentrations. The nano-flow is the method of choice for resolving complex peptide mixtures (Gaspari and Cuda 2011).

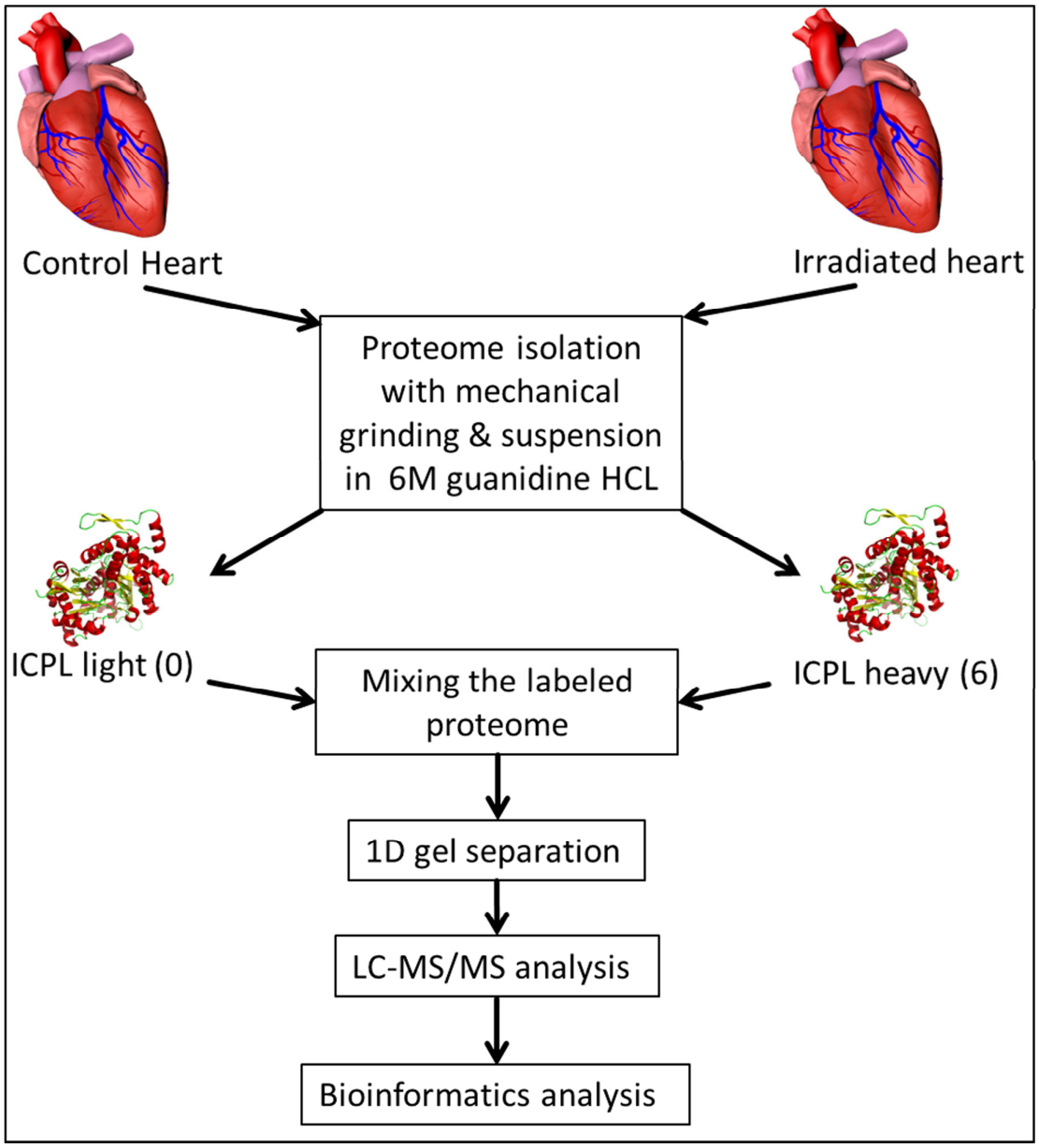

Figure 4: Generic representation of comparative proteomic analysis. *The key steps are tissue lysis, ICPL labeling, LC-MS analysis and bioinformatics evaluation*

1.7.6 Mass spectrometry

Mass spectrometer (MS) is the heart of proteomic analysis. Using the simple principle of measuring mass-to-charge (M/Z) ratio, it is possible to analyze a large spectrum of proteins and peptides. A typical mass spectrometer consists of an ionization source, a mass analyzer and a detector. Proteins or peptides are vaporized and ionized with ionization sources such

as electrospray (ESI), lasers (MALDI), chemicals (CI) etc. and sprayed into the mass spectrometer (Fenn, Mann et al. 1989, Castro, Koster et al. 1992).

In proteomics applications, quadrupole, time-of-flight (tof), ion trap, or orbitrap types of mass analyzers are routinely used. In recent commercially available instruments two or more mass analyzers are combined to get a better resolution. After the first measurement of the peptide mass the peptides are further fragmented with inert gas collision to its amino acid stages in the second detector to enable the identification of the peptide sequence. The ions striking on the surface of the detector produce a weak alternating current (AC) signal that is further amplified by the detector. In quantitative analysis, the intensity of differentially labeled peptides is compared to receive the relative amount of peptides (and corresponding proteins) in the different samples (Bantscheff, Lemeer et al. 2012).

In this study, the mass-based separation of the labeled proteins was performed by 1D SDS-PAGE gel. Each SDS gel lane representing one total proteome was cut in two and the proteins were subjected to in-gel digestion with trypsin (Sigma Aldrich) (Merl, Ueffing et al. 2012). The digested peptides were separated by nano-HPLC and mass spectroscopic analysis performed with an LTQ Orbitrap XL mass spectrometer (Thermo Scientific) (Hauck, Dietter et al. 2010). Up to ten of the most intense ions were selected for fragmentation in the linear ion trap and target peptides already selected for MS/MS were dynamically excluded for 60 seconds.

The MS/MS spectra were searched against the Ensembl mouse database (Version: 2.4, 56416 sequences) using the Mascot search engine (version 2.3.02; Matrix Science) with the following parameters: a precursor mass error tolerance of 10 ppm and a fragment tolerance of 0.6 Da. One missed cleavage was allowed. Carbamidomethylation was set as the fixed modification. Oxidized methionine and ICPL-0 and ICPL-6 for lysine residues and N-termini of peptides were set as the variable modifications.

1.7.7 Bioinformatics tools for MS data analysis

Bioinformatics analysis has two different goals. The first goal is to convert the raw data obtained from the mass spectrometer to a meaningful list of identified and quantified proteins. This step is important in deciding about the quality and possible exclusion of

disqualified spectra that are obtained from the mass spectrometer run. The second goal is to extract the biological significance from differentially regulated proteins. Both steps require the use of data mining tools to provide statistical calculations and manual literature and data base search.

Software tools such as Proteome Discoverer, MaxQuant, ICPL-quant, and Pro-genesis are used for the first step of reading the raw mass spectra and comparing the peptide masses to those found in global databases such as Ensembl, Protein Database (PDB), SwissProt, and UniProt. The direct comparison of spectral library to the databases leads to the generation of protein lists with features including p-value, fold change, PEP intensities, and number of unique peptides identified and quantified (sequence coverage) (Cox and Mann 2008, Colaert, Barsnes et al. 2011). In comparative proteomics, these attributes allow the significance of the deregulated proteins to be determined. In this study, data processing for the identification and quantitation of ICPL-duplex labeled proteins was performed using Proteome Discoverer version 1.3.0.339 (Thermo Scientific).

In the second step bioinformatics tools are used to investigate the biological networks based on the significantly changed proteins from first step. Many data mining tools such as Ingenuity Pathway Analysis (http://www.ingenuity.com/), STRING protein networks (Szklarczyk, Franceschini et al. 2015), and Gene Ontology (GO) using PANTHER classification system (Mi, Muruganujan et al. 2013) can be used for analyses of the proteomics datasets.

1.7.8 Supporting experiments

Mass spectrometry-based comparative methods trace small changes at the level of total protein. However, they are currently unable to reveal alterations in the post-translational modifications of proteins. The level of protein modifications such as phosphorylation and acetylation is well-known to be altered in cellular and molecular processes. In order to track those changes the classical laboratory techniques such as western blotting are very useful. Western blotting, also known as immunoblotting, is widely applied to detect and quantify specific proteins with the help of antigen-antibody reaction from complex protein extracts. Proteins are separated using gel electrophoresis and transferred on nitrocellulose membrane and targeted with specific antibodies (Towbin, Staehelin et al. 1979). This method provides the opportunity to quantify the levels of total as well as modified proteins.

Immunoblotting of protein extracts from control and irradiated tissues can used to validate proteomic data.

Some proteins such as enzymes and transcription factors, have specific activity that can be measured with enzyme-linked immunosorbent assay (ELISA). This technique is useful in measuring the activity of a target protein and comparing it with the total amount of this protein (Yalow and Berson 1960). Histological analysis is a valuable tool in cardiac pathophysiological studies. The localization and amount of differentially expressed proteins can be studied using various stainings for tissue sections.

The materials and methods, results and discussions from this study are included in the following publications.

Chapter 2: Results and discussion

2.1 *In-utero* Low-dose Irradiation Leads to Persistent Alterations in the Mouse Heart Proteome

2.1.1 Aim and summary

Prenatal development of the heart is very important for the postnatal function. Environmental stress can cause disturbances during the prenatal phase. No proteomics studies on the heart have been performed to unravel the changes induced by ionizing radiation *in utero*. The aim of this study was to analyze the long-term (6 months and 2 year of age) alterations on the proteome level after *in-utero* exposure to low-dose ionizing radiation. Pregnant mice were irradiated (X-ray) with total body exposure on embryonic day 11. The doses ranging from 0.02 Gy to 1.0 Gy were delivered and the hearts were isolated and examined with the ICPL triplex method for proteomic quantification.

The protein profiles in irradiated hearts indicate a progressive impairment in cardiac function. The changes were significantly visible at a dose as low as 0.1 Gy in both time points studied (6 months, 2 years). At the 1.0 Gy dose the persistent damage to structural components and alterations in mitochondrial proteins were observed. The Ingenuity Pathway Analysis indicated that the kinase family protein MAP4K4 is inhibited at the 1 Gy *in-utero* dose, even after 2 years. The changes in MAP4K4 were validated by biochemical methods.

Our study contributes to the understanding of the effects of ionizing radiation exposure *in utero*. Our data suggests that the *in-utero* exposure to IR leads to persistent proteome alteration at 6 months and is progressively seen at 2 years. Although the results from this *in-utero* study remain to be further confirmed, this study that is first of its kind pinpoints the biological mechanisms that need further evaluation.

2.1.2 Contribution

This study was performed in co-operation between Institute of Radiation Biology (ISB), the Research Unit Protein Science (PROT) of Helmholtz Zentrum München and the Radiobiology Unit, Belgian Nuclear Research Centre (SCK-CEN) Belgium. Dr. Tine Verreet from SCK-CEN did the *in-utero* animal irradiation; Dr. Juliane Merl-Pham from PROT ran the LC-MS/MS, I

isolated the proteins from the control and irradiated mice hearts, labeled them with ICPL and performed the downstream data analysis. Additionally I also performed the immunoblotting and the enzyme activity assays. Moreover, I designed all the tables, figures and wrote the manuscript with the help of PD Dr. Soile Tapio, Dr. Omid Azimzadeh and Prof. Dr. Michael J. Atkinson. Dr. Stefanie M Hauck and Dr. Mohammed A. Benotmane helped in the scientific discussion.

2.1.3 Publication

The following paper was published as an original research paper on June 8th 2016 in PLosOne

In-utero Low-dose Irradiation Leads to Persistent Alterations in the Mouse Heart Proteome

Mayur V. Bakshi, Omid Azimzadeh, Juliane Merl-Pham, Tine Verreet, Stefanie M. Hauck, Mohammed A. Benotmane, Michael J. Atkinson, Soile Tapio

PLoS One. 2016 Jun 8; 11(6):e0156952.

DOI: 10.1371/journal.pone.0156952. eCollection 2016.

PLOS | ONE

RESEARCH ARTICLE

In-Utero Low-Dose Irradiation Leads to Persistent Alterations in the Mouse Heart Proteome

Mayur V. Bakshi[1], Omid Azimzadeh[1], Juliane Merl-Pham[2], Tine Verreet[4,5], Stefanie M. Hauck[2], Mohammed A. Benotmane[4], Michael J. Atkinson[1,3], Soile Tapio[1]*

1 Helmholtz Zentrum München, German Research Center for Environmental Health GmbH, Institute of Radiation Biology, D-85764 Neuherberg, Germany, **2** Helmholtz Zentrum München, German Research Center for Environmental Health GmbH, Research Unit Protein Science, D-80939 Munich, Germany, **3** Chair of Radiation Biology, Technical University of Munich, D-80333 Munich, Germany, **4** Radiobiology Unit, Belgian Nuclear Research Centre, SCK-CEN, B-2400 Mol, Belgium, **5** Laboratory of Neural Circuit Development and Regeneration, Animal Physiology and Neurobiology Section, Department of Biology, KU Leuven, B-3000 Leuven, Belgium

* soile.tapio@helmholtz-muenchen.de

OPEN ACCESS

Citation: Bakshi MV, Azimzadeh O, Merl-Pham J, Verreet T, Hauck SM, Benotmane MA, et al. (2016) *In-Utero* Low-Dose Irradiation Leads to Persistent Alterations in the Mouse Heart Proteome. PLoS ONE 11(6): e0156952. doi:10.1371/journal.pone.0156952

Editor: Nukhet Aykin-Burns, University of Arkansas for Medical Sciences; College of Pharmacy, UNITED STATES

Received: January 15, 2016

Accepted: May 23, 2016

Published: June 8, 2016

Data Availability Statement: The raw data files from the mass spectrometry analysis have been deposited under the following link: http://storedb.org/store_v3/study.jsp?studyId=1019.

Funding: The research leading to these results is supported by a grant from the European Community's Seventh Framework Program (EURATOM), Contract No. 295823 (PROCARDIO) and Contract No. 295552 (CEREBRAD). The funders had no role in study design, data collection and analysis, decision to publish, or preparation of the manuscript.

Abstract

Prenatal exposure to stress such as increased level of reactive oxygen species or antiviral therapy are known factors leading to adult heart defects. The risks following a radiation exposure during fetal period are unknown, as are the mechanisms of any potential cardiac damage. The aim of this study was to gather evidence for possible damage by investigating long-term changes in the mouse heart proteome after prenatal exposure to low and moderate radiation doses. Pregnant C57Bl/6J mice received on embryonic day 11 (E11) a single total body dose of ionizing radiation that ranged from 0.02 Gy to 1.0 Gy. The offspring were sacrificed at the age of 6 months or 2 years. Quantitative proteomic analysis of heart tissue was performed using Isotope Coded Protein Label technology and tandem mass spectrometry. The proteomics data were analyzed by bioinformatics and key changes were validated by immunoblotting. Persistent changes were observed in the expression of proteins representing mitochondrial respiratory complexes, redox and heat shock response, and the cytoskeleton, even at the low dose of 0.1 Gy. The level of total and active form of the kinase MAP4K4 that is essential for the embryonic development of mouse heart was persistently decreased at the radiation dose of 1.0 Gy. This study provides the first insight into the molecular mechanisms of cardiac impairment induced by ionizing radiation exposure during the prenatal period.

Introduction

Ionizing radiation is now recognized as a risk factor for cardiovascular disease [1]. It is suggested that children may be more susceptible to future radiation-induced heart impairment than adults [2]. Given the well-documented association between prenatal radiation exposure

Competing Interests: The authors have declared that no competing interests exist.

Abbreviations: Gy, Gray; IPA, Ingenuity Pathway Analysis; H/L, heavy to light ratio; ICPL, isotope coded protein label; LC-MS, liquid chromatography mass spectrometry.

and both childhood cancer [3] and developmental impairments [4,5], the incidence of hypertension, hypercholesterolemia and cardiovascular disease was investigated in atomic bomb survivors exposed *in utero* [6]. Although no significant excess in the risk for cardiovascular disease was found, there was a suggestion of an increased risk when fatal and nonfatal cardiovascular disease cases were combined. This study has statistical limitations due to the low number (506) of *in-utero* exposed subjects studied and their relatively young age (under 60 years) at the time of examination [6].

The embryonic development of the murine fetal heart is a very dynamic process as the typical gestation period only lasts three weeks. A. particular window of susceptibility extends from embryonic day E9 to E12. When corrected for size and embryonic time scale, the anatomy and growth of mouse and human hearts are quite similar [7], suggesting that mouse models can be successfully used to study the heart development.

The activation of the MAP kinase cascade plays an important role in the heart chamber formation of the fetus [8]. Data from human studies suggest that environmental stress factors such as hypoxia, increased level of reactive oxygen species or antiviral therapy adversely influence this process [9,10]. It is reasonable to suggest that ionizing radiation may have similar adverse effects on the fetal heart development. However, no experimental data concerning radiation-induced cardiac defects after prenatal exposure are available at the moment.

The aim of this study was to evaluate the long-term consequences of low and moderate *in-utero* (E11) radiation doses using the C57Bl/6J mouse model. The lowest radiation dose used here is comparable to that received in coronary computed tomography angiogram (20 mGy). The higher doses of 0.1 and 1.0 Gy have been measured in accidental and occupational situations, even in females [6,11]. Both male and female offspring were included in the study. A global quantitative proteomics analysis with a liquid chromatography-tandem mass spectrometry (LC–MS/MS) identification of dysregulated proteins was performed. Proteins altered in expression could be clustered to several categories including mitochondrial, acute phase and structural proteins. Significant proteome alterations were detectable two years post-irradiation even after exposure to a dose of 0.1 Gy.

Materials and Methods

In-utero irradiation

All animal experiments were performed in accordance with the European Communities Council Directive of November 24, 1986 (86/609/EEC) and approved by the local ethical board Studiecentrum voor Kernenergie-Centre d'Étude de l'énergie Nucléaire/Vlaamse Instelling voor Technologisch Onderzoek (SCK-CEN/VITO) (ref. 02–012). C57Bl/6J were purchased from Janvier (Bio-services, Uden, The Netherlands) and housed under standard laboratory conditions (12 h light/dark cycle). Mice were mated during a 2-hourtime period in the morning, at the start of the light phase (7.30 h until 9.30 h), in order to ensure synchronous timing of embryonic development. Subsequently, pregnant females were whole body irradiated at E11 (0.02/0.05, 0.1 and 1.0 Gy) at a dose rate of 0.35 Gy/min using a Pantak RX tube operating at 250 kV, 15 mA (1 mm Cu-filtered X-rays). The calibration of the X-ray tube was performed using an ionization chamber. Control pregnant females were sham-irradiated. The overall health of the mice was monitored weekly. No adverse health consequences were observed in the irradiated mice. All mice were sacrificed via cervical dislocation, the male offspring after 6 months and the female offspring 2 years after birth. Hearts were excised and maintained at -80°C until further analysis. The time points referred to in this paper (6 m, 2 y) are calculated from the birth, not from the irradiation.

Isolation of total heart protein

The frozen hearts were pulverized in liquid nitrogen using mortar and pestle. The powdered tissue was immediately suspended in 6 M guanidine hydrochloride (SERVA) with phosphatase and protease inhibitor cocktails (Roche). The samples were centrifuged at 13,000 g and the supernatants were collected. Protein concentration of each supernatant was measured with Bradford assay [12].

ICPL labeling

Fifty (50) μg of protein from each supernatant was labeled with Isotope Coded Protein Label (ICPL) technology. Triplex set of labels (light, medium and heavy) were used as follows: control was labeled with light labels while irradiated heart proteomes (0.02/0.05 Gy, 0.1 Gy) were labeled with medium and heavy isotopes as described previously [13]. Duplex set of labels was used for the dose of 1.0 Gy: control was labeled with a light label and the irradiated sample with a heavy label. Three biological replicates were used for each dose and for the respective control groups. The labeled proteins were mixed, precipitated and dissolved in Laemmeli sample buffer [14]. The proteins were separated by SDS-PAGE gel electrophoresis and stained using Coomassie Blue.

Mass spectrometric analysis

Mass spectrometric analysis was done as described previously [15]. Shortly, the Coomassie Blue stained protein lanes were cut into 5 slices and individually in-gel digested with trypsin (Sigma Aldrich). The digested peptides were fractionated on nano-HPLC and subsequently analyzed with an Orbitrap-XL mass spectrometer (Thermo Scientific) as described previously [16].

The MS/MS spectra were searched against the Ensembl mouse database (Version: 2.4, 56 416 sequences) using the Mascot search engine (version 2.3.02; Matrix Science) with the following parameters: a precursor mass error tolerance of 10 ppm and a fragment tolerance of 0.6 D. One missed cleavage was allowed. Carbamidomethylation was set as the fixed modification. Oxidized methionine and ICPL-0, ICPL-4 and ICPL-6 for lysine residues and N-termini of peptides were set as the variable modifications.

Data processing for the identification and quantitation of ICPL-triplex labeled proteins was performed using Proteome Discoverer version 1.3.0.339 (Thermo Scientific). The MASCOT Percolator node-based algorithm was used to discriminate correct from incorrect peptide spectrum matches. The q value of the percolator algorithm was set to 0.01 representing strict peptide ranking. Thus, only the best ranked peptides were used. Further, these peptides were filtered against a Decoy database resulting in a false discovery rate (FDR) of each LC-MS-run; the significance threshold of the FDR was set to 0.01 to ensure that only highly confident peptides were used for protein quantification [17]. Proteins identified by at least two unique peptides in two out of three biological replicates, and having an H/L variability of less than 30% were considered for further evaluation. Proteins identified by a single peptide were manually scrutinized and regarded as unequivocally identified if they fulfilled the following four criteria: (a) they had fragmentation spectra with a long, nearly complete y- and/or b-series; (b) all lysines were modified; (c) the numbers of lysines predicted from the mass difference of the labeled pair matched the number of lysines in the given sequence from the search query and (d) at least one mass of a modified lysine was included in the detected partial fragment series [18]. Proteins with ratios of H/L label greater than 1.30-fold or less than 0.769-fold were defined as being significantly differentially expressed.

Access to raw data files from LC-MS/MS runs

The raw data files from the mass spectrometry analysis have been deposited under the following link-http://storedb.org/store_v3/study.jsp?studyId=1019

Bioinformatics analysis

Protein-protein interactions and signaling networks were searched using INGENUITY Pathway Analysis (IPA) (http://www.INGENUITY.com) [19] and STRING protein database (http://string-db.org) [20]. The Ensembl protein accession numbers, including the relative expression values of all significantly deregulated proteins, were uploaded to IPA and STRING to elucidate possible interactions.

Immunoblotting analysis

Immunoblotting of protein lysates from control and irradiated tissues was performed as described [21]. In short, proteins were separated using 1D gel electrophoresis and transferred to nitrocellulose membranes (GE Healthcare) using a TE 77 semidry blotting system (GE Healthcare) at 0.8 mA/cm for 1 h. Membranes were saturated for one hour with 8% milk powder in TBS (50 mM Tris-HCl, pH 7.6 and 150 mM NaCl) containing 0.1% Tween 20 (TBS/T). Blots were incubated overnight at 4°C with antibodies against vimentin (Abcam ab92547), LIM domain-binding protein 3 (Abcam ab154183), peroxiredoxin-5 (Abcam ab119712), apolipoprotein E (Abcam ab1906) and phospho Map4K4-ser801 (BioSource bs-5493R).

After washing three times in TBS/T, blots were incubated for one hour at room temperature with horseradish peroxidase-conjugated or alkaline phosphatase anti-mouse or anti-rabbit secondary antibody (Santa Cruz Biotechnology) in blocking buffer (TBS/T with 8% w/v milk powder). Immuno-detection was performed with ECL advance Western blotting detection kit (GE Healthcare). The protein bands were quantified using Total Lab (TL100) software (http://www.totallab.com). ATP synthase ß (Abcam ab14730) was used for normalization as it showed no significant change in the proteomics analysis.

MAP4K4 ELISA assay

To test the amount of total MAP4K4 same amount of protein (100 μg) from each sample was used for the enzyme-linked immunosorbent assay (ELISA) assay that was performed according to manufacturer's guidelines (MyBioSource MBS9317805).

Statistical analysis

Statistical analysis was performed using Graph Pad Prism (release 4). Immunoblotting results were evaluated using non-paired Student´s t-test. Data are presented as means + standard deviation (SD). A p-value of less than 0.05 was considered to denote statistical significance. Three biological replicates were used in all experiments.

Results

Proteome alteration increases with the radiation dose

The proteomic analysis at 6 months using male offspring identified a total of 1196 proteins (682 quantified) of which 19 (1.6%) and 29 proteins (2.4%) were significantly deregulated at 0.02 Gy and 0.1 Gy, respectively (Tables A and B in S2 File). At 6 months, the number of identified proteins after 1.0 Gy was 1188 (644 quantified) of which 34 proteins (2.9%) were significantly deregulated (Table C in S2 File). The protein expression changes induced at the lowest

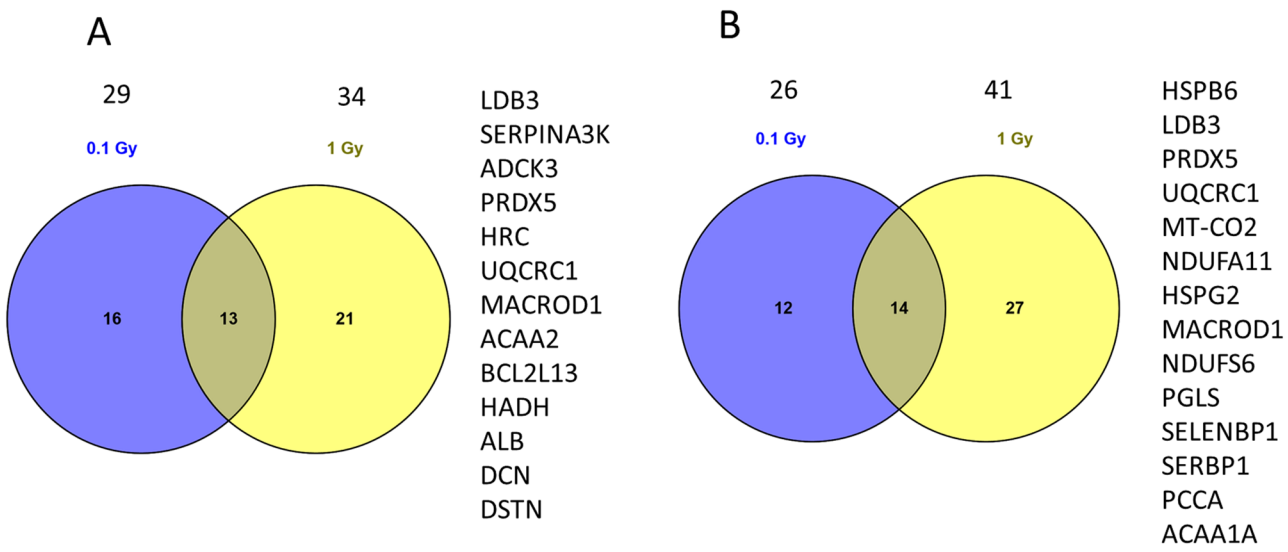

Fig 1. Venn diagrams showing the number of all and shared deregulated proteins at doses of 0.1 Gy and 1.0 Gy. (A) The numbers of deregulated proteins at 6 months and (B) 2 years are indicated above the circles. The list of shared proteins at these time points is shown on the right.

doi:10.1371/journal.pone.0156952.g001

dose (0.02 Gy) showed little overlap with those seen at the higher doses with only seven proteins shared with the deregulated proteins at the dose of 0.1 Gy or 1.0 Gy. However, thirteen significantly deregulated proteins were shared between 0.1 Gy and 1.0 Gy doses, including peroxiredoxin 5 (PRDX5), LIM domain-binding protein-3 (LDB3), and several mitochondrial proteins (Fig 1A).

As only a few proteome alterations were seen at the dose of 0.02 Gy, the effect of a slightly higher but still a low radiation dose (0.05 Gy) was investigated at a later time point (2 years). To estimate the effect of the gender in the radiation response female offspring was used at this time point. The proteomics analysis at 0.05 Gy and 0.1 Gy identified a total of 983 proteins (528 quantified) of which 11 (1.1%) and 26 proteins (2.7%) were significantly deregulated, respectively (Tables D and E in S2 File). At the 1.0 Gy dose 2 years post-irradiation, 988 proteins were identified (582 quantified), of which 41 proteins (4.2%) were significantly deregulated (Table F in S2 File). Again, the proteome response at the lowest dose was distinct from that of the higher doses with only six deregulated proteins shared with 0.1 Gy or 1.0 Gy. In contrast, the higher doses induced similar changes in the heart proteome. Fourteen significantly deregulated proteins were shared between these doses (Fig 1B). These included PRDX5, LDB3, heat shock protein HSPB6, and several mitochondrial proteins.

The proteome alteration at the highest dose (1.0 Gy) was investigated as a function of time. Ten deregulated proteins were found shared at 6 months and 2 years (Table 1), indicating a similar response in male and female mice. Members of mitochondrial complexes I and III, and hydroxyacyl-Coenzyme A dehydrogenase (HADH), involved in acetyl-CoA pathway, were found upregulated. Similarly, HSBP6, PRDX5, and LDB3 were upregulated whereas the structural protein vimentin (VIM) and the lipid translocator apolipoprotein E (APOE) were found downregulated (Table 1). With the exception of transgelin 2 (TAGLN2), an actin binding protein and a marker of differentiated smooth muscle [22], all shared proteins showed a similar direction of deregulation at the two time points. All differentially regulated proteins showed a greater fold change in expression at 2 years than at 6 months, suggesting a progressive proteome alteration.

Table 1. Significantly deregulated proteins after 1.0 Gy *in-utero* dose common to time points of 6 months and 2 years.

Protein name	Fold change		Function
	6 m	2 y	
Heat shock protein, alpha-crystallin-related, B6	2.3	3.7	Cardiac apoptosis
LIM-domain binding protein 3	2.2	2.4	Developmentally regulated in cardiac muscle
Peroxiredoxin 5	1.8	2.0	Response to mitochondrial oxidative stress
Hydroxyacyl-Coenzyme A dehydrogenase	1.6	1.7	Acetyl-CoA pathway
MACRO domain containing 1	1.5	1.7	Ribose deacetylase
Ubiquinol-cytochrome c reductase core protein 1	1.4	2.0	Mitochondrial respiratory Complex III
NADH dehydrogenase (ubiquinone) flavoprotein 2	1.3	1.4	Mitochondrial respiratory Complex I
Transgelin 2	0.7	1.4	Marker of differentiated smooth muscle
Vimentin	0.7	0.6	Structural constituent
Apolipoprotein E	0.6	0.4	Lipid transportation

doi:10.1371/journal.pone.0156952.t001

Taken together, these data indicate a dose-dependent increase in the number of deregulated proteins at both time points. The proteome response at the lowest doses used here (0.02 Gy, 0.05 Gy) showed little similarity with that at the higher doses. Nevertheless, the protein LDB3 that is essential for the structure of sarcomeres was found upregulated at all doses and time points.

Deregulated proteins form mitochondrial, acute phase, and structural protein clusters

Proteins, the expression of which was altered at the lowest radiation doses, i.e. 0.02 Gy and 0.05 Gy, (6 months and 2 years, respectively) could not be clustered to form an interactive network using STRING analysis. This suggested that no particular biological pathway was significantly affected at these doses.

Significantly deregulated proteins at doses of 0.1 Gy or 1.0 Gy could be clustered in categories as follows: mitochondrial proteins, acute phase response and structural proteins (cytoskeleton) (Fig 2). In most cases, the number of proteins in a particular network increased with dose at both time points, supporting a dose-dependent increase of proteome alterations that was also suggested by the proteomics analysis. In case of mitochondrial proteins, several members of the respiratory complexes I, III and IV showed persistent upregulation, ubiquinol-cytochrome c reductase (UQCRC1) being a central member of all networks. Although the networks of acute phase and structural proteins were represented as deregulated at both time points, the members of these networks changed in a time-dependent manner. For example, a transient deregulation was seen in the serpine family of proteins at 1.0 Gy at 6 months but not at 2 years. Some of these changes may also be due to a gender-specific alteration of the cardiac proteome.

Immunoblotting confirms the results of the proteomic analysis

In order to validate the proteomics data, the expression of proteins representing the biological categories of cellular structure, metabolism or oxidative stress was investigated by immunoblotting (Fig 3). In agreement with the proteomics data, immunoblotting showed increase in the amount of LDB3 and PRDX5 whereas a decrease in the level of structural protein vimentin and lipid transporter APOE was observed after the 1.0 Gy dose at both time points (Figs A-D in S1 File).

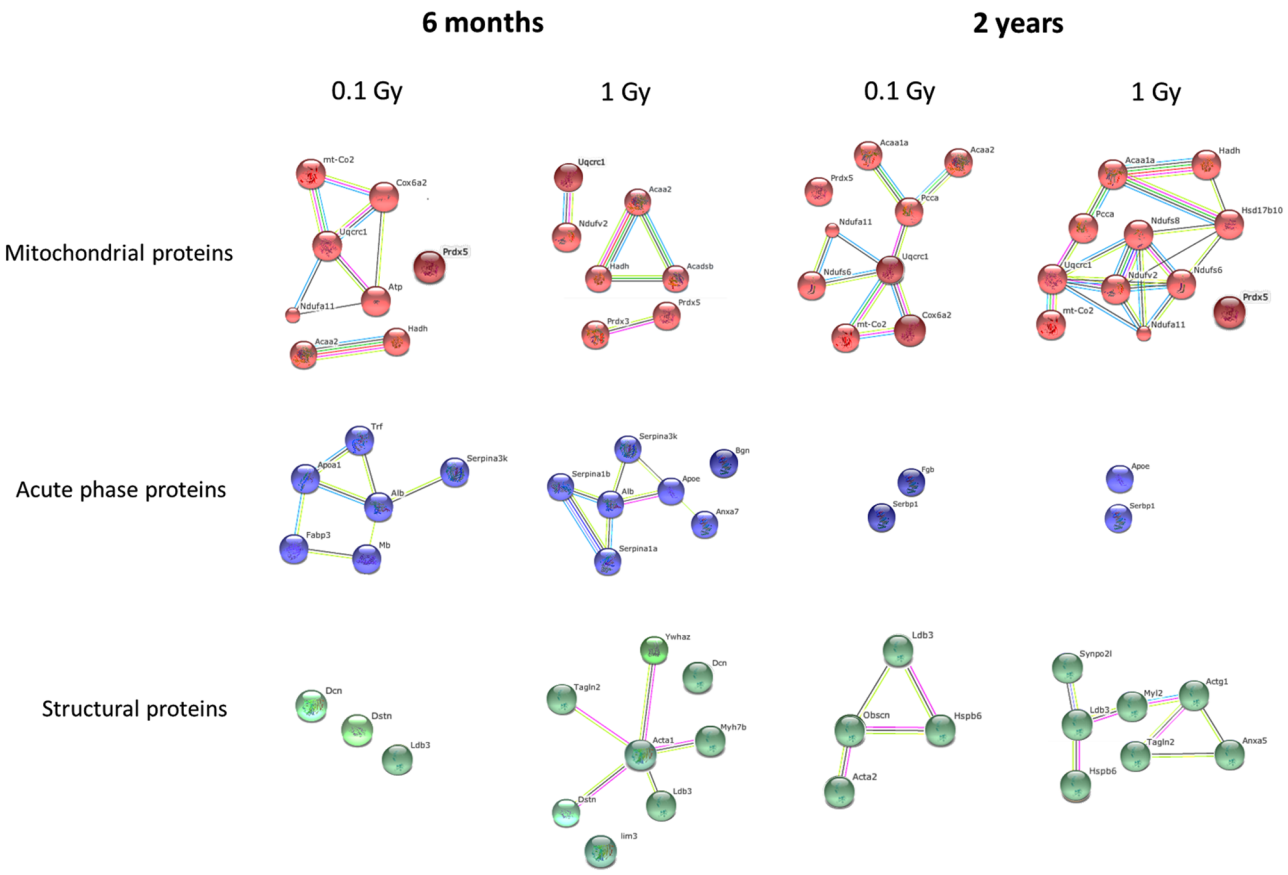

Fig 2. STRING protein networks of significantly changed proteins at prenatal (E11) radiation exposure of 0.1 Gy and 1.0 Gy. Common networks between 6-month- and 2-year-time points are shown. Mitochondrial proteins, acute phase proteins and structural proteins represent the major protein classes of proteins affected by the pre-natal irradiation.

doi:10.1371/journal.pone.0156952.g002

Expressions of the total MAP4K4 and phospho-MAP4K4 are decreased after 1.0 Gy

Ingenuity Pathway Analysis (IPA) predicted the inhibition of mitogen-activated protein kinase kinase kinase kinase 4 (MAP4K4) at 6 and 24 months after a dose of 1.0 Gy (Fig 4) but not at lower doses.

The relative quantification of the level of phosphorylated (active) MAP4K4 (Ser-801) using immunoblotting showed a significant decrease at 6 months (Fig 5A and Fig D in S1 File). At 2 years, the significance of downregulation was not reached ($p = 0.1714$) (Fig 5A).

To confirm the predicted inhibition of MAP4K4, the total amount was measured using the control and 1.0 Gy irradiated cardiac tissue. A significant decrease in the level of total kinase expression was observed at both time points in irradiated hearts (Fig 5B).

Discussion

There is a considerable lack of data concerning late effects of radiation-induced damage in the prenatal period. This study is to our knowledge the first to investigate persistent molecular changes in the murine heart after *in-utero* exposure to low and moderate doses of ionizing radiation. The doses used here, ranging from 0.02 to 1.0 Gy, are comparable to those found in medical diagnostic situations, atomic bombings and occupationally exposed populations [23,24].

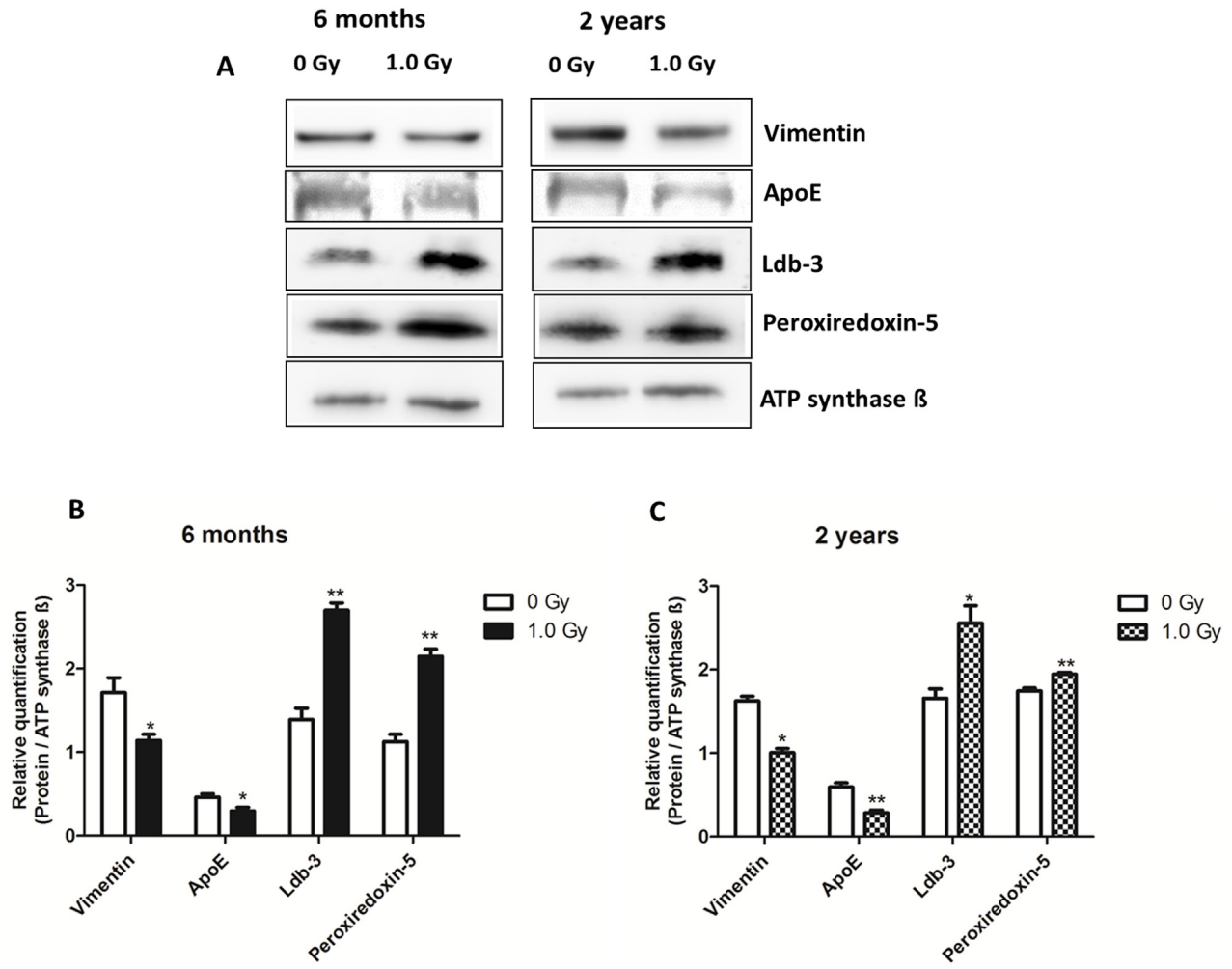

Fig 3. Immunoblot validation of proteomics data at 1.0 Gy using antibodies against vimentin (VIM), apolipoprotein E (APOE), LIM domain-binding protein (LDB3), and peroxiredoxin 5 (PRDX5). (A) The immunoblot images of VIM, APOE (6 months), PRDX5, and LDB3 are shown. The bar charts at 6 months (B) and 2 years (C) represent the average ratios with standard deviation (SD) of relative protein expression in control and 1.0 Gy irradiated samples after background correction and normalization to ATP synthase ß. (unpaired Student´s t-test; *p $\leq$0.05; **p$\leq$0.01; n = 3).

doi:10.1371/journal.pone.0156952.g003

We show here that many mitochondrial proteins show differential expression after prenatal irradiation (E11) already at the dose of 0.1 Gy. Recent data strongly suggest that the switch to aerobic metabolism in the murine embryonic heart occurs around embryonic day E11.5 [25], close to the time point of irradiation in this study. It has been shown that at E9.5 mitochondrial electron transfer chain (ETC) activity and oxidative phosphorylation (OXPHOS) are not coupled, even though the complexes are present. At E11.5, mitochondria appear functionally more mature, ETC activity and OXPHOS are coupled and respond to ETC inhibitors [25]. The time window of OXPHOS activation may be especially susceptible to radiation-induced mitochondrial impairment. In this study, many members of respiratory Complexes I and IV are found differentially regulated after prenatal exposure, this being in agreement with the data following neonatal irradiation with same doses as used here [21]. In addition, upregulation of Complex III proteins is seen in this study. Our previous data on locally irradiated adult (8 weeks) mouse hearts (2 Gy) also highlight mitochondrial respiratory complexes as radiation targets in the

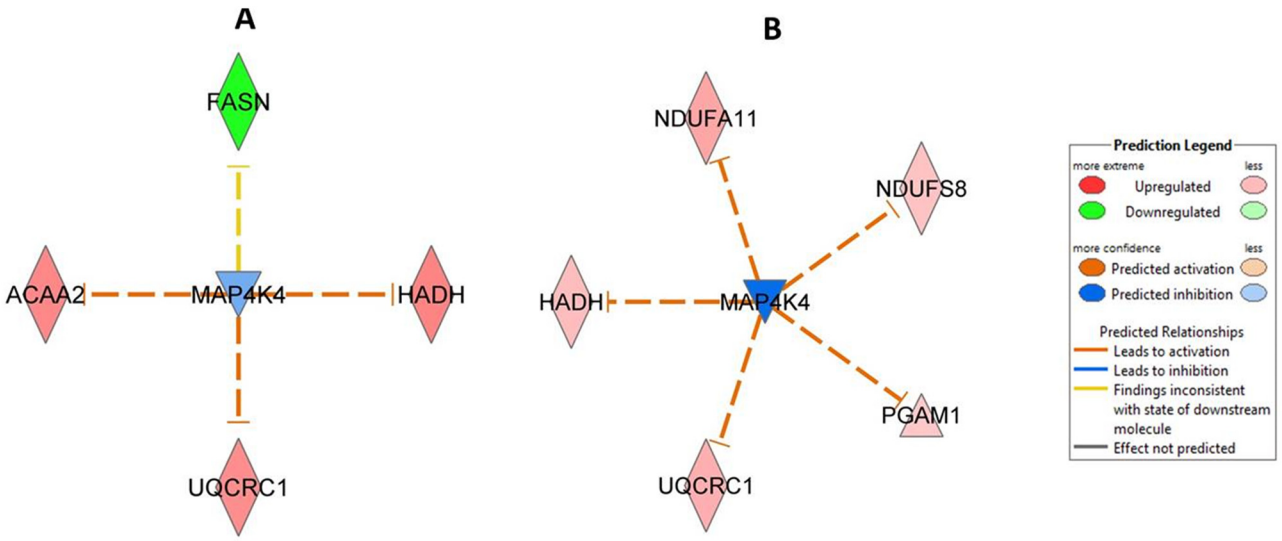

Fig 4. Ingenuity Pathway Analysis networks showing predicted inhibition of protein kinase MAP4K4. (A) Predicted networks after *in utero* irradiation at 1.0 Gy, 6 months and (B) 1.0 Gy, 2 year are shown. Three biological replicates were used in all experiments. ACAA2, acetyl-Coenzyme A acyltransferase 2; FASN, fatty acid synthase; HADH, hydroxyacyl-Coenzyme A dehydrogenase; UQCRC1, ubiquinol-cytochrome c reductase core protein 1; NDUFA11, NADH dehydrogenase (ubiquinone) 1 alpha subcomplex 11; NDUFS8, NADH dehydrogenase (ubiquinone) Fe-S protein 8; PGAM1, phosphoglycerate mutase 1; MAP4K4, Mitogen-activated protein kinase kinase kinase kinase 4.

doi:10.1371/journal.pone.0156952.g004

heart but mice irradiated in the adulthood show downregulation, not upregulation, of the complex proteins [26]. This was connected with increased reactive oxygen species formation and protein oxidation, even 40 weeks after the radiation exposure [27]. The prenatal irradiation used here does not increase protein oxidation in the heart (data not shown) although the persistent upregulation of PRDX5 is indicative of long-term oxidative stress [28,29]. The upregulation of respiratory chain proteins may indicate a protective response to the early transient radiation insult [30].

A second group of significantly deregulated proteins found in this study are the heat shock proteins. Similar to mitochondrial proteins, the marked upregulation of heat shock protein B6 (HSPB6, formerly heat shock protein 20) that is observed at the 1.0 Gy dose already after 6 months and at all doses after 2 years, may indicate a response to persistent radiation-induced damage. HSPB6 plays a key role in protection against apoptosis, remodeling, and ischemia/reperfusion injury [31,32]. It has been implicated in modulation of cardiac contractility through sarcoplasmic reticulum calcium cycling [33].

Also involved in the cardiac contractility is the protein LDB3, also known as Cypher or Z-band alternatively spliced PDZ-motif (ZASP). It is the only protein found upregulated at all doses and time points. It stabilizes the cardiac sarcomere during contraction, through interactions with actin [34]. Mutations in LDB3 cause several forms of heart disease including dilated cardiomyopathy [35,36]. Another Z-disc protein, SYNPO2L, highly expressed in the mouse embryonic heart [37] and essential for heart function [38], is found almost twofold upregulated two years after the prenatal radiation dose of 1.0 Gy.

A transient deregulation (both up- and downregulation) at six months is seen of many members of the serpin family, especially at 1.0 Gy. The serpin family comprises a structurally similar, yet functionally diverse, set of proteins. Named originally for their function as serine proteinase inhibitors, many of its members are not inhibitors but rather chaperones, involved in cellular storage and transport [39]. An almost twofold upregulation is found at 1.0 Gy for

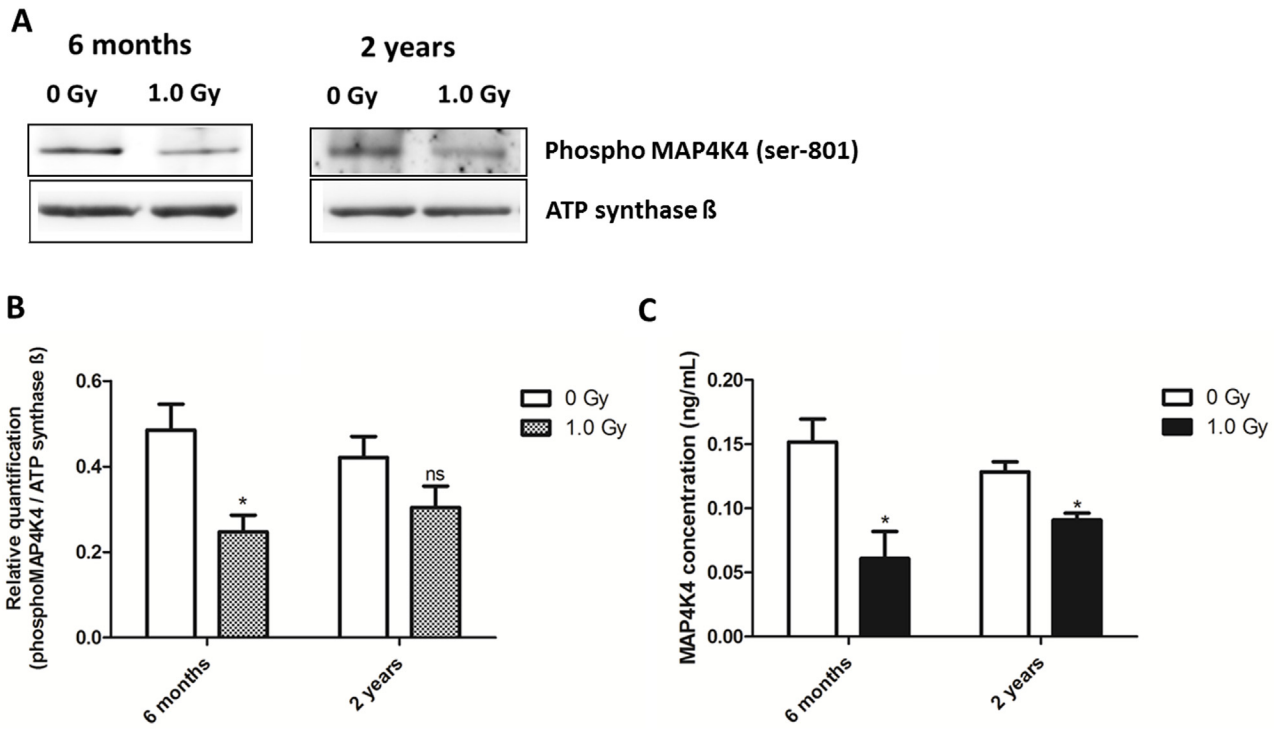

Fig 5. Characterization of MAP4K4 in the control and 1.0 Gy-irradiated mouse heart. (A) The immunoblot images of phospho-MAP4K4 (Ser-801) in the 1.0 Gy irradiated hearts compared to the controls at 6 months and 2 years is shown. (B) Columns represent the average ratios with standard deviation (SD) of relative protein expression in control and 1.0 Gy irradiated samples after background correction and normalization to ATP synthase ß (unpaired Student´s t-test; *p ≤0.05; ns, non-significant; n = 3). (C) The total amount of MAP4K4 measured using ELISA in control and 1.0 Gy irradiated heart tissue shows significant radiation-induced decrease at 6 months and 2 years (unpaired Student´s *t*-test; *$p \leq 0.05$; ns, non-significant; n = 3).

doi:10.1371/journal.pone.0156952.g005

the expression of SERPINA1A, alpha-1-antitrypsin orthologue, the deletion of which is embryonically lethal [40]. Alpha-1-antitrypsin expression has been associated with atherosclerosis progression in human [41].

An alteration of the cardiac cytoskeleton is suggested already at 0.1 Gy. The proteins from the structural component category such as annexin 5, transgelin (2 years), obscurin, and different forms of actin and myosin show increased expression. Obscurin plays a role in the formation of new sarcomeres during myofibril assembly [42] and mutations in this protein have been associated with dilated [43] and hypertrophic cardiomyopathy [44]. In contrast, downregulation of the vimentin expression was observed here, in accordance with our previous studies using adult mice [26,27].

APOE has an important function in the heart by facilitating the transport of high density lipoproteins (HDL) and low density lipoproteins (LDL) across the plasma membrane [45]. The downregulation of APOE observed at both time points (1.0 Gy) may suggest increased lipid accumulation [46] as previously shown at high doses of ionizing radiation to the heart [47].

This study shows that *in-utero* irradiation (1.0 Gy) decreases the expression of total and active form of MAP4K4 by reducing the phosphorylation of serine-801. MAP4K4, a serine/threonine protein kinase [48], is essential in embryonic mesoderm formation leading to the origin of the cardiovascular system [49]. The deletion of the corresponding gene is lethal as the k.o. mice die between E9.5 and E10.5. (Xue, Wang et al. 2001). Little is known of its function in the heart but several isoforms of this enzyme were identified recently in the rat cardiac kinome [50]. Its expression was higher in neonatal ventricular myocytes compared to the adult ones.

MAP4K4 may play a role in the response to environmental stress and inflammation as silencing it in macrophages *in vivo* protected mice from lipopolysaccharide-induced lethality by inhibiting TNF-alpha and interleukin-1beta production [51]. The reduced amount of total and active form of MAP4K4 seen in this study may be protective against cardiac inflammation but more research is needed to clarify this.

As we find no great differences in the heart proteome responses of male and female mice, the gender-specific responses may be characteristic only to mice irradiated at a mature age. This is in agreement with our previous studies using both male and female mice that were irradiated early in life at postnatal day 10. These studies showed little difference in the hippocampal proteome after low and moderate doses of ionizing radiation [17,52].

Conclusions

This study suggests that biological pathways important at the time of irradiation (E11) are still found altered years after the initial insult. Such pathways include initiation of mitochondrial respiration and activation of MAP kinases in the mouse embryonic heart. The proteomic response after prenatal irradiation is different from that observed after radiation exposure at the adult age but bears resemblance to that found after radiation exposure at the early postnatal phase. Several structural proteins found dysregulated in this study are involved in the sarcomere formation and contractility. Both of these processes are rapidly developing at the time of the radiation exposure.

Supporting Information

S1 File. Supplementary Figures. Fig A: Images from immunoblotting of APOE and ATP synthase ß in control and 1.0 Gy irradiated heart lysates at 6 months and 2 years. Fig B: Images from immunoblotting of PRDX5 and ATP synthase ß in control and 1.0 Gy irradiated heart lysates at 6 months and 2 years. Fig C: Images from immunoblotting of LDB3 and ATP synthase ß in control and 1.0 Gy irradiated heart lysates at 6 months and 2 years. Fig D: Images from immunoblotting of phospho-MAP4K4 (Ser-801), vimentin and ATP synthase ß in control and 1.0 Gy irradiated heart lysates at 6 months and 2 years.
(PDF)

S2 File. Supplementary tables. Table A: Significantly deregulated proteins at 0.02 Gy, 6 months. Table B: Significantly deregulated proteins at 0.1 Gy, 6 months. Table C: Significantly deregulated proteins at 1.0 Gy dose, 6 months. Table D: Significantly deregulated proteins list at 0.05 Gy, 2 years. Table E: Significantly deregulated proteins at 0.1 Gy, 2 years. Table F: Significantly deregulated proteins at 1.0 Gy, 2 years.
(PDF)

Acknowledgments

We thank Stefanie Winkler, Mieke Neefs, Liselotte Leysen and Sandra Helm for technical assistance.

Author Contributions

Conceived and designed the experiments: MVB OA ST. Performed the experiments: MVB OA JMP. Analyzed the data: MVB OA ST. Contributed reagents/materials/analysis tools: TV SMH MAB. Wrote the paper: MVB OA MJA ST.

References

1. Little MP, Azizova TV, Bazyka D, Bouffler SD, Cardis E, Chekin S, et al. Systematic review and meta-analysis of circulatory disease from exposure to low-level ionizing radiation and estimates of potential population mortality risks. Environ Health Perspect 2012 120; 1503–1511. doi: 10.1289/ehp.1204982 PMID: 22728254
2. Armstrong GT, Liu Q, Yasui Y, Neglia JP, Leisenring W, Robison LL, et al. Late mortality among 5-year survivors of childhood cancer: a summary from the Childhood Cancer Survivor Study. J Clin Oncol 2009 27; 2328–2338. doi: 10.1200/JCO.2008.21.1425 PMID: 19332714
3. Williams PM, Fletcher S. Health effects of prenatal radiation exposure. Am Fam Physician 2010 82; 488–493. PMID: 20822083
4. Fattibene P, Mazzei F, Nuccetelli C, Risica S. Prenatal exposure to ionizing radiation: sources, effects and regulatory aspects. Acta Paediatr 1999 88; 693–702. PMID: 10447122
5. Otake M, Schull WJ, Yoshimaru H. A review of forty-five years study of Hiroshima and Nagasaki atomic bomb survivors. Brain damage among the prenatally exposed. J Radiat Res 1991 32 Suppl; 249–264. PMID: 1762113
6. Tatsukawa Y, Nakashima E, Yamada M, Funamoto S, Hida A, Akahoshi M, et al. Cardiovascular disease risk among atomic bomb survivors exposed in utero, 1978–2003. Radiat Res 2008 170; 269–274. doi: 10.1667/RR1434.1 PMID: 18763869
7. Wessels A, Sedmera D. Developmental anatomy of the heart: a tale of mice and man. Physiol Genomics 2003 15; 165–176. PMID: 14612588
8. Rose BA, Force T, Wang Y. Mitogen-activated protein kinase signaling in the heart: angels versus demons in a heart-breaking tale. Physiol Rev 2010 90; 1507–1546. doi: 10.1152/physrev.00054.2009 PMID: 20959622
9. Raddatz E, Gardier S, Sarre A. Physiopathology of the embryonic heart (with special emphasis on hypoxia and reoxygenation). Ann Cardiol Angeiol (Paris) 2006 55; 79–89.
10. Chapple SJ, Puszyk WM, Mann GE. Keap1-Nrf2 regulated redox signaling in utero: Priming of disease susceptibility in offspring. Free Radic Biol Med 2015.
11. Azizova TV, Muirhead CR, Druzhinina MB, Grigoryeva ES, Vlasenko EV, Sumina MV, et al. Cardiovascular diseases in the cohort of workers first employed at Mayak PA in 1948–1958. Radiat Res 2010 174; 155–168. doi: 10.1667/RR1789.1 PMID: 20681782
12. Bradford MM. A rapid and sensitive method for the quantitation of microgram quantities of protein utilizing the principle of protein-dye binding. Anal Biochem 1976 72; 248–254. PMID: 942051
13. Yentrapalli R, Azimzadeh O, Barjaktarovic Z, Sarioglu H, Wojcik A, Harms-Ringdahl M, et al. Quantitative proteomic analysis reveals induction of premature senescence in human umbilical vein endothelial cells exposed to chronic low-dose rate gamma radiation. Proteomics 2013 13; 1096–1107. doi: 10.1002/pmic.201200463 PMID: 23349028
14. Laemmli UK. Cleavage of structural proteins during the assembly of the head of bacteriophage T4. Nature 1970 227; 680–685. PMID: 5432063
15. Bakshi MV, Azimzadeh O, Barjaktarovic Z, Kempf SJ, Merl-Pham J, Hauck SM, et al. Total body exposure to low-dose ionizing radiation induces long-term alterations to the liver proteome of neonatally exposed mice. J Proteome Res 2015 14; 366–373. doi: 10.1021/pr500890n PMID: 25299163
16. Hauck SM, Dietter J, Kramer RL, Hofmaier F, Zipplies JK, Amann B, et al. Deciphering membrane-associated molecular processes in target tissue of autoimmune uveitis by label-free quantitative mass spectrometry. Mol Cell Proteomics 2010 9; 2292–2305. doi: 10.1074/mcp.M110.001073 PMID: 20601722
17. Kempf SJ, Casciati A, Buratovic S, Janik D, von Toerne C, Ueffing M, et al. The cognitive defects of neonatally irradiated mice are accompanied by changed synaptic plasticity, adult neurogenesis and neuroinflammation. Mol Neurodegener 2014 9; 57. doi: 10.1186/1750-1326-9-57 PMID: 25515237
18. Sarioglu H, Brandner S, Jacobsen C, Meindl T, Schmidt A, Kellermann J, et al. Quantitative analysis of 2,3,7,8-tetrachlorodibenzo-p-dioxin-induced proteome alterations in 5L rat hepatoma cells using isotope-coded protein labels. Proteomics 2006 6; 2407–2421. PMID: 16548065
19. Mayburd AL, Martlinez A, Sackett D, Liu H, Shih J, Tauler J, et al. Ingenuity network-assisted transcription profiling: Identification of a new pharmacologic mechanism for MK886. Clin Cancer Res 2006 12; 1820–1827. PMID: 16551867
20. Szklarczyk D, Franceschini A, Wyder S, Forslund K, Heller D, Huerta-Cepas J, et al. STRING v10: protein-protein interaction networks, integrated over the tree of life. Nucleic Acids Res 2015 43; D447–452. doi: 10.1093/nar/gku1003 PMID: 25352553

21. Bakshi MV, Barjaktarovic Z, Azimzadeh O, Kempf SJ, Merl J, Hauck SM, et al. Long-term effects of acute low-dose ionizing radiation on the neonatal mouse heart: a proteomic study. Radiat Environ Biophys 2013 52; 451–461. doi: 10.1007/s00411-013-0483-8 PMID: 23880982
22. Assinder SJ, Stanton JA, Prasad PD. Transgelin: an actin-binding protein and tumour suppressor. Int J Biochem Cell Biol 2009 41; 482–486. doi: 10.1016/j.biocel.2008.02.011 PMID: 18378184
23. ICRP. Pregnancy and medical radiation. Ann ICRP 2000 30; iii–viii, 1–43. PMID: 11108925
24. ACOG. ACOG Committee Opinion. Number 299, September 2004 (replaces No. 158, September 1995). Guidelines for diagnostic imaging during pregnancy. Obstet Gynecol 2004 104; 647–651. PMID: 15339791
25. Beutner G, Eliseev RA, Porter GA Jr. Initiation of electron transport chain activity in the embryonic heart coincides with the activation of mitochondrial complex 1 and the formation of supercomplexes. PLoS One 2014 9; e113330. doi: 10.1371/journal.pone.0113330 PMID: 25427064
26. Barjaktarovic Z, Schmaltz D, Shyla A, Azimzadeh O, Schulz S, Haagen J, et al. Radiation-induced signaling results in mitochondrial impairment in mouse heart at 4 weeks after exposure to X-rays. PLoS One 2011 6; e27811. doi: 10.1371/journal.pone.0027811 PMID: 22174747
27. Barjaktarovic Z, Shyla A, Azimzadeh O, Schulz S, Haagen J, Dorr W, et al. Ionising radiation induces persistent alterations in the cardiac mitochondrial function of C57BL/6 mice 40 weeks after local heart exposure. Radiother Oncol 2013 106; 404–410. doi: 10.1016/j.radonc.2013.01.017 PMID: 23522698
28. Zhou Y, Kok KH, Chun AC, Wong CM, Wu HW, Lin MC, et al. Mouse peroxiredoxin V is a thioredoxin peroxidase that inhibits p53-induced apoptosis. Biochem Biophys Res Commun 2000 268; 921–927. PMID: 10679306
29. Banmeyer I, Marchand C, Clippe A, Knoops B. Human mitochondrial peroxiredoxin 5 protects from mitochondrial DNA damages induced by hydrogen peroxide. FEBS Lett 2005 579; 2327–2333. PMID: 15848167
30. Li N, Brun T, Cnop M, Cunha DA, Eizirik DL, Maechler P. Transient oxidative stress damages mitochondrial machinery inducing persistent beta-cell dysfunction. J Biol Chem 2009 284; 23602–23612. doi: 10.1074/jbc.M109.024323 PMID: 19546218
31. Fan GC, Chu G, Mitton B, Song Q, Yuan Q, Kranias EG. Small heat-shock protein Hsp20 phosphorylation inhibits beta-agonist-induced cardiac apoptosis. Circ Res 2004 94; 1474–1482. PMID: 15105294
32. Fan GC, Ren X, Qian J, Yuan Q, Nicolaou P, Wang Y, et al. Novel cardioprotective role of a small heat-shock protein, Hsp20, against ischemia/reperfusion injury. Circulation 2005 111; 1792–1799. PMID: 15809372
33. Qian J, Vafiadaki E, Florea SM, Singh VP, Song W, Lam CK, et al. Small heat shock protein 20 interacts with protein phosphatase-1 and enhances sarcoplasmic reticulum calcium cycling. Circ Res 2011 108; 1429–1438. doi: 10.1161/CIRCRESAHA.110.237644 PMID: 21493896
34. Faulkner G, Pallavicini A, Formentin E, Comelli A, Ievolella C, Trevisan S, et al. ZASP: a new Z-band alternatively spliced PDZ-motif protein. J Cell Biol 1999 146; 465–475. PMID: 10427098
35. Li Z, Ai T, Samani K, Xi Y, Tzeng HP, Xie M, et al. A ZASP missense mutation, S196L, leads to cytoskeletal and electrical abnormalities in a mouse model of cardiomyopathy. Circ Arrhythm Electrophysiol 2010 3; 646–656. doi: 10.1161/CIRCEP.109.929240 PMID: 20852297
36. Vatta M, Mohapatra B, Jimenez S, Sanchez X, Faulkner G, Perles Z, et al. Mutations in Cypher/ZASP in patients with dilated cardiomyopathy and left ventricular non-compaction. J Am Coll Cardiol 2003 42; 2014–2027. PMID: 14662268
37. van Eldik W, Beqqali A, Monshouwer-Kloots J, Mummery C, Passier R. Cytoskeletal heart-enriched actin-associated protein (CHAP) is expressed in striated and smooth muscle cells in chick and mouse during embryonic and adult stages. Int J Dev Biol 2011 55; 649–655. doi: 10.1387/ijdb.103207wv PMID: 21948713
38. Beqqali A, Monshouwer-Kloots J, Monteiro R, Welling M, Bakkers J, Ehler E, et al. CHAP is a newly identified Z-disc protein essential for heart and skeletal muscle function. J Cell Sci 2010 123; 1141–1150. doi: 10.1242/jcs.063859 PMID: 20215401
39. Heit C, Jackson BC, McAndrews M, Wright MW, Thompson DC, Silverman GA, et al. Update of the human and mouse SERPIN gene superfamily. Hum Genomics 2013 7; 22. doi: 10.1186/1479-7364-7-22 PMID: 24172014
40. Wang D, Wang W, Dawkins P, Paterson T, Kalsheker N, Sallenave JM, et al. Deletion of Serpina1a, a murine alpha1-antitrypsin ortholog, results in embryonic lethality. Exp Lung Res 2011 37; 291–300. doi: 10.3109/01902148.2011.554599 PMID: 21574874
41. Talmud PJ, Martin S, Steiner G, Flavell DM, Whitehouse DB, Nagl S, et al. Progression of atherosclerosis is associated with variation in the alpha1-antitrypsin gene. Arterioscler Thromb Vasc Biol 2003 23; 644–649. PMID: 12692006

42. Borisov AB, Kontrogianni-Konstantopoulos A, Bloch RJ, Westfall MV, Russell MW. Dynamics of obscurin localization during differentiation and remodeling of cardiac myocytes: obscurin as an integrator of myofibrillar structure. J Histochem Cytochem 2004 52; 1117–1127. PMID: 15314079

43. Makarenko I, Opitz CA, Leake MC, Neagoe C, Kulke M, Gwathmey JK, et al. Passive stiffness changes caused by upregulation of compliant titin isoforms in human dilated cardiomyopathy hearts. Circ Res 2004 95; 708–716. PMID: 15345656

44. Arimura T, Matsumoto Y, Okazaki O, Hayashi T, Takahashi M, Inagaki N, et al. Structural analysis of obscurin gene in hypertrophic cardiomyopathy. Biochem Biophys Res Commun 2007 362; 281–287. PMID: 17716621

45. Mahley RW. Apolipoprotein E: cholesterol transport protein with expanding role in cell biology. Science 1988 240; 622–630. PMID: 3283935

46. Nakashima Y, Plump AS, Raines EW, Breslow JL, Ross R. ApoE-deficient mice develop lesions of all phases of atherosclerosis throughout the arterial tree. Arterioscler Thromb 1994 14; 133–140. PMID: 8274468

47. Stewart FA, Heeneman S, Te Poele J, Kruse J, Russell NS, Gijbels M, et al. Ionizing radiation accelerates the development of atherosclerotic lesions in ApoE-/- mice and predisposes to an inflammatory plaque phenotype prone to hemorrhage. Am J Pathol 2006 168; 649–658. PMID: 16436678

48. Dan I, Watanabe NM, Kusumi A. The Ste20 group kinases as regulators of MAP kinase cascades. Trends Cell Biol 2001 11; 220–230. PMID: 11316611

49. Zhang SX, Garcia-Gras E, Wycuff DR, Marriot SJ, Kadeer N, Yu W, et al. Identification of direct serum-response factor gene targets during Me2SO-induced P19 cardiac cell differentiation. J Biol Chem 2005 280; 19115–19126. PMID: 15699019

50. Fuller SJ, Osborne SA, Leonard SJ, Hardyman MA, Vaniotis G, Allen BG, et al. Cardiac protein kinases: the cardiomyocyte kinome and differential kinase expression in human failing hearts. Cardiovasc Res 2015 108; 87–98. doi: 10.1093/cvr/cvv210 PMID: 26260799

51. Aouadi M, Tesz GJ, Nicoloro SM, Wang M, Chouinard M, Soto E, et al. Orally delivered siRNA targeting macrophage Map4k4 suppresses systemic inflammation. Nature 2009 458; 1180–1184. doi: 10.1038/nature07774 PMID: 19407801

52. Kempf SJ, Sepe S, von Toerne C, Janik D, Neff F, Hauck SM, et al. Neonatal Irradiation Leads to Persistent Proteome Alterations Involved in Synaptic Plasticity in the Mouse Hippocampus and Cortex. J Proteome Res 2015.

2.2 Long-term effects of acute low-dose ionizing radiation on the neonatal mouse heart: a proteomic study

2.2.1 Aim and summary

Infants and children are more susceptible for radiation-induced cardiovascular disease (CVD). The biological changes behind the increased risk for CVD after low-dose exposure in the early developmental phase are unknown. So far, long-term effects of low-dose ionizing radiation on neonates were not studied by global proteome profiling.

The aim of this study was to investigate the long-term alterations on the proteome level after exposure to total body low-dose ionizing radiation at neonatal stage. Neonatal mice were irradiated on postnatal day 10 with whole body ^{60}Co gamma-irradiation, with doses ranging from 0.02 Gy to1.0 Gy. The mice were sacrificed at 7 months of age and hearts were isolated. Global quantitative proteomic study was performed using ICPL (duplex) labeling and LC-MS/MS analysis. We identified 32, 31, 66, and 34 significantly deregulated proteins after doses of 0.02, 0.1, 0.5, and 1.0 Gy, respectively. The four doses shared 9 deregulated proteins, belonging to inflammatory response, antioxidant activity and cytoskeletal protein categories. The transcription factor peroxisome proliferator-activated receptor alpha (PPARA) was predicted to be a common upstream regulator of several deregulated proteins. The phosphorylation level of PPARA was found to be significantly reduced from the dose of 0.1 Gy onwards, correlating with its altered activity.

This study indicates that both adaptive and maladaptive responses to the initial radiation insult occur, leading to persistent damage. It will contribute to the understanding of the long-term consequences of radiation-induced injury and developmental alterations in the neonatal heart.

2.2.2 Contribution

This study is the first and essential work to test the main hypothesis of this thesis concerning the role of age at exposure. This study was performed with the help of Sonja Buratovic (University of Uppsala) and Dr. Juliane Merl-Pham. Dr. Sonja Buratovic irradiated the mice and Dr. Merl-Pham performed the LC-MS/MS run. The heart proteome isolation ICPL labeling and data analysis was my major contribution. All the immunoblotting

experiments for cytoskeletal protein as well as the experiment concerning phosphorylation of PPARA were done by me. The figures and tables and the text for the publication was created by me with guidance from PD Dr. Soile Tapio and Prof. Dr. Michael J. Atkinson. The co-authors Dr. Omid Azimzadeh, Dr. Stefanie M Hauck and Prof. Per Eriksson helped in the scientific discussion.

2.2.3 Publication

The following paper was published as an original manuscript in 2013 in Radiation Environmental Biophysics

Long-term effects of acute low-dose ionizing radiation on the neonatal mouse heart: a proteomic study

Mayur V. Bakshi, Zarko Barjaktarovic, Omid Azimzadeh, Stefan J. Kempf, Juliane Merl, Stefanie M. Hauck, Per Eriksson, Sonja Buratovic, Michael J. Atkinson, Soile Tapio

Radiat Environ Biophys 52(4): 451-461.

DOI 10.1007/S00411-013-0483-8

Radiat Environ Biophys (2013) 52:451–461
DOI 10.1007/s00411-013-0483-8

ORIGINAL PAPER

Long-term effects of acute low-dose ionizing radiation on the neonatal mouse heart: a proteomic study

Mayur V. Bakshi · Zarko Barjaktarovic · Omid Azimzadeh · Stefan J. Kempf · Juliane Merl · Stefanie M. Hauck · Per Eriksson · Sonja Buratovic · Michael J. Atkinson · Soile Tapio

Received: 6 March 2013 / Accepted: 11 July 2013 / Published online: 24 July 2013

Abstract Epidemiological studies establish that children and young adults are especially susceptible to radiation-induced cardiovascular disease (CVD). The biological mechanisms behind the elevated CVD risk following exposure at young age remain unknown. The present study aims to elucidate the long-term effects of ionizing radiation by studying the murine cardiac proteome after exposure to low and moderate radiation doses. NMRI mice received single doses of total body ^{60}Co gamma-irradiation on postnatal day 10 and were sacrificed 7 months later. Changes in cardiac protein expression were quantified using isotope-coded protein label and tandem mass spectrometry. We identified 32, 31, 66, and 34 significantly deregulated proteins after doses of 0.02, 0.1, 0.5, and 1.0 Gy, respectively. The four doses shared 9 deregulated proteins. Bioinformatics analysis showed that most of the deregulated proteins belonged to a limited set of biological categories, including metabolic processes, inflammatory response, and cytoskeletal structure. The transcription factor peroxisome proliferator-activated receptor alpha was predicted as a common upstream regulator of several deregulated proteins. This study indicates that both adaptive and maladaptive responses to the initial radiation damage persist well into adulthood. It will contribute to the understanding of the long-term consequences of radiation-induced injury and developmental alterations in the neonatal heart.

Keywords Low-dose ionizing radiation · Acute exposure · Total body irradiation · Cardiac effects · Fibrinogen · PPAR alpha · Proteomics · ICPL

Abbreviations

Gy	Gray
IPA	Ingenuity Pathway Analysis
CVD	Cardiovascular disease
H/L	Heavy to light ratio
ICPL	Isotope-coded protein label
LC–MS	Liquid chromatography mass spectrometry
PND	Postnatal day
TBI	Total body irradiation
PPAR	Peroxisome proliferator-activated receptor

Introduction

Epidemiological studies of A-bomb survivors from Hiroshima and Nagasaki provide evidence for the development of an increased risk of cardiovascular disease (CVD) many decades after the radiation exposure

Electronic supplementary material The online version of this article (doi:10.1007/s00411-013-0483-8) contains supplementary material, which is available to authorized users.

M. V. Bakshi · Z. Barjaktarovic · O. Azimzadeh · S. J. Kempf · M. J. Atkinson · S. Tapio (✉)
Institute of Radiation Biology, German Research Center for Environmental Health, Helmholtz Zentrum München, Neuherberg, Germany
e-mail: soile.tapio@helmholtz-muenchen.de

J. Merl · S. M. Hauck
Research Unit Protein Science, German Research Center for Environmental Health, Helmholtz Zentrum München, Neuherberg, Germany

P. Eriksson · S. Buratovic
Department of Environmental Toxicology, Uppsala University, Uppsala, Sweden

M. J. Atkinson
Department of Radiation Oncology, Klinikum Recht der Isar, Technical University of Munich, Munich, Germany

(Preston et al. 2003). Even relatively low radiation doses (0.5 Gy) may elevate the risk of late CVD in this cohort, especially if the age at exposure was below 40 years (Shimizu et al. 2010). Survivors of childhood cancer who have received radiation therapy are also highly susceptible to increased risk CVD later in life (Aleman et al. 2003; Armstrong et al. 2009; Tukenova et al. 2010; Shankar et al. 2008). The underlying biological mechanisms responsible for elevated CVD risk at young age after ionizing radiation are unknown.

The A-bomb and cancer survivor cohorts represent quite different types of exposures in terms of both the applied dose (acute vs. fractionated over many weeks) and the anatomical location. The medical cohorts received multiple fractions of local irradiation, while the A-bomb survivors were exposed to an acute total body irradiation (TBI). Cardiac effects after equivalent exposures differ as TBI may affect the heart both directly and indirectly through damage to other organs such as lung (Ghobadi et al. 2012) and kidneys (Moulder et al. 2004). Nevertheless, these studies consistently show that age at exposure is an important parameter influencing the risk of CVD later in life. In addition to biological factors, this may be due to the fact that cardiovascular effects have more time to develop in those exposed at young age than in adults.

A comparison of the long-term cardiovascular damage after TBI and local thorax irradiation was made in young 5-week-old rats, following changes in heart function and coronary vessel morphology after a single dose of 10 Gy (Baker et al. 2009). TBI, but not an equivalent local thorax dose, impaired cardiac function, indicated by a decreased strain pattern after 240 days. Similar damage had previously been observed after local thorax irradiation, but after the application of considerably higher doses (20–70 Gy) (Lauk 1986; Yeung et al. 1989).

We have previously studied the early changes in cardiac proteome of C57BL/6 mice after exposure to acute TBI with a gamma dose of 3 Gy (Azimzadeh et al. 2011). Significant biological responses observed within the first 24 h included inflammation, antioxidative defense, and reorganization of structural proteins. Mitochondrial proteins represented the protein class most sensitive to ionizing radiation (Azimzadeh et al. 2011, 2012). In numerous biochemical and functional studies of cardiomyocytes and heart tissue, impairment of mitochondrial function has been directly linked to the development of CVD and radiation (Takano et al. 2003; Dhalla et al. 2000; Ballinger 2005; Misra et al. 2009; Barjaktarovic et al. 2011, 2013).

The aim of the present study was to investigate the long-term cardiac effects following low-dose total body irradiation of developing neonatal mice hearts. For this purpose, we used the outbred NMRI mice strain to study the effects of ionizing radiation on the neonatal heart as this strain has a degree of genetic variance similar to what would be expected in the human population. The mice were exposed to TBI on postnatal day 10 (PND 10) using doses ranging from 0.02 to 1.0 Gy. The cardiac tissue proteome changes were analyzed 7 months postirradiation using isotope-coded protein labeling (ICPL) and tandem mass spectrometry (LC–MS/MS).

Experimental procedures

Mouse total body irradiation (TBI)

Mice were bred and irradiated at the Svedberg Laboratory, Uppsala University, in accordance with the guidelines of Swedish Committee for Ethical Experiments on Laboratory Animals (approval number C 347/10). NMRI male mice were exposed to a single acute dose of TBI at PND 10 using a ^{60}Co gamma radiation source (dose rate 0.023 Gy/min) delivering doses of 0.02, 0.1, 0.5, and 1.0 Gy. Control mice were sham-irradiated. The radiation exposure did not cause any additional stress to the mice. An ionization chamber (Markus chamber type 23343.PTW-Freiburg) was used to validate the radiation exposure. After arrival in Germany at the age of 5 months, the mice received a routine treatment for intestinal parasites with Ivomac (Merial, 0.03 mg/mouse) (Baumans et al. 1988). Animals were sacrificed at the age of 7 months when they were fully grown but not yet aged, via cervical dislocation. Hearts were excised, thoroughly rinsed in PBS to remove excessive blood, snap-frozen, and stored at −80 °C until required.

Isolation and extraction of whole heart proteome

Whole frozen hearts were powdered in liquid nitrogen using a cooled mortar and pestle. The tissue powder was re-suspended in ICPL lysis buffer containing guanidine hydrochloride (SERVA) with protease and phosphatase inhibitor cocktails following the manufacturer's instructions (Roche Diagnostics). The supernatants were stored at −20 °C until analysis.

Proteomic analysis

Protein quantification and labeling

The protein concentration in the tissue lysates was determined by Bradford assay following the manufacturer's instructions (Thermo Fisher) (Bradford 1976).

The ICPL labeling was done as previously reported (Sarioglu et al. 2006; Azimzadeh et al. 2011, Sarioglu et al. 2006). Briefly, three biological replicates containing

100 μg of protein were prepared from both control and irradiated cardiac tissue and labeled with ICPL reagents (SERVA) following the manufacturer's instructions. ICPL-0 was used for control tissue and ICPL-6 for irradiated tissue. A bovine serum albumin standard with a defined ratio (1:1) of heavy and light ICPL labels was used as an internal standard for quantification. The heavy and light labeled replicates were combined prior to separation using 12 % SDS gel electrophoresis before staining with colloidal Coomassie solution.

LC–ESI–MS/MS analysis

After Coomassie blue staining, each SDS gel lane was cut into two and subjected to in-gel digestion with trypsin (Sigma Aldrich) as described previously (Merl et al. 2012). The digested peptides were separated by nano-HPLC and mass spectroscopic analysis performed with an LTQ Orbitrap XL mass spectrometer (Thermo Scientific) as described (Hauck et al. 2010). Up to ten of the most intense ions were selected for fragmentation in the linear ion trap, and target peptides already selected for MS/MS were dynamically excluded for 60 s.

The MS/MS spectra were searched against the Ensembl mouse database (Version: 2.4, 56 416 sequences) using the Mascot search engine (version 2.3.02; Matrix Science) with the following parameters: a precursor mass error tolerance of 10 ppm and a fragment tolerance of 0.6 D. One missed cleavage was allowed. Carbamidomethylation was set as the fixed modification. Oxidized methionine and ICPL-0 and ICPL-6 for lysine residues and N-termini of peptides were set as the variable modifications.

Data processing for the identification and quantitation of ICPL-duplex labeled proteins was performed using Proteome Discoverer version 1.3.0.339 (Thermo Scientific). The MASCOT Percolator algorithm was used for discriminating between correct and incorrect spectrum identifications (Brosch et al. 2009) with a maximum q value of 0.01. The proteins identified by at least two unique peptides in two out of three biological replicates and quantified by the H/L variability of less than 30 % were considered for further evaluation. Proteins identified with a single peptide were manually scrutinized and regarded as unequivocally identified if they fulfilled the following four criteria: (1) they had fragmentation spectra with a long, nearly complete y- and/or b-series; (2) all lysines were modified; (3) the numbers of lysines predicted from the mass difference of the labeled pair had to match the number of lysines in the given sequence from the search query, and (4) at least one mass of a modified lysine was included in the detected partial fragment series (Sarioglu et al. 2006). Proteins with ratios of H/L label greater than 1.30-fold or less than 0.769-fold ($p < 0.05$; Perseus statistical tool) were defined as being significantly differentially expressed. The significance of the fold-change was determined by technical variability based on the average values of the coefficient of variation (CV) of a spiked standard protein mixture. The average %CV obtained for H/L ratio of spiked protein was 18 % for bovine serum albumin (Supplementary Table S1) in all MS/MS runs. The biological significance of this fold-change cutoff is in good agreement with previously published data (Sarioglu et al. 2006; Papaioannou et al. 2011).

Pathway and functional correlation analysis

Gene Ontology (GO) analysis

Differentially expressed proteins in all samples were categorized using the protein analysis through evolutionary relationships (PANTHER), bioinformatics tool (http://www.pantherdb.org) (Thomas et al. 2006) for Gene Ontology (GO) category "biological processes".

Protein–protein interaction and signaling network

The analyses of protein–protein interaction and signaling networks were performed by the two bioinformatics tools: Ingenuity Pathway Analysis (IPA) (INGENUITY System. http://www.ingenuity.com) (Mayburd et al. 2006) and STRING protein database (http://string-db.org/) (Szklarczyk et al. 2011). The protein accession numbers including the relative expression values (fold-change) of each deregulated protein were uploaded to IPA and STRING to investigate interactions between these proteins.

Immunoblotting analysis

Immunoblotting of protein extracts from control and irradiated tissues was used to validate the proteomic data. Proteins were separated by 1-D gel electrophoresis and transferred to nitrocellulose membranes (GE Healthcare) using a TE 77 semidry blotting system (GE Healthcare) at 0.8 mA/cm for 1 h. Membranes were saturated for 1 h with 8 % advance blocking reagent (GE Healthcare) in TBS (50 mM Tris–HCl, pH 7.6 and 150 mM NaCl) containing 0.1 % Tween 20 (TBS/T). Blots were incubated overnight at 4 °C with antibodies against phospho-PPAR alpha (Ser-12) (Abcam), anti-heavy chain cardiac myosin antibody (Abcam), and anti-desmin antibody (Abcam).

After washing three times in TBS/T, blots were incubated for 1 h at room temperature with horseradish peroxidise-conjugated anti-mouse or anti-rabbit secondary antibody (Santa Cruz Biotechnology) in blocking buffer (TBS/T with 5 % w/v advance blocking reagent). Immunodetection was performed with ECL advance Western blotting detection kit (GE Healthcare). The protein bands

were quantified using ImageQuant 5.2 software (GE Healthcare) by integration of all pixel values in the band area after background correction. ATP synthase ß (Abcam) was used for normalization as our proteomic data showed no deregulation of this protein.

Statistical analysis

Statistical analysis was performed using Graph Pad Prism (release 4) and Perseus software (http://maxquant.org/). Immunoblotting results were evaluated using non-paired Student′s t test. Data are presented as mean ± standard deviation (SD). A p value of less than 0.05 was considered to denote statistical significance. Three biological replicates were used for all experiments.

Results

The aim of this study was to analyze the long-term effects of low and moderate radiation exposures on the proteome of the developing murine heart. As a model, we used the outbred NMRI mouse strain exposed to TBI early in life (PND10) and analyzed changes in protein expression 7 months later.

Proteomic analysis

The cardiac tissue of the irradiated mice showed alterations in the heart proteome compared with control animals, even after the lowest dose (0.02 Gy) used. The numbers of identified proteins were 856, 778, 753, and 725 after radiation doses of 0.02, 0.1, 0.5, and 1.0 Gy, respectively. The numbers of quantified proteins in these exposed groups were 546, 498, 507, and 489, respectively.

Out of all quantified proteins, 32 (0.02 Gy), 31 (0.1 Gy), 66 (0.5 Gy), and 34 (1.0 Gy) were significantly deregulated using the statistical criteria described before. All significantly deregulated proteins are listed in Supplementary Tables S2–S5. There was no relationship between dose and the number of deregulated proteins, the dose of 0.5 Gy showing more deregulated proteins than other doses.

Nine proteins were found to be significantly deregulated at all radiation doses (Table 1). These represented structural proteins such as actin and myosin and inflammatory proteins such as fibrinogens (alpha, beta and gamma). Two isoforms of carbonic anhydrase that function as free radical scavengers were also commonly down-deregulated. In addition, the ribosomal protein L19 was up-regulated at all doses (Table 1).

A number of the deregulated proteins were shared between different doses, and these are illustrated in Fig. 1. Twelve proteins were shared between the two lowest doses of 0.02 and 0.1 Gy (Table S2), including hemopexin (down-regulated) and cyclooxygenase-2 (up-regulated). Sixteen proteins were overlapping between the highest two doses of 0.5 and 1.0 Gy (Table S5), containing proteins involved in lipid metabolism, such as phytanoyl-CoA dioxygenase (PHYHD1) and apolipoprotein A-I (APOA1).

Bioinformatics analysis

Gene Ontology studies

"Metabolic processes", "cellular processes," and "transport" were the major categories of biological processes that were affected (Fig. 2). In the category "metabolic

Table 1 Shared significantly deregulated proteins between all radiation doses

Ensembl gene ID	Gene name	Protein	Fold changes in the different doses				Biological functions
			0.02 Gy	0.1 Gy	0.5 Gy	1.0 Gy	
ENSMUSP00000103181	RPL19	Ribosomal protein L19	1.648	1.426	3.124	2.868	Protein synthesis
ENSMUSP00000029630	FGA	Alpha fibrinogen	0.646	0.579	0.597	0.496	Blood clotting and inflammatory responses
ENSMUSP00000039472	FGB	Beta fibrinogen	0.727	0.628	0.634	0.417	Blood clotting and inflammatory responses
ENSMUSP00000037018	FGG	Gamma fibrinogen	0.655	0.763	0.593	0.497	Blood clotting and inflammatory responses
ENSMUSP00000091925	CAR1	Carbonic anhydrase 1	0.493	0.405	0.532	0.463	Antioxidative response
ENSMUSP00000029078	CAR2	Carbonic anhydrase 2	0.575	0.468	0.568	0.582	Antioxidative response
ENSMUSP00000030187	TLN1	Talin 1	0.404	0.327	0.388	0.405	Structural constituent of cytoskeleton
ENSMUSP00000099867	MYH7	Myosin 7, heavy chain	1.853	0.337	0.176	0.537	Structural constituent of cytoskeleton
ENSMUSP00000071486	ACTG1	Gamma actin	0.680	0.644	0.585	0.544	Structural constituent of cytoskeleton

processes," the primary metabolic processes (lipid, protein, and carbohydrate metabolism) were those mostly affected by radiation. Lipid transport was significantly changed, as indicated by the deregulation of the ApoA class of proteins. The biological process "cellular compartment organization" revealed substantial down-regulation of structural proteins such as actin, talin, myosin, and desmin.

Protein–protein interaction and signaling network analysis

IPA of networking and protein–protein interactions revealed that "cell-to-cell signaling" and "cellular interaction" were the most common molecular and cellular functions affected at all doses (Tables S2–S5).

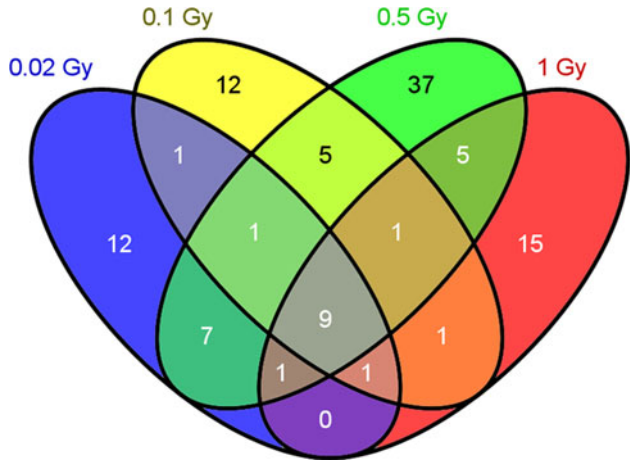

Fig. 1 Venn diagram showing the number of shared proteins affected in all irradiated samples

Interestingly, the transcription factor peroxisome proliferator-activated receptor alpha (PPAR alpha) was predicted to be a mediator of the observed protein changes, quite independent of the radiation dose applied (Fig. 3). PPAR alpha targets that show down-regulation were the apolipoproteins (APOA1, APOA4) and the fibrinogens (FGA, FGB, FGG), while the mitochondrial complex IV subunit COX2 was showing up-regulation.

At the dose of 0.5 Gy, the networking of these proteins was additionally analyzed using the STRING software tool. Three radiation-induced clusters of proteins became apparent representing amino acid and fatty acid metabolism, inflammatory responses, and structural proteins (Fig. 4).

Taken together, GO, IPA, and STRING analyses suggested an alteration in lipid metabolism with a possible role of PPAR alpha as a central regulator after radiation.

Immunoblotting analysis

In agreement with the predicted activation of PPAR-alpha-dependent pathways, the phosphorylation status of cardiac tissue revealed a significant decrease in the serine-12 phosphorylated form of PPAR alpha at the doses of 0.1, 0.5, and 1 Gy, while the lowest dose of 0.02 Gy showed no significant change (Fig. 5, Fig S1, Fig S2). As phosphorylation of PPAR alpha leads to its deactivation (Burns and Vanden Heuvel 2007), this result is consistent with an increased transcription of PPAR alpha targets. No change was observed in the level of total PPAR alpha (Figure S2).

Two structural proteins showing radiation-induced changes, myosin heavy chain and desmin, were also

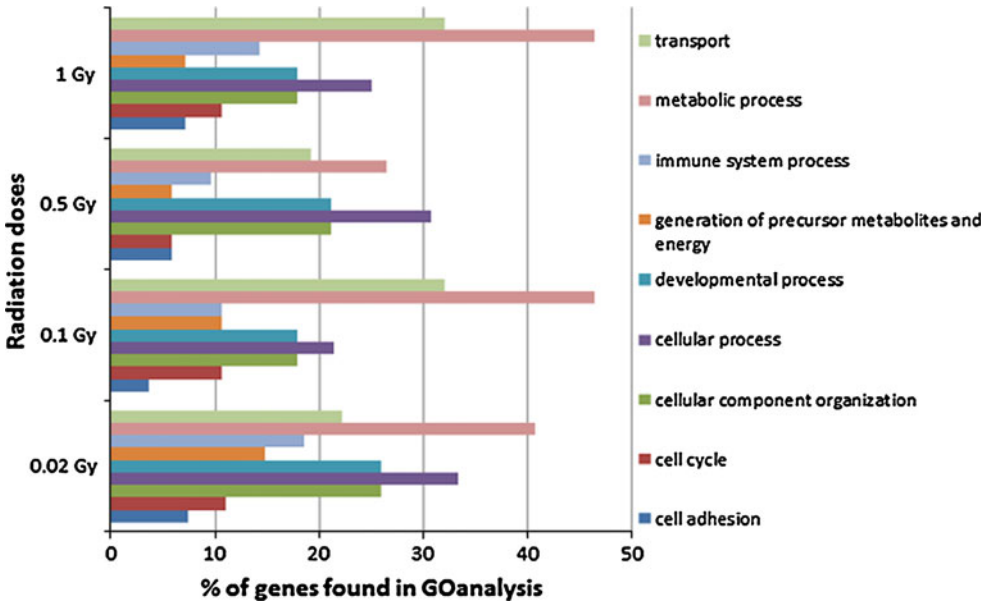

Fig. 2 Gene Ontology analysis of mice irradiated with different doses. Proteins are categorized according to the GO term "biological processes"

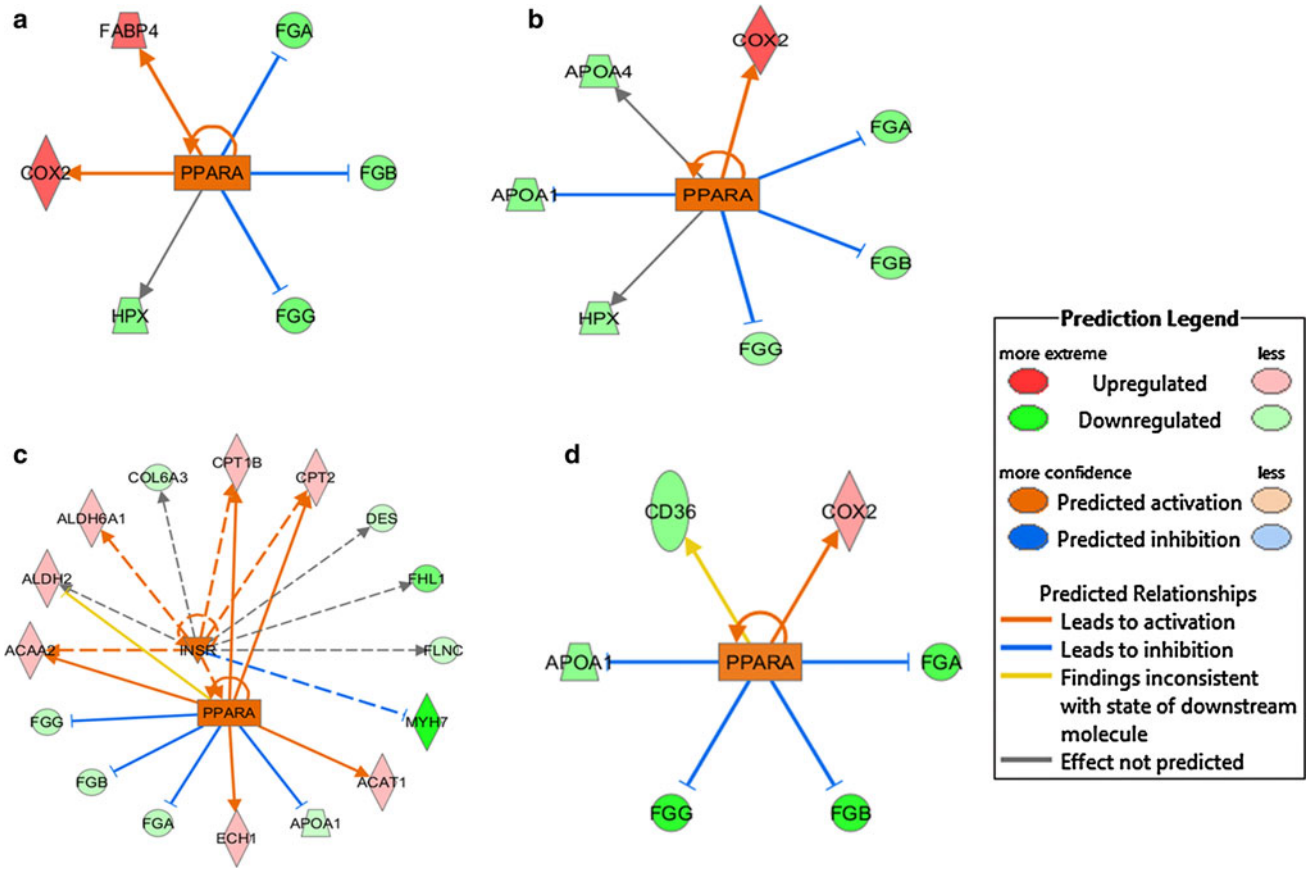

Fig. 3 Ingenuity Pathway Analysis networks showing transcriptional factor PPAR alpha as an upstream regulator. The networks corresponding to doses of 0.02 Gy (**a**), 0.1 Gy (**b**), 0.5 Gy (**c**), and 1.0 Gy (**d**) are shown. PPAR alpha is predicted activated in all networks. The proteins indicated in *red* are up-regulated and those indicated in *green* are down-regulated. Three biological replicates were used in all experiments. ACAA2, acetyl-Coenzyme A acyltransferase 2; ACAT1, acetyl-Coenzyme A acetyltransferase 1; ALDH2, aldehyde dehydrogenase mitochondrial precursor; ALDH6A1, aldehyde dehydrogenase family 6 subfamily A1; APOA1, apolipoprotein A-I; CD36, CD36 antigen; COL6A3, collagen type VI alpha 3; COX2, cytochrome c oxidase subunit 2; CPT1B, carnitine palmitoyltransferase 1b, muscle; CPT2, carnitine palmitoyltransferase 2; DES, desmin; ECH1, enoyl coenzyme A hydratase 1, peroxisomal; FABP4, fatty acid binding protein 4 adipocyte; FGA, fibrinogen alpha; FGB, fibrinogen beta; FGG, fibrinogen gamma; FHL1, four and a half LIM domains protein 1; FLNC, filamin C gamma; HPX, hemopexin; INSR, insulin receptor; MYH7, myosin heavy polypeptide 7; PPARA, peroxisome proliferator-activated receptor alpha (color figure online)

quantified by immunoblotting (Fig. S2). Both were found to be significantly down-regulated (Fig. 6), again consistent with our proteomics data.

Discussion

Epidemiological data suggest an increased radiation sensitivity of the cardiovascular system in children and young adults receiving radiation exposure to the heart, albeit with a very prolonged latency to appearance of CVD. The long-term follow-up of A-bomb survivors suggests that there is an excess risk even at the low doses that may be encountered from repeated medical procedures (Shimizu et al. 2010).

Our study now provides the first indications of the mechanisms underlying the long-term damage following a single low-dose exposure to ionizing radiation of the developing heart. The doses used here ranged from very low (0.02 Gy) to moderate (1.0 Gy), in order to provide an insight into the possible risk at low doses that may be received from realistic exposure scenarios.

Our results indicate that there were considerable changes in the cardiac proteome even at the lowest dose of 0.02 Gy. Furthermore, the functional spectra of the affected pathways were quite similar between the different doses (Fig. 2). More strikingly, several proteins commonly deregulated at all doses were potential downstream targets of a single transcriptional regulator, PPAR alpha (Fig. 3) (Azimzadeh et al. 2013). The levels of the phospho-PPAR alpha were significantly down-regulated at the higher doses of 0.1, 0.5, and 1 Gy. As phosphorylation of PPAR alpha leads to its deactivation (Burns and Vanden Heuvel 2007), this result is consistent with an increased transcription of PPAR alpha targets.

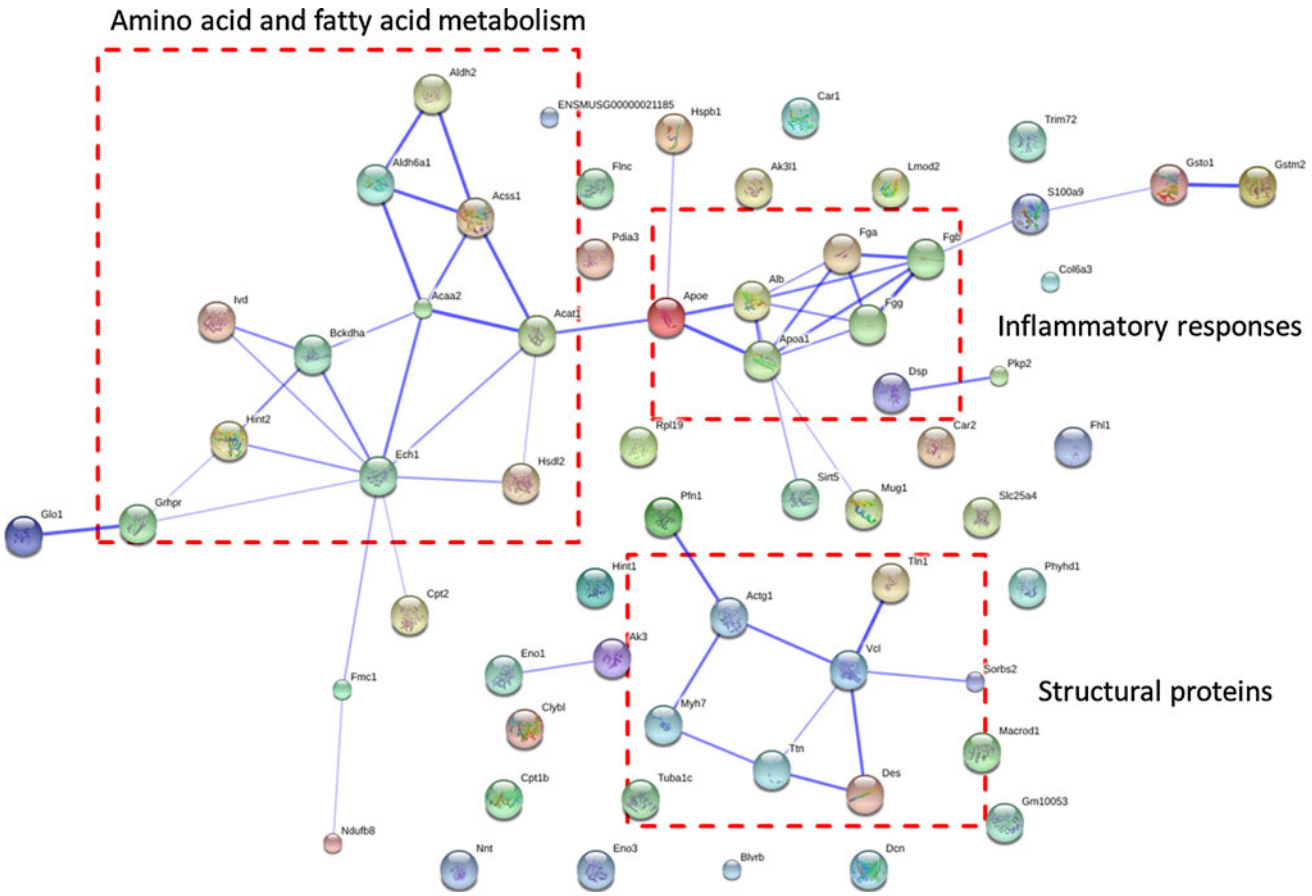

Fig. 4 STRING protein network showing different classes of proteins significantly deregulated at the dose of 0.5 Gy. Major proteins from the network clustered in the amino acid and lipid metabolism, inflammatory responses and cytoskeletal structure

PPAR alpha plays an important role during perinatal cardiac development, when the heart undergoes a switch in energy substrate preference from glucose in the fetal period to fatty acids following birth (Lehman and Kelly 2002). The postnatal activation of the mitochondrial energy production pathway involves the up-regulated expression of fatty acid oxidation enzymes, as well as other proteins important in mitochondrial energy transduction and production pathways (van der Lee et al. 2000). This postnatal transcriptional switch is regulated by the activation of PPAR alpha (Djouadi et al. 1999). This is consistent with our observation with mice irradiated at young age revealing radiation-induced up-regulation of enzymes involved in fatty acid metabolism (ECH1, ACAT1, CPT1B, ACAA2, CPT2) and of mitochondrial proteins (NDUFB8, ATP5J2, SLC25A4, COX2), as well as the decrease in phosphorylated PPAR alpha protein indicating an increased activity of PPAR alpha in cardiomyocytes (Barger et al. 2000). This may be a sign of adaptation in order to prohibit a developmental impairment of the heart.

PPAR alpha is activated in a complex manner by both ligand-dependent and ligand-independent mechanisms (Lazennec et al. 2000; Vanden Heuvel et al. 2003). Natural ligands of PPAR alpha include fatty acids and eicosanoids (Murakami et al. 1999), while ligand-independent activation is the result of cross talk between kinases and phosphatases (Burns and Vanden Heuvel 2007).

Later in life, PPAR alpha continues to regulate the expression of a large number of proteins involved in lipid and carbohydrate metabolism (van Raalte et al. 2004; Fruchart et al. 1999). In our study, the expression of apolipoproteins APOA1 and APOA4 was found to be down-regulated in the irradiated hearts compared with the control. APOA1, the major protein of the HDL complex, has the ability to act as an extracellular acceptor of cholesterol, thereby promoting cholesterol efflux from the heart and other tissues to the liver for subsequent excretion (Boisvert et al. 1999). In addition, HDL has other properties, including antioxidant, anti-inflammatory, and antithrombotic effects that may also be antiatherogenic (Barter et al. 2007). PPAR alpha has been shown to reduce plasma HDL in mice (Peters et al. 1997). Consequently, and in accordance with our proteomics data, PPAR alpha activation in mouse reduced APOA1 mRNA expression (Vu-Dac et al. 1998).

Recent data support the central coordinating role of PPAR alpha in the regulation of both inflammatory and

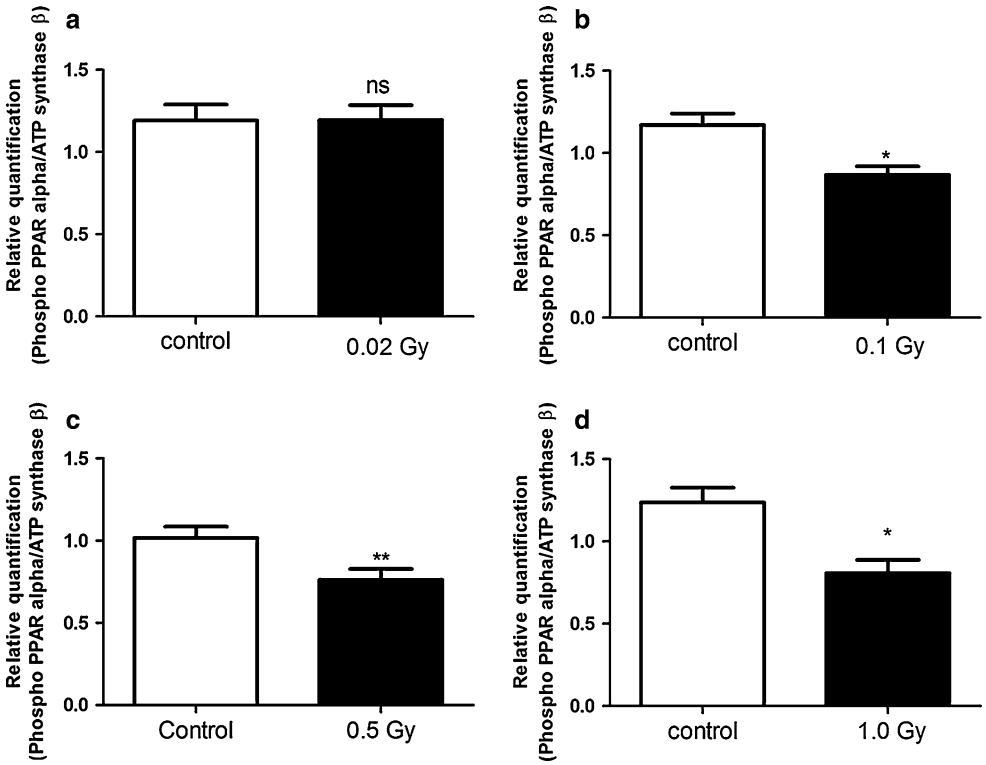

Fig. 5 Immunoblot validation of predicted activation of PPAR alpha using anti-phospho-PPAR alpha at doses of 0.02 (**a**), 0.1 (**b**), 0.5 (**c**), and 1 Gy (**d**). A significant down-regulation of the inactive form phospho-PPAR alpha is shown at higher doses (**b**, **c**, **d**). Columns represent the average ratios with standard deviation (SD) of relative protein expression in control and 0.5 Gy irradiated samples after background correction and normalization to ATP synthase ß. (unpaired Student′s *t* test; $^{*}p \leq 0.05$; $^{**}p \leq 0.01$; $n = 3$)

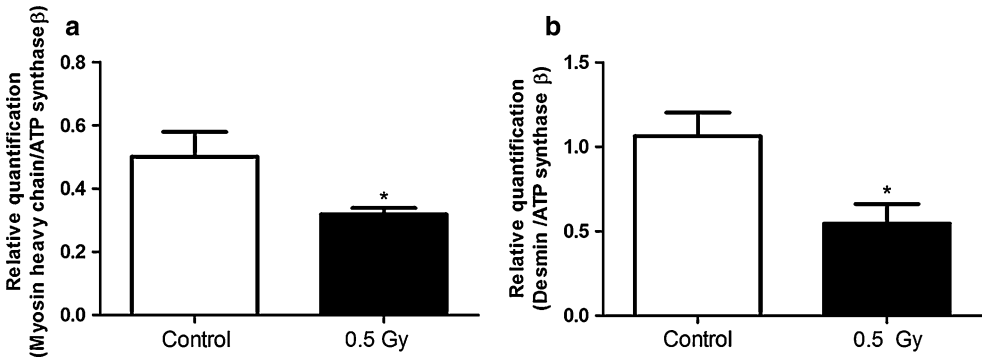

Fig. 6 Immunoblot validation of proteomic results (0.5 Gy) using anti-heavy myosin (**a**) and anti-desmin (**b**) antibodies. A significant down-regulation of the levels of myosin and desmin is shown. Columns represent the average ratios with standard deviation (SD) of relative protein expression in control and 0.5 Gy irradiated samples after background correction and normalization to ATP synthase ß. (unpaired Student′s *t* test; $^{*}p \leq 0.05$; $^{**}p \leq 0.01$; $n = 3$)

vascular responses, processes known to contribute to the development of CVD (Fruchart 2009; Smeets et al. 2007). The anti-inflammatory action of active PPAR alpha has been associated with the transcriptional inhibition of genes coding for fibrinogen and other acute-phase proteins (Gervois et al. 2001). Our proteomics analysis showed a down-regulation of fibrinogens in the heart tissue, indicating an ongoing radiation-induced anti-inflammatory process. Fibrinogen plays two essential roles in the body: It is along with other acute-phase proteins immediately elevated with tissue inflammation or tissue destruction, but also a vital part of the coagulation process (Gervois et al. 2001). When fibrinogen acts as an "acute-phase reactant," it rises sharply during tissue inflammation or injury. Radiation-induced increases in acute-phase proteins have been observed immediately after irradiation of the murine heart (TBI of 3 Gy) (Azimzadeh et al. 2011). The long-term anti-inflammatory effect that we observe here may be a protective response to the initial injury.

Among numerous defense mechanisms against oxidative injury in the heart, glutathione S-transferases play a crucial role (Roth et al. 2011). We observed deregulation of glutathione S-transferases mu and omega, both of which are involved in cellular redox homeostasis. Our data also show

a dose-independent down-regulation of two carbonic anhydrase isoenzymes, indicating an effect on the antioxidative system (Basel et al. 2012). High carbonic anhydrase-2 levels have been shown to promote cardiomyocyte hypertrophy (Alvarez et al. 2007; Brown et al. 2012) and were found in hypertrophic failing hearts (Alvarez et al. 2013). Early induction of antioxidative defense has been previously observed in murine hearts exposed to TBI (3 Gy) (Azimzadeh et al. 2011).

The higher doses (0.1, 0.5, and 1.0 Gy) used in this study induced significant down-regulation in the levels of those cardiac proteins involved in contraction and cytoskeletal organization, such as actin, decorin, talin, and myosin. High doses of TBI have been shown to induce similar alterations in cardiac myosin isozymes (Litten et al. 1990) and increase the risk of degeneration of heart structure and of cardiac dysfunction in rat (Baker et al. 2009). Our previous data also show acute radiation-induced decrease in key cardiac structural proteins immediately after TBI (3 Gy) (Azimzadeh et al. 2011) that are sustained even 40 weeks after a moderate (2 Gy) local cardiac irradiation (Barjaktarovic et al. 2013) in C57BL/6 mice. Despite such evidence of progressive structural damage to the myocardium and microvasculature, only modest changes in murine cardiac function occur even after a high local heart dose of 16 Gy (Seemann et al. 2012). However, despite the absence of overt damage, this dose lead to a sudden cardiac death between 30 and 40 weeks in 38 % of the mice (Seemann et al. 2012).

Conclusions

This study of the long-term effects of TBI on the developing murine heart illuminates two diverse responses. On the one hand, activation of PPAR alpha across the wide dose range of 0.02–1 Gy is predicted from the induction of fatty acid metabolism and anti-inflammatory and antioxidative activities. The data emphasize the importance of this transcriptional regulator in the radiation response of neonatal hearts, probably due to its essential role in pre- and postnatal phases of cardiac function. The observed changes may be considered to be a regenerative adaptation to the initial radiation-induced damage.

On the other hand, doses of 0.5 Gy and above result in a reduced expression of cytoskeletal proteins, indicating degenerative changes to the heart structure and thus maladaptation to the damage. Structural degeneration may be an indication of the non-proliferative nature of the cardiac tissue. Structural remodeling has been observed frequently in several previous studies as a dose-dependent phenomenon. We suggest that compensatory mechanisms may maintain cardiac integrity due to the modest doses used here. However, it cannot be excluded that detrimental effects of the compensatory process may themselves later contribute to the increased risk of CVD seen in the long term after radiation exposure.

Acknowledgments The research leading to these results is supported by a grant from the European Community's Seventh Framework Program (EURATOM) Contract No. 295823 (PROCARDIO) and Contract No. 295552 (CEREBRAD). We thank Stefanie Winkler for her technical assistance.

References

Aleman BM, van den Belt-Dusebout AW, Klokman WJ, Van't Veer MB, Bartelink H, van Leeuwen FE (2003) Long-term cause-specific mortality of patients treated for Hodgkin's disease. J Clin Oncol 21(18):3431–3439. doi:10.1200/jco.2003.07.131

Alvarez BV, Johnson DE, Sowah D, Soliman D, Light PE, Xia Y, Karmazyn M, Casey JR (2007) Carbonic anhydrase inhibition prevents and reverts cardiomyocyte hypertrophy. J Physiol 579(Pt 1):127–145. doi:10.1113/jphysiol.2006.123638

Alvarez BV, Quon AL, Mullen J, Casey JR (2013) Quantification of carbonic anhydrase gene expression in ventricle of hypertrophic and failing human heart. BMC Cardiovasc Disord 13:2. doi:10.1186/1471-2261-13-2

Armstrong GT, Liu Q, Yasui Y, Neglia JP, Leisenring W, Robison LL, Mertens AC (2009) Late mortality among 5-year survivors of childhood cancer: a summary from the Childhood Cancer Survivor Study. J Clin Oncol 27(14):2328–2338. doi:10.1200/jco.2008.21.1425

Azimzadeh O, Scherthan H, Sarioglu H, Barjaktarovic Z, Conrad M, Vogt A, Calzada-Wack J, Neff F, Aubele M, Buske C, Atkinson MJ, Tapio S (2011) Rapid proteomic remodeling of cardiac tissue caused by total body ionizing radiation. Proteomics 11(16):3299–3311. doi:10.1002/pmic.201100178

Azimzadeh O, Scherthan H, Yentrapalli R, Barjaktarovic Z, Ueffing M, Conrad M, Neff F, Calzada-Wack J, Aubele M, Buske C, Atkinson MJ, Hauck SM, Tapio S (2012) Label-free protein profiling of formalin-fixed paraffin-embedded (FFPE) heart tissue reveals immediate mitochondrial impairment after ionising radiation. J Proteomics 75(8):2384–2395. doi:10.1016/j.jprot.2012.02.019

Azimzadeh O, Sievert W, Sarioglu H, Yentrapalli R, Barjaktarovic Z, Sriharshan A, Ueffing M, Janik D, Aichler M, Atkinson MJ, Multhoff G, Tapio S (2013) PPAR alpha: a novel radiation target in locally exposed Mus musculus heart revealed by quantitative proteomics. J Proteome Res 12(6):2700–2714. doi:10.1021/pr400071g

Baker JE, Fish BL, Su J, Haworth ST, Strande JL, Komorowski RA, Migrino RQ, Doppalapudi A, Harmann L, Allen Li X, Hopewell JW, Moulder JE (2009) 10 Gy total body irradiation increases risk of coronary sclerosis, degeneration of heart structure and function in a rat model. Int J Radiat Biol 85(12):1089–1100

Ballinger SW (2005) Mitochondrial dysfunction in cardiovascular disease. Free Radic Biol Med 38(10):1278–1295

Barger PM, Brandt JM, Leone TC, Weinheimer CJ, Kelly DP (2000) Deactivation of peroxisome proliferator-activated receptor-alpha during cardiac hypertrophic growth. J Clin Invest 105(12):1723–1730. doi:10.1172/jci9056

Barjaktarovic Z, Schmaltz D, Shyla A, Azimzadeh O, Schulz S, Haagen J, Dörr W, Sarioglu H, Schäfer A, Atkinson MJ, Zischka H, Tapio S (2011) Radiation–induced signaling results in

mitochondrial impairment in mouse heart at 4 weeks after exposure to X-rays. PLoS ONE 6(12):e27811. doi:10.1371/journal.pone.0027811

Barjaktarovic Z, Shyla A, Azimzadeh O, Schulz S, Haagen J, Dörr W, Sarioglu H, Atkinson M, Zischka H, Tapio S (2013) Ionising radiation induces persistent alterations in the cardiac mitochondrial function of C57BL/6 mice 40 weeks after local heart exposure. Radiother Oncol (in press)

Barter PJ, Puranik R, Rye KA (2007) New insights into the role of HDL as an anti-inflammatory agent in the prevention of cardiovascular disease. Curr Cardiol Rep 9(6):493–498

Basel H, Kavak S, Demir H, Meral I, Ekim H, Bektas H (2012) Effect of levosimendan injection on oxidative stress of rat myocardium. Toxicol Ind Health. doi:10.1177/0748233712436643

Baumans V, Havenaar R, van Herck H (1988) The use of repeated treatment with Ivomec and Neguvon spray in the control of murine fur mites and oxyurid worms. Lab Anim 22(3):246–249

Boisvert WA, Black AS, Curtiss LK (1999) ApoA1 reduces free cholesterol accumulation in atherosclerotic lesions of ApoE-deficient mice transplanted with ApoE-expressing macrophages. Arterioscler Thromb Vasc Biol 19(3):525–530

Bradford MM (1976) A rapid and sensitive method for the quantitation of microgram quantities of protein utilizing the principle of protein-dye binding. Anal Biochem 72:248–254

Brosch M, Yu L, Hubbard T, Choudhary J (2009) Accurate and sensitive peptide identification with Mascot Percolator. J Proteome Res 8(6):3176–3181. doi:10.1021/pr800982s

Brown BF, Quon A, Dyck JR, Casey JR (2012) Carbonic anhydrase II promotes cardiomyocyte hypertrophy. Can J Physiol Pharmacol 90(12):1599–1610. doi:10.1139/y2012-142

Burns KA, Vanden Heuvel JP (2007) Modulation of PPAR activity via phosphorylation. Biochim Biophys Acta 1771(8):952–960. doi:10.1016/j.bbalip.2007.04.018

Dhalla NS, Temsah RM, Netticadan T (2000) Role of oxidative stress in cardiovascular diseases. J Hypertens 18(6):655–673

Djouadi F, Brandt JM, Weinheimer CJ, Leone TC, Gonzalez FJ, Kelly DP (1999) The role of the peroxisome proliferator-activated receptor alpha (PPAR alpha) in the control of cardiac lipid metabolism. Prostaglandins Leukot Essent Fat Acids 60(5–6):339–343

Fruchart JC (2009) Peroxisome proliferator-activated receptor-alpha (PPARalpha): at the crossroads of obesity, diabetes and cardiovascular disease. Atherosclerosis 205(1):1–8. doi:10.1016/j.atherosclerosis.2009.03.008

Fruchart JC, Duriez P, Staels B (1999) Peroxisome proliferator-activated receptor-alpha activators regulate genes governing lipoprotein metabolism, vascular inflammation and atherosclerosis. Curr Opin Lipidol 10(3):245–257

Gervois P, Vu-Dac N, Kleemann R, Kockx M, Dubois G, Laine B, Kosykh V, Fruchart JC, Kooistra T, Staels B (2001) Negative regulation of human fibrinogen gene expression by peroxisome proliferator-activated receptor alpha agonists via inhibition of CCAAT box/enhancer-binding protein beta. J Biol Chem 276(36):33471–33477. doi:10.1074/jbc.M102839200

Ghobadi G, van der Veen S, Bartelds B, de Boer RA, Dickinson MG, de Jong JR, Faber H, Niemantsverdriet M, Brandenburg S, Berger RM, Langendijk JA, Coppes RP, van Luijk P (2012) Physiological interaction of heart and lung in thoracic irradiation. Int J Radiat Oncol Biol Phys 84(5):e639–e646. doi:10.1016/j.ijrobp.2012.07.2362

Hauck SM, Dietter J, Kramer RL, Hofmaier F, Zipplies JK, Amann B, Feuchtinger A, Deeg CA, Ueffing M (2010) Deciphering membrane-associated molecular processes in target tissue of autoimmune uveitis by label-free quantitative mass spectrometry. Mol Cell Proteomics MCP 9(10):2292–2305. doi:10.1074/mcp.M110.001073

Lauk S (1986) Strain differences in the radiation response of the rat heart. Radiother Oncol 5(4):333–335

Lazennec G, Canaple L, Saugy D, Wahli W (2000) Activation of peroxisome proliferator-activated receptors (PPARs) by their ligands and protein kinase A activators. Mol Endocrinol (Baltimore, Md) 14(12):1962–1975

Lehman JJ, Kelly DP (2002) Transcriptional activation of energy metabolic switches in the developing and hypertrophied heart. Clin Exp Pharmacol Physiol 29(4):339–345

Litten RZ, Fein HG, Gainey GT, Walden TL, Smallridge RC (1990) Alterations in rat cardiac myosin isozymes induced by whole-body irradiation are prevented by 3,5,3′-L-triiodothyronine. Metabolism 39(1):64–68

Mayburd AL, Martlinez A, Sackett D, Liu H, Shih J, Tauler J, Avis I, Mulshine JL (2006) Ingenuity network-assisted transcription profiling: identification of a new pharmacologic mechanism for MK886. Clin Cancer Res 12(6):1820–1827

Merl J, Ueffing M, Hauck SM, von Toerne C (2012) Direct comparison of MS-based label-free and SILAC quantitative proteome profiling strategies in primary retinal Muller cells. Proteomics 12(12):1902–1911. doi:10.1002/pmic.201100549

Misra MK, Sarwat M, Bhakuni P, Tuteja R, Tuteja N (2009) Oxidative stress and ischemic myocardial syndromes. Med Sci Monit 15(10):RA209–RA219

Moulder JE, Fish BL, Cohen EP (2004) Impact of angiotensin II type 2 receptor blockade on experimental radiation nephropathy. Radiat Res 161(3):312–317

Murakami K, Ide T, Suzuki M, Mochizuki T, Kadowaki T (1999) Evidence for direct binding of fatty acids and eicosanoids to human peroxisome proliferators-activated receptor alpha. Biochem Biophys Res Commun 260(3):609–613. doi:10.1006/bbrc.1999.0951

Papaioannou MD, Lagarrigue M, Vejnar CE, Rolland AD, Kuhne F, Aubry F, Schaad O, Fort A, Descombes P, Neerman-Arbez M, Guillou F, Zdobnov EM, Pineau C, Nef S (2011) Loss of Dicer in Sertoli cells has a major impact on the testicular proteome of mice. Mol Cell proteomics MCP 10(4):M900587MCP900200. doi:10.1074/mcp.M900587-MCP200

Peters JM, Hennuyer N, Staels B, Fruchart JC, Fievet C, Gonzalez FJ, Auwerx J (1997) Alterations in lipoprotein metabolism in peroxisome proliferator-activated receptor alpha-deficient mice. J Biol Chem 272(43):27307–27312

Preston DL, Shimizu Y, Pierce DA, Suyama A, Mabuchi K (2003) Studies of mortality of atomic bomb survivors. Report 13: solid cancer and noncancer disease mortality: 1950-1997. Radiat Res 160(4):381–407

Roth E, Marczin N, Balatonyi B, Ghosh S, Kovacs V, Alotti N, Borsiczky B, Gasz B (2011) Effect of a glutathione S-transferase inhibitor on oxidative stress and ischemia-reperfusion-induced apoptotic signalling of cultured cardiomyocytes. Exp Clin Cardiol 16(3):92–96

Sarioglu H, Brandner S, Jacobsen C, Meindl T, Schmidt A, Kellermann J, Lottspeich F, Andrae U (2006) Quantitative analysis of 2,3,7,8-tetrachlorodibenzo-p-dioxin-induced proteome alterations in 5L rat hepatoma cells using isotope-coded protein labels. Proteomics 6(8):2407–2421

Seemann I, Gabriels K, Visser NL, Hoving S, te Poele JA, Pol JF, Gijbels MJ, Janssen BJ, van Leeuwen FW, Daemen MJ, Heeneman S, Stewart FA (2012) Irradiation induced modest changes in murine cardiac function despite progressive structural damage to the myocardium and microvasculature. Radiother Oncol 103(2):143–150. doi:10.1016/j.radonc.2011.10.011

Shankar SM, Marina N, Hudson MM, Hodgson DC, Adams MJ, Landier W, Bhatia S, Meeske K, Chen MH, Kinahan KE, Steinberger J, Rosenthal D (2008) Monitoring for cardiovascular disease in survivors of childhood cancer: report from the

Cardiovascular Disease Task Force of the Children's Oncology Group. Pediatrics 121(2):e387–e396. doi:10.1542/peds.2007-0575

Shimizu Y, Kodama K, Nishi N, Kasagi F, Suyama A, Soda M, Grant EJ, Sugiyama H, Sakata R, Moriwaki H, Hayashi M, Konda M, Shore RE (2010) Radiation exposure and circulatory disease risk: Hiroshima and Nagasaki atomic bomb survivor data, 1950-2003. BMJ (Clinical research ed) 340:b5349

Smeets PJ, Planavila A, van der Vusse GJ, van Bilsen M (2007) Peroxisome proliferator-activated receptors and inflammation: take it to heart (Oxford, England). Acta Physiologica 191(3):171–188. doi:10.1111/j.1748-1716.2007.01752.x

Szklarczyk D, Franceschini A, Kuhn M, Simonovic M, Roth A, Minguez P, Doerks T, Stark M, Muller J, Bork P, Jensen LJ, von Mering C (2011) The STRING database in 2011: functional interaction networks of proteins, globally integrated and scored. Nucleic Acids Res 39(Database issue):D561–D568. doi:10.1093/nar/gkq973

Takano H, Zou Y, Hasegawa H, Akazawa H, Nagai T, Komuro I (2003) Oxidative stress-induced signal transduction pathways in cardiac myocytes: involvement of ROS in heart diseases. Antioxid Redox Signal 5(6):789–794

Thomas PD, Kejariwal A, Guo N, Mi H, Campbell MJ, Muruganujan A, Lazareva-Ulitsky B (2006) Applications for protein sequence-function evolution data: mRNA/protein expression analysis and coding SNP scoring tools. Nucleic Acids Res 34(Web Server issue):W645–W650

Tukenova M, Guibout C, Oberlin O, Doyon F, Mousannif A, Haddy N, Guerin S, Pacquement H, Aouba A, Hawkins M, Winter D, Bourhis J, Lefkopoulos D, Diallo I, de Vathaire F (2010) Role of cancer treatment in long-term overall and cardiovascular mortality after childhood cancer. J Clin Oncol 28(8):1308–1315

van der Lee KA, Vork MM, De Vries JE, Willemsen PH, Glatz JF, Reneman RS, Van der Vusse GJ, Van Bilsen M (2000) Long-chain fatty acid-induced changes in gene expression in neonatal cardiac myocytes. J Lipid Res 41(1):41–47

van Raalte DH, Li M, Pritchard PH, Wasan KM (2004) Peroxisome proliferator-activated receptor (PPAR)-alpha: a pharmacological target with a promising future. Pharm Res 21(9):1531–1538

Vanden Heuvel JP, Kreder D, Belda B, Hannon DB, Nugent CA, Burns KA, Taylor MJ (2003) Comprehensive analysis of gene expression in rat and human hepatoma cells exposed to the peroxisome proliferator WY14,643. Toxicol Appl Pharmacol 188(3):185–198

Vu-Dac N, Chopin-Delannoy S, Gervois P, Bonnelye E, Martin G, Fruchart JC, Laudet V, Staels B (1998) The nuclear receptors peroxisome proliferator-activated receptor alpha and Rev-erbalpha mediate the species-specific regulation of apolipoprotein A-I expression by fibrates. J Biol Chem 273(40):25713–25720

Yeung TK, Lauk S, Simmonds RH, Hopewell JW, Trott KR (1989) Morphological and functional changes in the rat heart after X irradiation: strain differences. Radiat Res 119(3):489–499

2.3 Total Body Exposure to Low-Dose Ionizing Radiation Induces Long- Term Alterations to the Liver Proteome of Neonatally Exposed Mice

2.3.1 Aim and summary

Previous data show the negative impact of ionizing radiation on the liver function. In the previous study of this thesis on the radiation effects on neonatal mouse heart, PPARA alpha was convincingly identified as a cardiac target of low doses of ionizing radiation. PPARA also plays a very crucial role in liver for HDL and LDL metabolism. Experimental data also show that PPARA activity in liver is strongly associated with serum lipid profile.

This study was designed to investigate the acute and long-term global liver proteome using low-dose total body irradiated animals. Mice were irradiated at postnatal day 10 using ^{137}Cs gamma irradiation source with doses of 0.02, 0.05, 0.1, 0.5 and 1 Gy and the animals were sacrificed after 7 months. Liver tissues from control (sham) and irradiated animals were removed and total proteome was isolated using 6 M guanidine hydrochloride. ICPL duplex labelling was performed and quantitative proteome profiling was done using LC-MS/MS. Serum from these animals was tested for triglyceride (TG) and free fatty acid (FFA) content.

Inhibition of glycolysis pyruvate dehydrogenase pathway was indicated immediately after irradiation. In addition, alteration in structural proteins was observed directly (1 day) after the radiation exposure but they were no longer detectable after seven months, indicating the repair capacity of liver after low and moderate doses of IR. However, persistent alteration in lipid metabolism and activity of transcription factor PPARA were observed. Serum TG and FFA levels were also found persistently altered.

Together with our previous data on the cardiac effects in these mice, these results underscore the importance of PPARA -driven systemic effects after low-dose irradiation in neonates. Therapeutic substances controlling the activity of PPARA and lipid metabolism may act as radioprotective agents.

2.3.2 Contributions

This study was performed with the help of Sonja Buratovic (Uppsala University) and Dr. Juliane Merl-Pham (PROT/HMGU). Dr. Buratovic irradiated the animals; Dr. Merl-Pham ran

the LC-MS/MS analysis. I isolated the heart proteomes, labeled with ICPL and did all the downstream data analysis. I also performed all the immunoblottings and PDH assays. Moreover, I isolated nuclear fractions from the liver tissue and measured the PPARA activity by transcription factor activity assay. I also measured the serum TG and FFA levels. The text, tables, figures and supporting material of the publication was produced by me with the help of PD Dr. Soile Tapio and Prof. Dr. Michael J. Atkinson.

2.3.3 Publication

Total Body Exposure to Low-Dose Ionizing Radiation Induces Long- Term Alterations to the Liver Proteome of Neonatally Exposed Mice

Mayur V. Bakshi, Omid Azimzadeh, Zarko Barjaktarovic, Stefan J. Kempf, Juliane Merl-Pham, Stefanie M. Hauck, Sonja Buratovic, Per Eriksson, Michael J. Atkinson and Soile Tapio

The following paper was published as an original manuscript in Oct. 2014 in Journal of proteome research. Special Issue: Environmental Impact on Health

J. Proteome Res., 2015, 14 (1), pp 366–373

DOI: 10.1021/pr500890n

Journal of proteome research

Article

pubs.acs.org/jpr

Total Body Exposure to Low-Dose Ionizing Radiation Induces Long-Term Alterations to the Liver Proteome of Neonatally Exposed Mice

Mayur V. Bakshi,[†] Omid Azimzadeh,[†] Zarko Barjaktarovic,[†] Stefan J. Kempf,[†] Juliane Merl-Pham,[‡] Stefanie M. Hauck,[‡] Sonja Buratovic,[§] Per Eriksson,[§] Michael J. Atkinson,[†,∥] and Soile Tapio*[,†]

[†]Institute of Radiation Biology, [‡]Research Unit Protein Science, Helmholtz Zentrum München, German Research Center for Environmental Health, 85764 Neuherberg, Germany

[§]Department of Environmental Toxicology, Uppsala University, 75236 Uppsala, Sweden

[∥]Chair of Radiation Biology, Technical University of Munich, 81675 Munich, Germany

Supporting Information

ABSTRACT: Tens of thousands of people are being exposed daily to environmental low-dose gamma radiation. Epidemiological data indicate that such low radiation doses may negatively affect liver function and result in the development of liver disease. However, the biological mechanisms behind these adverse effects are unknown. The aim of this study was to investigate radiation-induced damage in the liver after low radiation doses. Neonatal male NMRI mice were exposed to total body irradiation on postnatal day 10 using acute single doses ranging from 0.02 to 1.0 Gy. Early (1 day) and late (7 months) changes in the liver proteome were tracked using isotope-coded protein label technology and quantitative mass spectrometry. Our data indicate that low and moderate radiation doses induce an immediate inhibition of the glycolysis pathway and pyruvate dehydrogenase availability in the liver. Furthermore, they lead to significant long-term alterations in lipid metabolism and increased liver inflammation accompanying inactivation of the transcription factor peroxisome proliferator-activated receptor alpha. This study contributes to the understanding of the potential risk of liver damage in populations environmentally exposed to ionizing radiation.

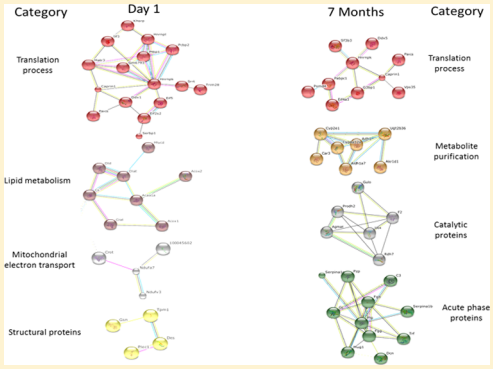

KEYWORDS: *Low-dose ionizing radiation, liver, metabolic crosstalk, PPAR alpha, proteomics, ICPL*

INTRODUCTION

Exposure to ionizing radiation is omnipresent. We are constantly exposed to cosmic radiation and to gamma-rays from naturally occurring radionuclides in the ground, building materials, food, and drink.[1] In addition, accidental nuclear scenarios lead to environmental contamination of unknown levels. Tens of thousands of people including children are living in polluted areas and are being exposed daily to low-dose gamma radiation. Most epidemiological studies concerning radiation-induced health effects are being conducted in medically or occupationally exposed populations, and very little is known about the consequences of environmental radiation.[1]

Classically, liver has been considered to be a radiation-sensitive organ.[2] Several studies using acute high doses of radiation (>10 Gy) have shown clear structural damage and hepatic toxicity in this organ.[3,4] Most of these data originate from locally irradiated liver tumor patients.[3] In accordance, animal studies using single high (25 Gy) and cumulative fractionated doses (total dose of 60 Gy) have indicated macroscopically detectable scarring and changes in liver function caused by deregulation of metabolic enzymes.[5] Ionizing radiation has been shown to increase the inflammatory status of the liver.[6] An inflammatory environment promotes the development of various liver diseases such as hepatitis as well as hepatocellular carcinoma.[7] Interestingly, the recent data from atomic bomb survivors that received only moderate to low radiation doses show significantly increased mortality due to liver cancer in this cohort.[8]

The liver is the metabolic center of the body; major metabolic activities and detoxification are performed by liver mitochondria via metabolic pathways such as lipid metabolism and the TCA cycle. The early postnatal period plays a pivotal role in structural and functional development of this organ with far-reaching consequences throughout the lifetime;[9] it has been suggested that nonalcoholic fatty liver may have roots in the neonatal period.[10] For hepatocytes, the main cellular components of the liver, the neonatal period means a time of adaptation to the new metabolic environment, mainly due to a switch in energy substrate preference from glucose in the fetal period to fatty acids following birth.[11] The neonatal liver

Special Issue: Environmental Impact on Health

Received: August 25, 2014
Published: October 9, 2014

undergoes several changes in its functional capacity during the early postnatal period.[12]

Previous data show that mice irradiated during the neonatal period are more susceptible to life shortening than those exposed in the intrauterine or adult period.[13] Liver cancer is significantly induced in neonatal mice at total body doses around 0.5 Gy.[14] The decreased capacity of the newborn liver, due to its low CYP450 content, to metabolize, detoxify, and excrete drugs[15] may be responsible for the increased susceptibility to ionizing radiation. However, very little is known about the biological mechanisms leading to radiation-induced liver damage. In particular, practically nothing is known about the dose dependence of this damage.

The aim of the current study was to elucidate immediate and late effects on liver of low-dose ionizing radiation given at early age. For this purpose, we used NMRI mice as a model. The mice were exposed to total body irradiation (TBI) on postnatal day 10 (PND 10) using doses ranging from 0.02 to 1.0 Gy. Early (1 day) and late (7 months) changes in the liver tissue were tracked by quantitative proteomics technology. As observed previously in the heart,[16,17] transcription factor peroxisome proliferator-activated receptor alpha (PPAR alpha) was found to play a central role in the regulation of the radiation-induced metabolic changes in the liver.

EXPERIMENTAL SECTION

Total Body Irradiation of Mice

Experiments were carried out in accordance with the European Communities Council Directive of 24 November 1986 (86/609/EEC), after approval from the local ethical committees (Uppsala University and the Agricultural Research Council) and by the Swedish Committee for Ethical Experiments on Laboratory Animals.

For early effect studies, male NMRI mice (Charles River) were exposed to single acute dose of total body irradiation (TBI) at PND 10 using a Cs-137 gamma radiation source (dose rate 0.2 Gy/min), delivering doses of 0.05, 0.1, 0.5, and 1.0 Gy (The Rudbeck Laboratory, Uppsala University). For late effects, mice were exposed to a single acute dose of TBI at PND 10 using a Co-60 gamma radiation source (dose rate 0.02 Gy/min), delivering doses of 0.02, 0.1, 0.5, and 1.0 Gy (The Svedberg Laboratory, Uppsala University). An ionization chamber (Markus chamber type 23343.PTW-Freiburg) was used to validate the radiation exposure as described previously.[18] Control mice were sham-irradiated, and the dose was validated as mentioned above. Control and irradiated animals were sacrificed at the age of 11 days or 7 months via cervical dislocation. Livers were excised, thoroughly rinsed in phosphate-buffered saline to remove blood, snap-frozen, and stored at −80 °C. In total, 60 mice were used for this study.

Isolation and Extraction of Whole Liver Proteome

Whole frozen livers were powdered in liquid nitrogen using a cooled mortar and pestle. The tissue powder was resuspended in ICPL lysis buffer containing 6 M guanidine hydrochloride (SERVA) with protease and phosphatase inhibitor cocktails (Roche Diagnostics). The lysates were stored at −20 °C until analysis.

Proteomic Analysis

Protein Quantification and Labeling. The protein concentration in the tissue lysates was determined by Bradford assay following the manufacturer's instructions (Thermo Fisher).[19]

The ICPL labeling was done as previously reported.[16] Briefly, individual protein lysates (100 μg in 100 μL of 6 M guanidine hydrochloride from each biological sample) were reduced, alkylated, and labeled with the respective ICPL reagent (SERVA) as follows: ICPL-0 was used for sham-irradiated control tissue, and ICPL-6, for the corresponding irradiated tissue. The heavy and light labeled replicates were combined prior to separation using 12% SDS gel electrophoresis and stained with colloidal Coomassie Blue solution. Three biological replicates per dose and time point were analyzed in all experiments.

LC−ESI−MS/MS Analysis. After staining, each SDS gel lane was cut into four equal slices and subjected to in-gel digestion with trypsin (Sigma-Aldrich) as described previously.[20] The generated peptides were separated by nano-HPLC, and mass spectrometric analysis was performed with an LTQ Orbitrap XL mass spectrometer (Thermo Scientific) as described before.[21] Up to 10 of the most intense ions were selected for fragmentation in the linear ion trap, and target peptides already selected for MS/MS were dynamically excluded for 60 s.

The MS/MS spectra were searched against the Ensembl mouse database (version 2.4, 56 416 sequences) using the MASCOT search engine (version 2.3.02; Matrix Science) with the following parameters: a precursor mass error tolerance of 10 ppm and a fragment tolerance of 0.6 Da. One missed cleavage was allowed. Carbamidomethylation was set as the fixed modification. Oxidized methionine and ICPL-0 and ICPL-6 for lysine residues and N-termini of peptides were set as the variable modifications.

Data processing for the identification and quantitation of ICPL-duplex labeled proteins was performed using Proteome Discoverer, version 1.3.0.339 (Thermo Scientific). The MASCOT node uses the ions score for an MS/MS match. MASCOT Percolator node uses algorithm to discriminate correct from incorrect peptide spectrum matches and calculates accurate statistics, such as the q-value (FDR) and posterior error probability (PEP), to improve the number of confidently identified peptides at a given false discovery rate.[22] It also assigns a statistically meaningful q-value to each PSM and the probability of the individual PSM being incorrect. The peptides passing the filter settings were grouped into the identified proteins. The proteins identified by at least two unique peptides in two out of three biological replicates, and quantified with an H/L variability of less than 30%, were considered for further evaluation. Proteins identified with a single peptide were manually scrutinized and regarded as unequivocally identified if they fulfilled the following four criteria: (a) they had fragmentation spectra with a long, nearly complete y- and/or b-series; (b) all lysines were modified; (c) the numbers of lysines predicted from the mass difference of the labeled pair had to match the number of lysines in the given sequence from the search query; and (d) at least one mass of a modified lysine was included in the detected partial fragment series.[23] Proteins with ratios of H/L label greater than 1.30-fold or less than 0.769-fold and having peptide q-value less than 0.01 in the Percolator high confidence peptide filter were defined as being significantly differentially expressed.

Data Deposition of Proteomics Experiments. The MSF files of the obtained after analyzing MS/MS spectra in

dx.doi.org/10.1021/pr500890n | J. Proteome Res. 2015, 14, 366−373

Proteome Discoverer can be found at http://storedb.org/project_details.php?projectid=39.

Bioinformatics Analysis

The analyses of protein−protein interaction and signaling networks were performed with two bioinformatics tools: Ingenuity Pathway Analysis (IPA) (INGENUITY System; http://www.ingenuity.com)[24] and STRING protein database (http://string-db.org/).[25] The protein accession numbers including the relative expression values (fold-change) of each deregulated protein were uploaded to IPA and STRING to identify possible interactions among these proteins.

Immunoblotting Analysis

Immunoblotting of protein extracts from control and irradiated tissues was used to validate the proteomic data. For nuclear fraction enrichment, immunoblotting was also used. Proteins were separated by 1D PAGE gel electrophoresis and transferred to nitrocellulose membranes (GE Healthcare) using a TE 77 semidry blotting system (GE Healthcare) at 0.8 mA/cm for 1 h. Membranes were saturated for 1 h with 8% advance blocking reagent (GE Healthcare) in TBS (50 mM Tris-HCl, pH 7.6, and 150 mM NaCl) containing 0.1% Tween-20 (TBS/T). Blots were incubated overnight at 4 °C with anti-tropomyosin-1 (alpha) (Abcam no. ab55915), anti-desmin (Abcam no. ab32362), anti-PCNA (PC10, for nuclear fraction) (Santa Cruz no. sc56), and anti-GAPDH (Santa Cruz no. sc-47724) (for nuclear fraction).

After washing three times in TBS/T, blots were incubated for 1 h at room temperature with horseradish peroxidise-conjugated anti-mouse or anti-rabbit secondary antibody (Santa Cruz Biotechnology) in blocking buffer (TBS/T with 5% w/v advance blocking reagent). Immunodetection was performed with ECL advance western blotting detection kit (GE Healthcare). The protein bands were quantified using total lab (TL) 100 software by integrating all pixel values in the band area after background correction. Tubulin alpha (GeneTex no. GTX72360) was used for normalization, as it was not significantly changed in proteomics analysis of the early 1.0 Gy dose.

Pyruvate Dehydrogenase Activity Assay

Pyruvate dehydrogenase (PDH) activity was measured using the dipstick assay kit in the control and 0.05, 0.1, 0.5, and 1.0 Gy treated liver samples from PND 11. The assay was performed following the manufacturer's guidelines (Abcam no. ab109882). The band intensities were quantified by using total lab (TL) 100 software.

PPAR Alpha Transcription Factor Activity Assay

Nuclear fractions from three biological replicates of control and 0.02, 0.1, 0.5, and 1.0 Gy irradiated livers after 7 months postirradiation were extracted using NE-PER nuclear and cytoplasmic extraction kit (Thermo Scientific no. 78833), and the protein concentration in the nuclear fractions was determined by Bradford assay following the manufacturer's instructions (Thermo Fisher).[19] Equal amounts of protein from control and irradiated samples were added on immobilized dsDNA-coated plates containing the peroxisome proliferator response element (PPRE). PPAR alpha was detected by addition of a specific primary antibody directed against PPAR alpha. After adding the secondary antibody, the activity was measured colorimetrically according to the manufacturer's guidelines (Abcam no. ab133107).

Serum FFA and TG Analysis

Serum of the animals 7 months postirradiation was collected immediately after sacrifice and stored at −80 °C for free fatty acid (FFA) and triglyceride (TG) quantification. Control and 0.02, 0.1, 0.5, and 1.0 Gy irradiated serum samples were analyzed. The quantification was done using BioVision colorimetric assay kits (TG cat no. K622-100 and FFA cat no. K612-100).

Statistical Analysis

Statistical analysis was performed using GraphPad Prism (release 4). Immunoblotting results were evaluated using unpaired Student's t test. Data are presented as mean + standard deviation (SD) or standard error of the mean (SEM). P-values equal to or smaller than 0.05 were considered to denote statistical significance. Three biological replicates were used for all experiments.

RESULTS

Proteomics Analysis

The total number of all identified and significantly deregulated proteins in each group are shown in Table 1. In the early (1 day) group, the proteomic alterations showed dose dependence, with the number of differentially regulated proteins being smallest at the lowest dose (0.05 Gy) and greatest at the highest dose (1.0 Gy) (Figure 1A). On the contrary, in the late-effect group (7 months), the highest number of deregulated proteins was observed at the dose of 0.1 Gy (Figure 1B).

Table 1. Numbers of All Proteins Identified and Significantly Deregulated in This Study[a]

	1 day post IR		7 months post IR	
dose (Gy)	total identified	significantly deregulated	total identified	significantly deregulated
0.05/0.02	1683	40	1669	42
0.1	1768	56	1528	76
0.5	1698	74	1484	60
1.0	1664	77	1440	64

[a]The different doses and time points are indicated.

The immediate effect of radiation on the liver proteome indicated that the three highest doses, i.e., 0.1, 0.5, and 1.0 Gy, had several differentially expressed proteins in common; 12 proteins were shared among all three of the highest doses, and 26 proteins were shared between the two highest doses (Figure 1A). Many of the shared proteins belonged to the glycolytic pathway, such as dihydrolipoamide S-acetyltransferase (DLAT), aldolase A (ALDO-A), and carnitine acetyltransferase (CRAT); all of these were downregulated. Two shared proteins were components of the mitochondrial respiratory chain complex I (NDUFV-3, NDUFV-7); both of these were downregulated (Supporting Information Table S1).

The major protein category representing the late proteome alterations was the inflammatory response, with proteins such as plasminogen and fibrinogens (FGG, FGB) being upregulated. Proteins of the beta oxidation process were also significantly affected, including enzymes such as ACAA1A (downregulated) and ALDH-1 (upregulated) (Supporting Information Table S2).

At both time points, the common affected process was translation; proteins such as CAPRIN-1, HNRNPK, and DDX-5 were found to be commonly upregulated. We observed

dx.doi.org/10.1021/pr500890n | J. Proteome Res. 2015, 14, 366−373

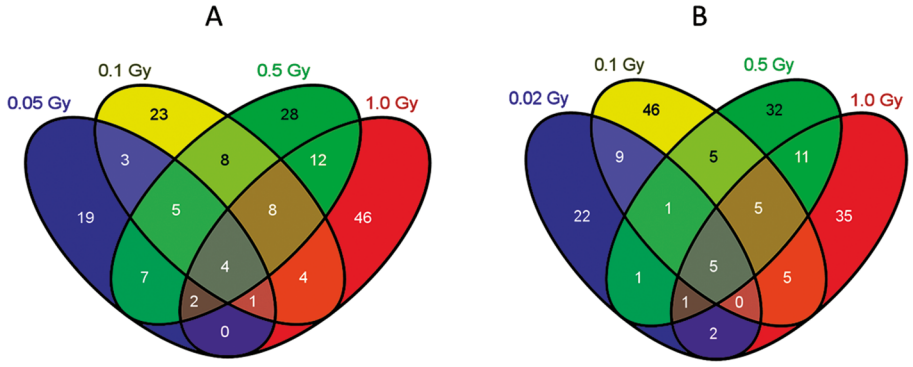

Figure 1. Venn diagram showing the number of significantly deregulated and shared proteins affected in all irradiated samples at 1 day (A) and 7 months postirradiation (B).

persistent alterations in liver structural proteins at the two highest doses at both time points. Structural proteins such as desmin, tropomyosin-1, and decorin were found to be downregulated (Supporting Information Tables S1c,d and S2c,d). The complete lists of significantly deregulated proteins and all identified and quantified peptides are shown in Tables S1−S4.

Bioinformatics Analysis

We analyzed the protein networks after exposure to 1.0 Gy using the STRING software tool (Supporting Information Figure S4). Both early and late time points showed an effect on the translation process. After 1 day of exposure, the most affected protein networks were lipid metabolism, mitochondrial electron transport, and structural proteins (Supporting Information Figure S4). The long-term effects at 7 months showed alterations in detoxification, catalytic proteins, and inflammation (Supporting Information Figure S4). The STRING analysis confirmed the results of IPA analysis.

To study protein networks involved in the radiation response, we used Ingenuity Pathway Analysis (IPA) software (Supporting Information Figures S5−S12). The analysis showed that the most important protein clusters at the lowest doses were hepatic system disease (0.05 Gy, early response) (Supporting Information Figure S5) and cellular assembly and organization (0.02 Gy, long-term response) (Supporting Information Figure S9). At higher doses (0.5 Gy, 1.0 Gy), lipid metabolism and energy production were the most significant networks both at early and late time points (Supporting Information Figures S8, S11, and S12). The immediate response to the dose of 1.0 Gy was characterized by the presence of stress response proteins such as glutathione S-transferase, theta 1 (upregulated) (Supporting Information Table S 1d). In the long-term effects, proteins belonging to the inflammatory responses group were significantly presented (Supporting Information Figures S11 and S12). The transcription factor PPAR alpha was predicted to be downregulated due to the deregulation of downstream targets such as hemopexin, fibrinogens beta and gamma, catalase, and CYP2C8 at the three highest doses (0.1, 0.5, 1.0 Gy) (Figure 2).

Immunoblotting Analysis

Western blotting analysis was done to validate the proteomics data. Both desmin and tropomyosin-1 showed significant downregulation at PND11 (1.0 Gy) (Figure 3 and Supporting Information Figure S1), which was in good agreement with our proteomics data. The enrichment of nuclear fraction from

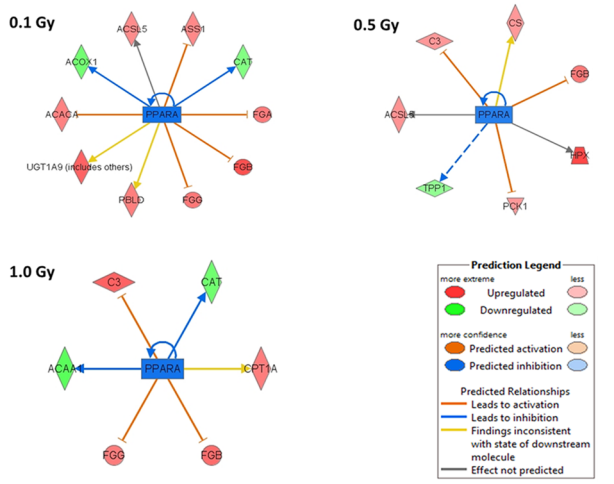

Figure 2. Ingenuity Pathway Analysis networks showing transcription factor PPAR alpha as an upstream regulator. PPAR alpha is predicted to be deactivated in all networks at the long-term time point. The proteins indicated in red are upregulated, and those indicated in green are downregulated. Three biological replicates were used in all experiments. ACACA, acetyl-coenzyme A carboxylase alpha; ACOX1, peroxisomal acyl-coenzyme A oxidase 1; ACCL5, acyl-CoA synthetase long-chain family member 5; ASS1, argininosuccinate synthetase 1; CAT, catalase; FGA, fibrinogen alpha; FGB, fibrinogen beta; FGG, fibrinogen gamma; PBLD1, phenazine biosynthesis-like protein domain containing 1; UGT1A9, UDP glucuronosyltransferase 1 family, polypeptide A9; CS, citrate synthase; C3, complement C3 precursor; HPX, hemopexin; PCK1, phosphoenolpyruvate carboxykinase 1; TPP1, tripeptidyl peptidase I; ACAA1, acetyl-coenzyme A acyltransferase 1A; CPT1A, carnitine palmitoyltransferase 1a; PPARA, peroxisome proliferator-activated receptor alpha.

irradiated live tissue was also confirmed using immunoblotting (Supporting Information Figure S2).

Pyruvate Dehydrogenase Assay

In order to verify the downregulation of the pyruvate complex and pyruvate kinase (PDK) that was indicated in the proteome changes at the early time point, we tested the activity of pyruvate dehydrogenase 1 day after radiation exposure; it showed a significant reduction by more than 2-fold at 0.5 and 1.0 Gy but not at lower doses (Figure 4 and Supporting Information Figure S3). This supported our proteomics data that showed significantly decreased expression of several pyruvate dehydrogenase subunits and pyruvate kinase at 0.5 and 1.0 Gy (Supporting Information Tables S1c,d).

dx.doi.org/10.1021/pr500890n | J. Proteome Res. 2015, 14, 366−373

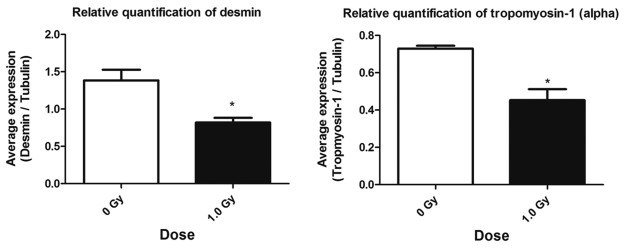

Figure 3. Immunoblot validation of proteomic results (1.0 Gy; PND 11) using anti-desmin and anti-tropomyosin-1 antibodies. A significant downregulation of the levels of desmin and tropomyosin-1 is shown. Columns represent the average ratios with standard deviation (SD) of relative protein expression in control and 1.0 Gy (PND 11) irradiated samples after background correction and normalization to tubulin alpha (unpaired Student's *t* test; $*p \leq 0.05$; $n = 3$).

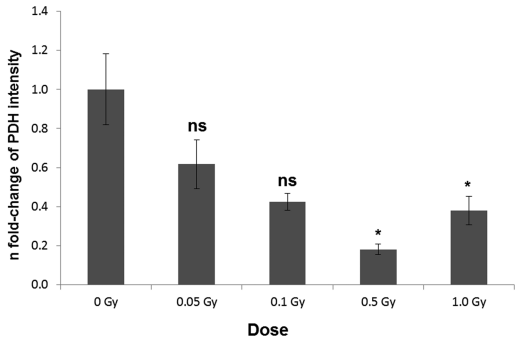

Figure 4. Liver pyruvate dehydrogenase (PDH) activity in the control and 0.05, 0.1, 0.5, and 1.0 Gy treated mice at PND 11. Bars represent *n* fold-changes with their corresponding standard error of the mean (SEM) from the biological replicates; statistical analysis was performed with unpaired Student's *t* test; $*p \leq 0.05$; ns, not significant; $n = 3$; data origin from two independent experiments to evaluate PDH activity at 1.0 and lower doses (0.5, 0.1, and 0.05 Gy) versus the respective controls.

PPAR Alpha Activity Assay

To confirm the prediction of PPAR alpha inactivation by IPA software (Figure 2), the activity of PPAR alpha was measured from nuclear extracts at the late time point (7 months). A significant dose-dependent decrease in the activity of this transcription factor was observed, starting from the dose of 0.1 Gy (Figure 5A).

Serum FFA and TG Analysis

Because PPAR alpha is well-known to control the free fatty acid (FFA) and triglyceride (TG) homeostasis in serum, we measured the serum concentrations of FFA and TG in control and 0.02, 0.1, 0.5, and 1.0 Gy irradiated animals (7 months postirradiation). The amount of FFA was found to be significantly elevated in the serum of irradiated mice at doses of 0.5 and 1.0 Gy but not at lower doses. In contrast, the level of TG showed a significant decrease at 0.5 and 1.0 Gy but not at lower doses (Figure 5B,C).

DISCUSSION

In this study, we investigated early and late alterations in the biological pathways triggered by low and moderate doses of total body ionizing radiation in the developing mouse liver. We show that doses as low as 0.1 Gy were able to inactivate PPAR alpha, a key regulator of hepatic fat oxidation, in a persistent manner.

Early Radiation Effects 1 Day after Irradiation

As a metabolic consequence of early radiation-induced effects, the expression of pyruvate kinase isozymes (PKM) and pyruvate dehydrogenase (PDH) were found to be significantly downregulated at all doses (Supporting Information Table S1). Because PKMs catalyze the final step in the glycolytic pathway, producing pyruvate and ATP in the presence of oxygen, their downregulation would result in less energy production through glycolysis but also less pyruvate, the main substrate of the citric acid cycle. Pyruvate not only acts as an energy substrate but also functions as a scavenger of hydrogen peroxide,[26] and its reduced level may result in increased oxidative stress in irradiated liver. The reduced level of PDH, transforming pyruvate into acetyl-CoA, was accompanied by downregulation of PDH activity (Figure 4). It has been shown previously that downregulation of PDH in liver is associated with increased insulin sensitivity,[27] which may decrease the metabolic flexibility of the liver, primarily between glucose and fatty acid oxidation.[28]

We observed an immediate effect on the glycolytic pathway, with many of its proteins (DLAT, ALDO-A, CRAT) being downregulated. Also, early on, some lipid metabolism enzymes, such as peroxisomal acyl-coenzyme A oxidase 1 (ACOX1) and peroxisomal acyl-coenzyme A oxidase 2 (ACOX2), were found to be deregulated. ACOX1 showed radiation-induced down-regulation, whereas ACOX2 was upregulated. ACOX1 is the first and rate-limiting enzyme of the inducible peroxisomal beta-oxidation system.[29,30] Its gene expression is positively regulated by PPAR alpha,[31] and shRNA-mediated PPAR alpha gene knockdown in primary human hepatocytes decreased expression levels of ACOX1 by more than 50%.[32] Mice lacking the ACOX1 gene develop hepatocellular carcinomas in 100% of animals between 10 and 15 months due to constitutive overexpression of PPAR alpha.[29]

Some mitochondrial electron transport chain proteins, all belonging to the respiratory Complex I, were also found to be downregulated (Supporting Information Table S1c,d). In accordance with previous data,[33] we found a decrease in the level of aconitase, a key enzyme in energy metabolism in mitochondria. Because aconitase is a sensitive target of reactive oxygen species and its loss limits citric acid cycle activity and mitochondrial respiratory capacity in vivo,[33] this may indicate early mitochondrial dysfunction and increased production of reactive oxygen species (ROS).[34,35] Data from animal studies indicate that neonatal liver mitochondria are very sensitive to oxidative stress.[36] Oxidative stress is considered to be the major reason for many metabolic disorders.[35,37,38]

In addition, an immediate effect of irradiation was seen in the downregulation of the expression of many structural proteins of the cytoskeleton and connective tissue (plectin, catenin, decorin, collagen, desmin, tropomyosin). The levels of desmin and tropomyosin-1 were found to be downregulated using both proteomics and immunoblotting. In hepatocytes, tropomyosin plays a role in stabilizing actin filaments.[39] The expression of desmin has been exclusively associated with hepatic stellate cells in the liver.[40] These changes indicate a rapid radiation-induced proteomic remodeling of the liver tissue.

Late PPAR Alpha-Mediated Metabolic Alterations after Low to Moderate Radiation Doses

On the basis of our proteomics data at 7 months postirradiation, PPAR alpha was predicted to be deactivated, as the expression of many of its target enzymes involved in lipid

dx.doi.org/10.1021/pr500890n | J. Proteome Res. 2015, 14, 366−373

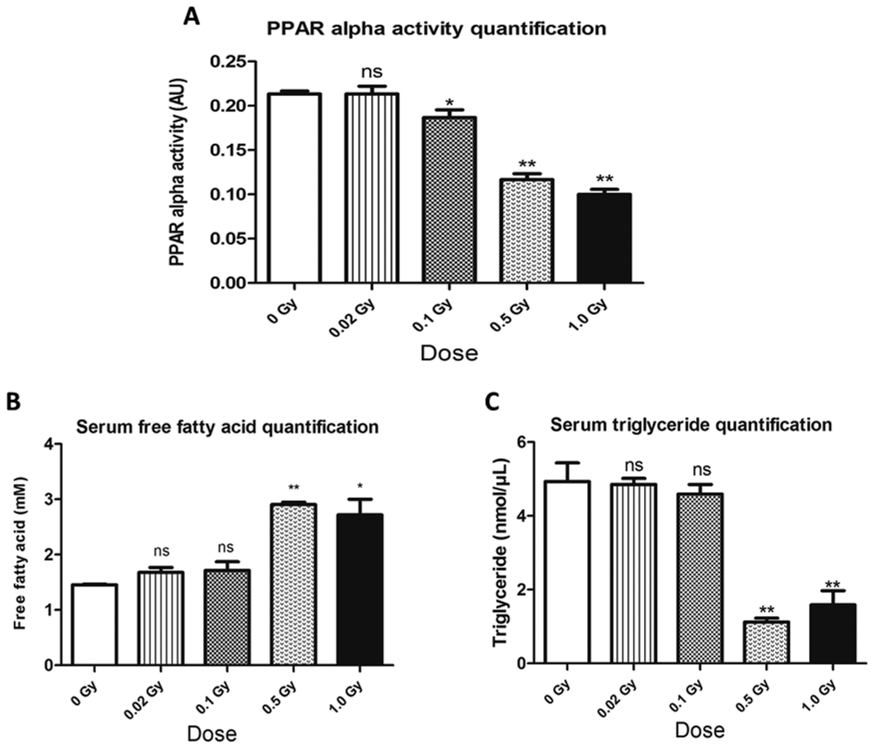

Figure 5. (A) Quantification of PPAR alpha activity in the liver of control and 0.02, 0.1, 0.5, and 1.0 Gy samples 7 months postirradiation (AU; arbitrary unit). (B, C) Quantification of triglycerides (B) and free fatty acid (C) in the serum samples of control and 0.02, 0.1, 0.5, and 1.0 Gy samples 7 months postirradiation (unpaired Student's *t* test; $*p \leq 0.05$; $**p \leq 0.01$; $n = 3$).

metabolism, such as ACOX1 and ACAA1, were downregulated, while inflammatory response proteins such as fibrinogens and hemopexin were found upregulated (Figure 2). Therefore, we measured the activity of PPAR alpha using nuclear extracts and found a clear decrease in PPAR alpha activity in the irradiated livers, even at a dose as low as 0.1 Gy (Figure 5A). The deactivation of PPAR alpha can be accomplished by both ligand-dependent and -independent mechanisms.[41,42] Unlike in the heart,[16] we did not find changes in the total or phosphorylated form of PPAR alpha in the irradiated liver (data not shown). Instead, a persistent increase in oxidative stress may contribute to the deactivation of PPAR alpha, as suggested by Azimzadeh et al.[17]

One of the hallmarks of inactivated PPAR alpha is its inability to use free fatty acids (FFA) for energy production.[43] In accordance with this, we found elevated levels of FFA in the serum of irradiated animals (0.5 and 1.0 Gy) (Figure 5B,C). In contrast, serum triglyceride (TG) levels in the irradiated mice were found to be decreased. The decreased levels of serum TG may result from the increased cardiac PPAR alpha activity in these animals,[16] as overexpression of PPAR alpha in the heart induces triglyceride accumulation in cardiomyocytes.[16,44] Our results and previous data suggest that there is an intensive crosstalk between heart and liver, especially in the neonatal phase.[45]

Late Increase in the Level of Cytochrome CYP450 Enzymes in Irradiated Liver

Cytochrome P450 comprises a large and diverse group of enzymes that catalyze the oxidation of organic substances. We found several types of CYP450 to be upregulated, especially Cyp2E1, which was persistently upregulated at doses of 0.1, 0.5, and 1.0 Gy (Supporting Information Table S2b–d). It has been shown previously that the expression of CYP2E1 is immediately induced after exposure to gamma rays (3 Gy) in rat liver.[33] A dose-dependent increase of CYP2E1 was also shown after fast neutron irradiation in mouse liver.[46] It has been demonstrated that under conditions with increased oxidative stress Cyp2E1 plays an important role in the induction of mitochondrial dysfunction.[47]

CONCLUSIONS

These data suggest a long-term radiation-induced dose-dependent inactivation of transcription factor PPAR alpha in liver, associated with mitochondrial dysfunction and increased oxidative stress. Total body radiation doses as low as 0.1 Gy given to neonatal mice resulted in both immediate and persistent adverse effects on metabolic pathways. Although doses lower than 0.1 Gy caused long-term alterations in the liver proteome, these very low doses did not result in significant changes in any of the functional assays performed in this study. In contrast, exposure to a dose of 0.5 Gy resulted in alterations in all end points that were investigated. Although the absence of evidence is not evidence of absence, it must be concluded that this study gives no support to long-term liver damage at doses lower than 0.1 Gy in a mouse model. Together with our previous data on the cardiac effects in these animals, these results underscore the importance of systemic effects after low radiation doses relevant in environmental exposure situations.

ASSOCIATED CONTENT

Supporting Information

Table S1: Significantly deregulated proteins in irradiated samples (postnatal day 11). Table S2: Significantly deregulated proteins in irradiated samples (7 months postirradiation). Table S3: All peptides identified and quantified after high confidence peptide filtering after day 1. Table S4: All peptides identified

dx.doi.org/10.1021/pr500890n | J. Proteome Res. 2015, 14, 366–373

and quantified after high confidence peptide filtering after 7 months. Figure S1: Immunoblotting images of different proteins expressed after a dose of 1.0 Gy. Figure S2: Immunoblotting image showing enrichment of nuclear fraction from irradiated liver tissue. Figure S3: Dip-stick assay showing relative abundance of pyruvate dehydrogenase in control and 0.05, 0.1, 0.5, and 1.0 Gy irradiated livers (postnatal day 11). Figure S4: STRING protein networks showing comparison between different classes of proteins significantly deregulated at the dose of 1.0 Gy at PND 11 and 7 months postirradiation time points. Figure S5: IPA summary analysis of 0.05 Gy early (PND11) liver analysis. Figure S6: IPA summary analysis of 0.1 Gy early (PND11) liver analysis. Figure S7: IPA summary analysis of 0.5 Gy early (PND11) liver analysis. Figure S8: IPA summary analysis of 1.0 Gy early (PND11) liver analysis. Figure S9: IPA summary analysis of 0.02 Gy long-term liver analysis. Figure S10: IPA summary analysis of 0.1 Gy long-term liver analysis. Figure S11: IPA summary analysis of 0.5 Gy long-term liver analysis. Figure S12: IPA summary analysis of 1.0 Gy long-term liver analysis. This material is available free of charge via the Internet at http://pubs.acs.org.

AUTHOR INFORMATION

Corresponding Author

*Tel.: +49 89 3187 3445; Fax: +49 89 3187 3378; E-mail: soile.tapio@helmholtz-muenchen.de.

Notes

The authors declare no competing financial interest.

ACKNOWLEDGMENTS

We thank Stefanie Winkler for technical assistance.

ABBREVIATIONS

Gy, Gray; TCA, tricarboxylic acid; IPA, Ingenuity Pathway Analysis; CVD, cardiovascular disease; H/L, heavy to light ratio; ICPL, isotope coded protein label; LC−MS, liquid chromatography mass spectrometry; PND, postnatal day; TBI, total body irradiation; PPAR, peroxisome proliferator-activated receptor; PDH, pyruvate dehydrogenase

REFERENCES

(1) Wakeford, R. The cancer epidemiology of radiation. *Oncogene* **2004**, *23*, 6404−28.
(2) Stryker, J. A. Science to practice: why is the liver a radiosensitive organ? *Radiology* **2007**, *242*, 1−2.
(3) Liu, W.; Haley, B. M.; Kwasny, M. J.; Li, J. J.; Grdina, D. J.; Paunesku, T.; Woloschak, G. E. The effects of radiation and dose-fractionation on cancer and non-tumor disease development. *Int. J. Environ. Res. Public Health* **2012**, *9*, 4688−703.
(4) Dawson, L. A.; Normolle, D.; Balter, J. M.; McGinn, C. J.; Lawrence, T. S.; Ten Haken, R. K. Analysis of radiation-induced liver disease using the Lyman NTCP model. *Int. J. Radiat. Oncol., Biol., Phys.* **2002**, *53*, 810−21.
(5) Rave-Fränk, M.; Malik, I.; Christiansen, H.; Naz, N.; Sultan, S.; Amanzada, A.; Blaschke, M.; Cameron, S.; Ahmad, S.; Hess, C.; Ramadori, G.; Moriconi, F. Rat model of fractionated (2 Gy/day) 60 Gy irradiation of the liver: long-term effects. *Radiat. Environ. Biophys.* **2013**, *52*, 321−38.
(6) Gridley, D. S.; Mao, X. W.; Cao, J. D.; Bayeta, E. J.; Pecaut, M. J. Protracted low-dose radiation priming and response of liver to acute gamma and proton radiation. *Free Radical Res.* **2013**, *47*, 811−20.
(7) Marra, F.; Tacke, F. Roles for chemokines in liver disease. *Gastroenterology* **2014**, *147*, 577−94.
(8) Ozasa, K.; Shimizu, Y.; Suyama, A.; Kasagi, F.; Soda, M.; Grant, E. J.; Sakata, R.; Sugiyama, H.; Kodama, K. Studies of the mortality of atomic bomb survivors, Report 14, 1950−2003: an overview of cancer and noncancer diseases. *Radiat. Res.* **2012**, *177*, 229−43.
(9) Kanamura, S.; Kanai, K.; Watanabe, J. Fine structure and function of hepatocytes during development. *J. Electron Microsc. Tech.* **1990**, *14*, 92−105.
(10) Beath, S. V. Hepatic function and physiology in the newborn. *Semin. Neonatol.* **2003**, *8*, 337−46.
(11) Lehman, J. J.; Kelly, D. P. Transcriptional activation of energy metabolic switches in the developing and hypertrophied heart. *Clin. Exp. Pharmacol. Physiol.* **2002**, *29*, 339−45.
(12) Grijalva, J.; Vakili, K. Neonatal liver physiology. *Semin. Pediatr. Surg.* **2013**, *22*, 185−9.
(13) Sasaki, S.; Fukuda, N. Temporal variation of excess mortality rate from solid tumors in mice irradiated at various ages with gamma rays. *J. Radiat Res.* **2005**, *46*, 1−19.
(14) Sasaki, S.; Fukuda, N. Dose-response relationship for induction of solid tumors in female B6C3F1 mice irradiated neonatally with a single dose of gamma rays. *J. Radiat. Res.* **1999**, *40*, 229−41.
(15) Faa, G.; Ekstrom, J.; Castagnola, M.; Gibo, Y.; Ottonello, G.; Fanos, V. A developmental approach to drug-induced liver injury in newborns and children. *Curr. Med. Chem.* **2012**, *19*, 4581−94.
(16) Bakshi, M. V.; Barjaktarovic, Z.; Azimzadeh, O.; Kempf, S. J.; Merl, J.; Hauck, S. M.; Eriksson, P.; Buratovic, S.; Atkinson, M. J.; Tapio, S. Long-term effects of acute low-dose ionizing radiation on the neonatal mouse heart: a proteomic study. *Radiat. Environ. Biophys* **2013**, *52*, 451−61.
(17) Azimzadeh, O.; Sievert, W.; Sarioglu, H.; Yentrapalli, R.; Barjaktarovic, Z.; Sriharshan, A.; Ueffing, M.; Janik, D.; Aichler, M.; Atkinson, M. J.; Multhoff, G.; Tapio, S. PAR alpha: a novel radiation target in locally exposed *Mus musculus* heart revealed by quantitative proteomics. *J. Proteome Res.* **2013**, *12*, 2700−14.
(18) Eriksson, P.; Fischer, C.; Stenerlow, B.; Fredriksson, A.; Sundell-Bergman, S. Interaction of gamma-radiation and methyl mercury during a critical phase of neonatal brain development in mice exacerbates developmental neurobehavioural effects. *Neurotoxicology* **2010**, *31*, 223−9.
(19) Bradford, M. M. A rapid and sensitive method for the quantitation of microgram quantities of protein utilizing the principle of protein-dye binding. *Anal. Biochem.* **1976**, *72*, 248−54.
(20) Merl, J.; Ueffing, M.; Hauck, S. M.; von Toerne, C. Direct comparison of MS-based label-free and SILAC quantitative proteome profiling strategies in primary retinal Muller cells. *Proteomics* **2012**, *12*, 1902−11.
(21) Hauck, S. M.; Dietter, J.; Kramer, R. L.; Hofmaier, F.; Zipplies, J. K.; Amann, B.; Feuchtinger, A.; Deeg, C. A.; Ueffing, M. Deciphering membrane-associated molecular processes in target tissue of autoimmune uveitis by label-free quantitative mass spectrometry. *Mol. Cell. Proteomics* **2010**, *9*, 2292−305.
(22) Brosch, M.; Yu, L.; Hubbard, T.; Choudhary, J. Accurate and sensitive peptide identification with Mascot Percolator. *J. Proteome Res.* **2009**, *8*, 3176−81.
(23) Sarioglu, H.; Brandner, S.; Jacobsen, C.; Meindl, T.; Schmidt, A.; Kellermann, J.; Lottspeich, F.; Andrae, U. Quantitative analysis of 2,3,7,8-tetrachlorodibenzo-p-dioxin-induced proteome alterations in 5L rat hepatoma cells using isotope-coded protein labels. *Proteomics* **2006**, *6*, 2407−21.
(24) Mayburd, A. L.; Martlinez, A.; Sackett, D.; Liu, H.; Shih, J.; Tauler, J.; Avis, I.; Mulshine, J. L. Ingenuity network-assisted transcription profiling: identification of a new pharmacologic mechanism for MK886. *Clin. Cancer Res.* **2006**, *12*, 1820−7.
(25) Szklarczyk, D.; Franceschini, A.; Kuhn, M.; Simonovic, M.; Roth, A.; Minguez, P.; Doerks, T.; Stark, M.; Muller, J.; Bork, P.; Jensen, L. J.; von Mering, C. The STRING database in 2011: functional interaction networks of proteins, globally integrated and scored. *Nucleic Acids Res.* **2011**, *39*, D561−8.

(26) Eghbal, M. A.; Pennefather, P. S.; O'Brien, P. J. H_2S cytotoxicity mechanism involves reactive oxygen species formation and mitochondrial depolarisation. *Toxicology* **2004**, *203*, 69−76.
(27) Choi, C. S.; Ghoshal, P.; Srinivasan, M.; Kim, S.; Cline, G.; Patel, M. S. Liver-specific pyruvate dehydrogenase complex deficiency upregulates lipogenesis in adipose tissue and improves peripheral insulin sensitivity. *Lipids* **2010**, *45*, 987−95.
(28) Zhang, S.; Hulver, M. W.; McMillan, R. P.; Cline, M. A.; Gilbert, E. R. The pivotal role of pyruvate dehydrogenase kinases in metabolic flexibility. *Nutr. Metab.* **2014**, *11*, 10.
(29) Meyer, K.; Jia, Y.; Cao, W. Q.; Kashireddy, P.; Rao, M. S. Expression of peroxisome proliferator-activated receptor alpha, and PPARalpha regulated genes in spontaneously developed hepatocellular carcinomas in fatty acyl-CoA oxidase null mice. *Int. J. Oncol.* **2002**, *21*, 1175−80.
(30) Meyer, K.; Lee, J. S.; Dyck, P. A.; Cao, W. Q.; Rao, M. S.; Thorgeirsson, S. S.; Reddy, J. K. Molecular profiling of hepatocellular carcinomas developing spontaneously in acyl-CoA oxidase deficient mice: comparison with liver tumors induced in wild-type mice by a peroxisome proliferator and a genotoxic carcinogen. *Carcinogenesis* **2003**, *24*, 975−84.
(31) Varanasi, U.; Chu, R.; Huang, Q.; Castellon, R.; Yeldandi, A. V.; Reddy, J. K. Identification of a peroxisome proliferator-responsive element upstream of the human peroxisomal fatty acyl coenzyme A oxidase gene. *J. Biol. Chem.* **1996**, *271*, 2147−55.
(32) Klein, K.; Thomas, M.; Winter, S.; Nussler, A. K.; Niemi, M.; Schwab, M.; Zanger, U. M. PPARA: a novel genetic determinant of CYP3A4 in vitro and in vivo. *Clin. Pharmacol. Ther.* **2012**, *91*, 1044−52.
(33) Chung, H. C.; Kim, S. H.; Lee, M. G.; Cho, C. K.; Kim, T. H.; Lee, D. H.; Kim, S. G. Mitochondrial dysfunction by gamma-irradiation accompanies the induction of cytochrome P450 2E1 (CYP2E1) in rat liver. *Toxicology* **2001**, *161*, 79−91.
(34) Drose, S.; Brandt, U. The mechanism of mitochondrial superoxide production by the cytochrome bc1 complex. *J. Biol. Chem.* **2008**, *283*, 21649−54.
(35) Barjaktarovic, Z.; Schmaltz, D.; Shyla, A.; Azimzadeh, O.; Schulz, S.; Haagen, J.; Dörr, W.; Sarioglu, H.; Schäfer, A.; Atkinson, M. J.; Zischka, H.; Tapio, S. Radiation-induced signaling results in mitochondrial impairment in mouse heart at 4 weeks after exposure to X-rays. *PLoS One* **2011**, *6*, e27811.
(36) Lazarin Mde, O.; Ishii-Iwamoto, E. L.; Yamamoto, N. S.; Constantin, R. P.; Garcia, R. F.; da Costa, C. E.; Vitoriano Ade, S.; de Oliveira, M. C.; Salgueiro-Pagadigorria, C. L. Liver mitochondrial function and redox status in an experimental model of non-alcoholic fatty liver disease induced by monosodium L-glutamate in rats. *Exp. Mol. Pathol.* **2011**, *91*, 687−94.
(37) Barjaktarovic, Z.; Shyla, A.; Azimzadeh, O.; Schulz, S.; Haagen, J.; Dorr, W.; Sarioglu, H.; Atkinson, M. J.; Zischka, H.; Tapio, S. Ionising radiation induces persistent alterations in the cardiac mitochondrial function of C57BL/6 mice 40 weeks after local heart exposure. *Radiother. Oncol.* **2013**, *106*, 404−10.
(38) Johnson, W. M.; Wilson-Delfosse, A. L.; Mieyal, J. J. Dysregulation of glutathione homeostasis in neurodegenerative diseases. *Nutrients* **2012**, *4*, 1399−440.
(39) Yokoyama, Y.; Kuramitsu, Y.; Takashima, M.; Iizuka, N.; Toda, T.; Terai, S.; Sakaida, I.; Oka, M.; Nakamura, K.; Okita, K. Proteomic profiling of proteins decreased in hepatocellular carcinoma from patients infected with hepatitis C virus. *Proteomics* **2004**, *4*, 2111−6.
(40) Nitou, M.; Ishikawa, K.; Shiojiri, N. Immunohistochemical analysis of development of desmin-positive hepatic stellate cells in mouse liver. *J. Anat.* **2000**, *197*, 635−46.
(41) Lazennec, G.; Canaple, L.; Saugy, D.; Wahli, W. Activation of peroxisome proliferator-activated receptors (PPARs) by their ligands and protein kinase A activators. *Mol. Endocrinol.* **2000**, *14*, 1962−75.
(42) Vanden Heuvel, J. P.; Kreder, D.; Belda, B.; Hannon, D. B.; Nugent, C. A.; Burns, K. A.; Taylor, M. J. Comprehensive analysis of gene expression in rat and human hepatoma cells exposed to the peroxisome proliferator WY14,643. *Toxicol. Appl. Pharmacol.* **2003**, *188*, 185−98.
(43) Francis, G. A.; Annicotte, J. S.; Auwerx, J. PPAR-alpha effects on the heart and other vascular tissues. *Am. J. Physiol.: Heart Circ. Physiol.* **2003**, *285*, H1−9.
(44) Palomer, X.; Salvado, L.; Barroso, E.; Vazquez-Carrera, M. An overview of the crosstalk between inflammatory processes and metabolic dysregulation during diabetic cardiomyopathy. *Int. J. Cardiol.* **2013**, *168*, 3160−72.
(45) Magida, J. A.; Leinwand, L. A. Metabolic crosstalk between the heart and liver impacts familial hypertrophic cardiomyopathy. *EMBO Mol. Med.* **2014**, *6*, 482−95.
(46) Jeong, W. I.; Do, S. H.; Kim, T. H.; Jeong, D. H.; Hong, I. H.; Ki, M. R.; Kwak, D. M.; Lee, S. S.; Jee, Y. H.; Kim, S. B.; Jeong, K. S. Acute effects of fast neutron irradiation on mouse liver. *J. Radiat. Res.* **2007**, *48*, 233−40.
(47) Qi, X. M.; Miao, L. L.; Cai, Y.; Gong, L. K.; Ren, J. ROS generated by CYP450, especially CYP2E1, mediate mitochondrial dysfunction induced by tetrandrine in rat hepatocytes. *Acta Pharmacol. Sin.* **2013**, *34*, 1229−36.

Chapter 3: Conclusions and Outlook

Epidemiological studies have shown that children and young adults are more susceptible for radiation-induced CVD. This study was carried out to investigate the proteome changes in the cardiac tissue after pre- and postnatal low and moderate doses of ionizing radiation in order to better understand whether the age at exposure plays a role in cardiac response to irradiation. Chapters 2.1 and 2.2 show the similarities and differences between radiation responses in the cardiac tissue after pre- and postnatal low doses irradiation. Chapter 2.3 shows the metabolic maladaptation and the cross talk between the heart and liver driven by PPARA after postnatal total body exposure.

3.1 Impairments in the heart after *in-utero* exposure to low-dose ionizing radiation

The prenatal exposure to ionizing radiation causes significant changes in the structural, mitochondrial and acute phase protein components of the proteome (Chapter 2.1). As mentioned in the introduction, the impairment in the structural formation of the heart is a cause for developmental heart disease. We see marked effects of low-dose ionizing radiation on the structural components of heart, associated with the activity of MAP4K4. Several structural proteins including different subunits of actin and myosin, vimentin, and obscurin and proteins associated with these (LDB3, HSBP6) were found to be among the deregulated proteins (Chapter 2.1). All these proteins have an important function in sarcomere formation and contractility, processes are that are rapidly developing at the time of the radiation exposure. This can be interpreted as the long-term consequence of the low-dose *in-utero* irradiation on the cardiac structure and function. Previous studies have shown that there is an active involvement of cytoskeletal proteins in hypertrophic heart failure and contractile dysfunction (Hein, Kostin et al. 2000, Katz 2000). Additional knowledge of consequences after *in-utero* irradiation can lead to the development of new means to improve prognosis and damage prevention of prenatal heart growth.

3.2 PPARA-driven metabolic imbalance after early postnatal low-dose irradiation

Metabolic maladaptation is a key process that was identified during this thesis work as deregulated after early postnatal total body irradiation. In the irradiated heart the nuclear transcription factor PPARA was found activated (Chapter 2.2) in contrast to its status in the liver where it was deactivated (Chapter 2.3). Mitochondrial ß-oxidation is the key source in the adult heart for energy production (Grynberg and Demaison 1996). Imbalances in the cardiac energy production caused by reactive oxygen species on mitochondrial respiratory complexes and ß-oxidation lead to cardiac arrhythmia, cardiomyopathy (Lorenzo, Ramirez et al. 2013, Yang, Bonini et al. 2014) and chronic heart failure (Ventura-Clapier, Garnier et al. 2004). In physiological conditions the heart and liver are synchronized for energy production by burning of free fatty acids that is regulated by the transcription factor PPARA (Francis, Annicotte et al. 2003). We have shown persistent changes in the serum concentration of triglycerides (TG) and free fatty acids (FFA) after neonatal total body irradiation. This indicates the presence of a systemic metabolic imbalance in heart and liver. Further studies on the function and mechanism of radiation-induced metabolic imbalance will lead to a better understanding of the developmental cardiac abnormalities. As it is known that PPARA is activated by both ligand-dependent and ligand-independent mechanisms and that PPARA ligands are essential for the activity of this transcription factor (Lazennec, Canaple et al. 2000, Vanden Heuvel, Kreder et al. 2003), these ligands are attractive candidates for designing novel therapeutic countermeasures in cardiac disease. Several clinical and preclinical studies have already demonstrated the beneficial effects of PPAR ligands on various cardiovascular risk factors (Francis, Annicotte et al. 2003, Staels, Maes et al. 2008, Cavender and Lincoff 2010, Chen, Liang et al. 2010). It should be investigated whether the administration of PPARA agonists may provide protection against postnatal radiation damage in the heart. Taken together, in the context of neonatal exposure it will be worthwhile to focus on the PPARA- driven metabolic pathways that integrate the energy demand of heart and liver.

3.3 Summary and outlook

To summarize the long-term consequences of pre- and postnatal irradiation, both similarities and differences are found (Figure 5). Both *in-utero* and postnatal exposure show alteration in the level of structural components of the heart. In prenatal exposure the MAPK signaling and in postnatal exposure the PPARA- driven metabolic signaling were imbalanced. This coincides with the activation of these pathways as MAP kinase pathway is essential for the prenatal heart chamber formation and PPARA activation is crucial during the postnatal metabolic switch from glucose to lipids (milk) in the energy production. Figure 5 shows that the main difference between the both exposures. This confirms our hypothesis that age at exposure determines the molecular damages in the heart by low doses of ionizing radiation. It also suggests that the biological pathways important at the time of irradiation are still found altered a long time after the initial insult.

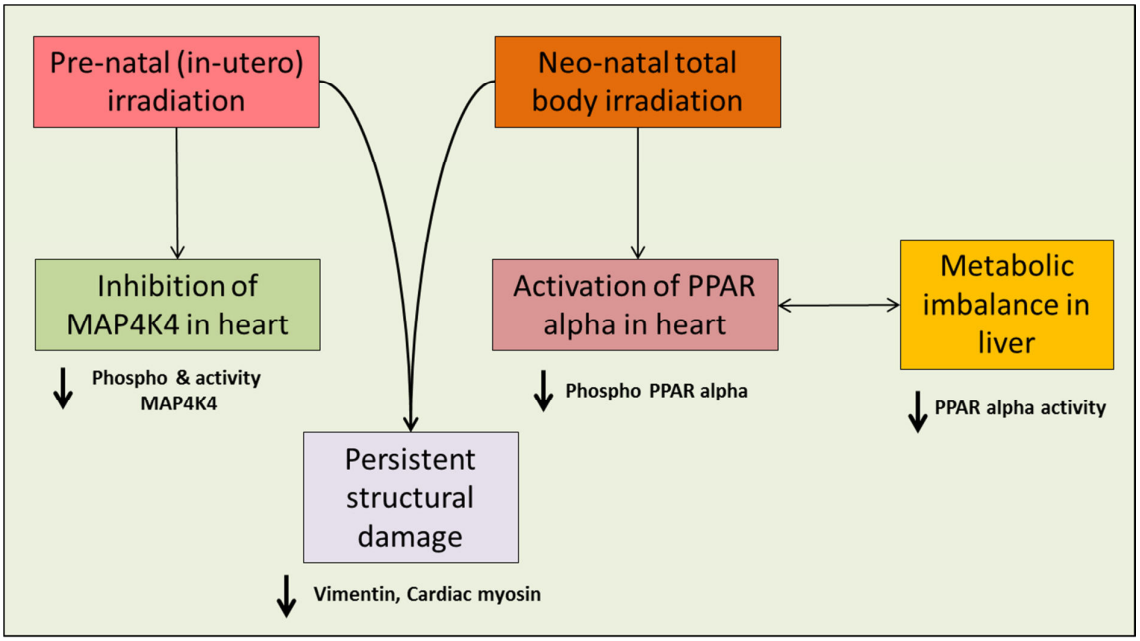

Figure 5: Molecular summary of the cardiac developmental alteration by total body low dose ionizing radiation in the mouse. *The prenatal irradiation causes persistent downregulation of the kinase MAP4K4 and alteration in structural protein expression. The postnatal ionizing radiation leads to the PPARA- driven metabolic imbalance between heart and liver and changes in the cytoskeletal proteome.*

This thesis represents the first effort to elucidate the molecular changes in developing heart after radiation insult. Significant changes in the proteomic profile were found at doses equal to or above 100 mGy but not at lower doses. Thus, these data give no direct support to the linear no- threshold model on the effects of ionizing radiation in the heart. However, further studies at low and moderate radiation doses are essential in order to minimize radiation-associated cardiovascular health risks, especially in fetuses and newborns.

References

Aleman, B. M., A. W. van den Belt-Dusebout, W. J. Klokman, M. B. Van't Veer, H. Bartelink and F. E. van Leeuwen (2003). "Long-term cause-specific mortality of patients treated for Hodgkin's disease." J Clin Oncol **21**(18): 3431-3439.

Anderson, R. H., S. Webb, N. A. Brown, W. Lamers and A. Moorman (2003). "Development of the heart: (2) Septation of the atriums and ventricles." Heart **89**(8): 949-958.

Anderson, R. H., S. Webb, N. A. Brown, W. Lamers and A. Moorman (2003). "Development of the heart: (3) formation of the ventricular outflow tracts, arterial valves, and intrapericardial arterial trunks." Heart **89**(9): 1110-1118.

Aoyama, T., J. M. Peters, N. Iritani, T. Nakajima, K. Furihata, T. Hashimoto and F. J. Gonzalez (1998). "Altered constitutive expression of fatty acid-metabolizing enzymes in mice lacking the peroxisome proliferator-activated receptor alpha (PPARalpha)." J Biol Chem **273**(10): 5678-5684.

Armstrong, G. T., Q. Liu, Y. Yasui, J. P. Neglia, W. Leisenring, L. L. Robison and A. C. Mertens (2009). "Late mortality among 5-year survivors of childhood cancer: a summary from the Childhood Cancer Survivor Study." J Clin Oncol **27**(14): 2328-2338.

Azimzadeh, O., W. Sievert, H. Sarioglu, R. Yentrapalli, Z. Barjaktarovic, A. Sriharshan, M. Ueffing, D. Janik, M. Aichler, M. J. Atkinson, G. Multhoff and S. Tapio (2013). "PPAR alpha: a novel radiation target in locally exposed Mus musculus heart revealed by quantitative proteomics." J Proteome Res **12**(6): 2700-2714.

Azizova, T. V., R. G. Haylock, M. B. Moseeva, M. V. Bannikova and E. S. Grigoryeva (2014). "Cerebrovascular diseases incidence and mortality in an extended Mayak Worker Cohort 1948-1982." Radiat Res **182**(5): 529-544.

Azizova, T. V., C. R. Muirhead, M. B. Moseeva, E. S. Grigoryeva, E. V. Vlasenko, N. Hunter, R. G. Haylock and J. A. O'Hagan (2012). "Ischemic heart disease in nuclear workers first employed at the Mayak PA in 1948-1972." Health Phys **103**(1): 3-14.

Baker, J. E., B. L. Fish, J. Su, S. T. Haworth, J. L. Strande, R. A. Komorowski, R. Q. Migrino, A. Doppalapudi, L. Harmann, X. Allen Li, J. W. Hopewell and J. E. Moulder (2009). "10 Gy total body irradiation increases risk of coronary sclerosis, degeneration of heart structure and function in a rat model." Int J Radiat Biol **85**(12): 1089-1100.

Baker, J. E., J. E. Moulder and J. W. Hopewell (2011). "Radiation as a Risk Factor for Cardiovascular Disease." Antioxidants & Redox Signaling **15**(7): 1945-1956.

Baluna, R. G., T. Y. Eng and C. R. Thomas (2006). "Adhesion molecules in radiotherapy." Radiat Res **166**(6): 819-831.

Bantscheff, M., S. Lemeer, M. M. Savitski and B. Kuster (2012). "Quantitative mass spectrometry in proteomics: critical review update from 2007 to the present." Anal Bioanal Chem **404**(4): 939-965.

Barjaktarovic, Z., A. Shyla, O. Azimzadeh, S. Schulz, J. Haagen, W. Dorr, H. Sarioglu, M. J. Atkinson, H. Zischka and S. Tapio (2013). "Ionising radiation induces persistent alterations in the cardiac mitochondrial function of C57BL/6 mice 40 weeks after local heart exposure." Radiother Oncol **106**(3): 404-410.

Berrington, A., S. C. Darby, H. A. Weiss and R. Doll (2001). "100 years of observation on British radiologists: mortality from cancer and other causes 1897-1997." Br J Radiol **74**(882): 507-519.

Bhatti, P., A. J. Sigurdson and K. Mabuchi (2008). "Can low-dose radiation increase risk of cardiovascular disease?" Lancet **372**(9640): 697-699.

Boerma, M. and M. Hauer-Jensen (2010). "Potential targets for intervention in radiation-induced heart disease." Curr Drug Targets **11**(11): 1405-1412.

Boerma, M., J. J. Kruse, M. van Loenen, H. R. Klein, C. I. Bart, C. Zurcher and J. Wondergem (2004). "Increased deposition of von Willebrand factor in the rat heart after local ionizing irradiation." Strahlenther Onkol **180**(2): 109-116.

Boerma, M., K. A. Roberto and M. Hauer-Jensen (2008). "Prevention and treatment of functional and structural radiation injury in the rat heart by pentoxifylline and alpha-tocopherol." Int J Radiat Oncol Biol Phys **72**(1): 170-177.

Boerma, M., J. Wang, J. Wondergem, J. Joseph, X. Qiu, R. H. Kennedy and M. Hauer-Jensen (2005). "Influence of mast cells on structural and functional manifestations of radiation-induced heart disease." Cancer Res **65**(8): 3100-3107.

Brand, T. (2003). "Heart development: molecular insights into cardiac specification and early morphogenesis." Dev Biol **258**(1): 1-19.

Breckenridge, R. (2014). "Molecular Control of Cardiac Fetal/Neonatal Remodeling." Journal of Cardiovascular Development and Disease **1**(1): 29.

Buckingham, M., S. Meilhac and S. Zaffran (2005). "Building the mammalian heart from two sources of myocardial cells." Nat Rev Genet **6**(11): 826-835.

Burns, K. A. and J. P. Vanden Heuvel (2007). "Modulation of PPAR activity via phosphorylation." Biochim Biophys Acta **1771**(8): 952-960.

Cai, C. L., X. Liang, Y. Shi, P. H. Chu, S. L. Pfaff, J. Chen and S. Evans (2003). "Isl1 identifies a cardiac progenitor population that proliferates prior to differentiation and contributes a majority of cells to the heart." Dev Cell **5**(6): 877-889.

Camerini, S. and P. Mauri (2015). "The role of protein and peptide separation before mass spectrometry analysis in clinical proteomics." J Chromatogr A **1381**: 1-12.

Cannon, B. (2013). "Cardiovascular disease: Biochemistry to behaviour." Nature **493**(7434): S2-3.

Castro, J. A., C. Koster and C. Wilkins (1992). "Matrix-assisted laser desorption/ionization of high-mass molecules by Fourier-transform mass spectrometry." Rapid Commun Mass Spectrom **6**(4): 239-241.

Cavender, M. A. and A. M. Lincoff (2010). "Therapeutic potential of aleglitazar, a new dual PPAR-alpha/gamma agonist: implications for cardiovascular disease in patients with diabetes mellitus." Am J Cardiovasc Drugs **10**(4): 209-216.

Chen, R., F. Liang, S. Morimoto, Q. Li, J. Moriya, J. Yamakawa, T. Takahashi, K. Iwai and T. Kanda (2010). "The effects of a PPARalpha agonist on myocardial damage in obese diabetic mice with heart failure." Int Heart J **51**(3): 199-206.

Chou, C. H., S. U. Chen and J. C. Cheng (2009). "Radiation-induced interleukin-6 expression through MAPK/p38/NF-kappaB signaling pathway and the resultant antiapoptotic effect on endothelial cells through Mcl-1 expression with sIL6-Ralpha." Int J Radiat Oncol Biol Phys **75**(5): 1553-1561.

Colaert, N., H. Barsnes, M. Vaudel, K. Helsens, E. Timmerman, A. Sickmann, K. Gevaert and L. Martens (2011). "Thermo-msf-parser: an open source Java library to parse and visualize Thermo Proteome Discoverer msf files." J Proteome Res **10**(8): 3840-3843.

Cousins, C., D. L. Miller, G. Bernardi, M. M. Rehani, P. Schofield, E. Vano, A. J. Einstein, B. Geiger, P. Heintz, R. Padovani and K. H. Sim (2013). "ICRP PUBLICATION 120: Radiological protection in cardiology." Ann ICRP **42**(1): 1-125.

Cox, J. and M. Mann (2008). "MaxQuant enables high peptide identification rates, individualized p.p.b.-range mass accuracies and proteome-wide protein quantification." Nat Biotechnol **26**(12): 1367-1372.

Darby, S. C., R. Doll and M. C. Pike (1985). "Detection of late effects of ionizing radiation: why deaths of A-bomb survivors are a valuable resource." Int J Epidemiol **14**(4): 637-639.

Dauly, C., D. H. Perlman, C. E. Costello and M. E. McComb (2006). "Protein separation and characterization by np-RP-HPLC followed by intact MALDI-TOF mass spectrometry and peptide mass mapping analyses." Journal of proteome research **5**(7): 1688-1700.

Davis, F. G., J. D. Boice, Jr., Z. Hrubec and R. R. Monson (1989). "Cancer mortality in a radiation-exposed cohort of Massachusetts tuberculosis patients." Cancer Res **49**(21): 6130-6136.

Dowell, R. T. (1984). "Metabolic and contractile function enhancement during rat heart postnatal development." Mech Ageing Dev **25**(3): 307-321.

Edvardsson, U., A. Ljungberg, D. Linden, L. William-Olsson, H. Peilot-Sjogren, A. Ahnmark and J. Oscarsson (2006). "PPARalpha activation increases triglyceride mass and adipose differentiation-related protein in hepatocytes." J Lipid Res **47**(2): 329-340.

Epstein, F. H. (1996). "Cardiovascular disease epidemiology: a journey from the past into the future." Circulation **93**(9): 1755-1764.

Eric J. Hall, A. J. G. (2006). "Radiobiology for Radiobiologist." **6th** 514.

Fenn, J. B., M. Mann, C. K. Meng, S. F. Wong and C. M. Whitehouse (1989). "Electrospray ionization for mass spectrometry of large biomolecules." Science **246**(4926): 64-71.

Fillmore, N., J. Mori and G. D. Lopaschuk (2014). "Mitochondrial fatty acid oxidation alterations in heart failure, ischaemic heart disease and diabetic cardiomyopathy." British Journal of Pharmacology **171**(8): 2080-2090.

Francis, G. A., J. S. Annicotte and J. Auwerx (2003). "PPAR-alpha effects on the heart and other vascular tissues." Am J Physiol Heart Circ Physiol **285**(1): H1-9.

Frey, N. and E. N. Olson (2003). "Cardiac hypertrophy: the good, the bad, and the ugly." Annu Rev Physiol **65**: 45-79.

Friess, J. L., A. Heselich, S. Ritter, A. Haber, N. Kaiser, P. G. Layer and C. Thielemann (2015). "Electrophysiologic and cellular characteristics of cardiomyocytes after X-ray irradiation." Mutat Res **777**: 1-10.

Gaspari, M. and G. Cuda (2011). "Nano LC-MS/MS: a robust setup for proteomic analysis." Methods Mol Biol **790**: 115-126.

Gessert, S. and M. Kuhl (2010). "The multiple phases and faces of wnt signaling during cardiac differentiation and development." Circ Res **107**(2): 186-199.

Grynberg, A. and L. Demaison (1996). "Fatty acid oxidation in the heart." J Cardiovasc Pharmacol **28 Suppl 1**: S11-17.

Hauck, S. M., J. Dietter, R. L. Kramer, F. Hofmaier, J. K. Zipplies, B. Amann, A. Feuchtinger, C. A. Deeg and M. Ueffing (2010). "Deciphering membrane-associated molecular processes in target tissue of autoimmune uveitis by label-free quantitative mass spectrometry." Mol Cell Proteomics **9**(10): 2292-2305.

Hauptmann, M., A. K. Mohan, M. M. Doody, M. S. Linet and K. Mabuchi (2003). "Mortality from diseases of the circulatory system in radiologic technologists in the United States." Am J Epidemiol **157**(3): 239-248.

Heallen, T., Y. Morikawa, J. Leach, G. Tao, J. T. Willerson, R. L. Johnson and J. F. Martin (2013). "Hippo signaling impedes adult heart regeneration." Development **140**(23): 4683-4690.

Heallen, T., M. Zhang, J. Wang, M. Bonilla-Claudio, E. Klysik, R. L. Johnson and J. F. Martin (2011). "Hippo pathway inhibits Wnt signaling to restrain cardiomyocyte proliferation and heart size." Science **332**(6028): 458-461.

Hein, S., S. Kostin, A. Heling, Y. Maeno and J. Schaper (2000). "The role of the cytoskeleton in heart failure." Cardiovasc Res **45**(2): 273-278.

Henson, K. E., P. McGale, C. Taylor and S. C. Darby (2013). "Radiation-related mortality from heart disease and lung cancer more than 20 years after radiotherapy for breast cancer." Br J Cancer **108**(1): 179-182.

Horvath, C. G., B. A. Preiss and S. R. Lipsky (1967). "Fast liquid chromatography: an investigation of operating parameters and the separation of nucleotides on pellicular ion exchangers." Anal Chem **39**(12): 1422-1428.

Howe, G. R., L. B. Zablotska, J. J. Fix, J. Egel and J. Buchanan (2004). "Analysis of the mortality experience amongst U.S. nuclear power industry workers after chronic low-dose exposure to ionizing radiation." Radiat Res **162**(5): 517-526.

Hurkmans, C. W., J. H. Borger, L. J. Bos, A. van der Horst, B. R. Pieters, J. V. Lebesque and B. J. Mijnheer (2000). "Cardiac and lung complication probabilities after breast cancer irradiation." Radiother Oncol **55**(2): 145-151.

Ieda, M., J.-D. Fu, P. Delgado-Olguin, V. Vedantham, Y. Hayashi, B. G. Bruneau and D. Srivastava (2010). "Direct Reprogramming of Fibroblasts into Functional Cardiomyocytes by Defined Factors." Cell **142**(3): 375-386.

Ieda, M., T. Tsuchihashi, K. N. Ivey, R. S. Ross, T.-T. Hong, R. M. Shaw and D. Srivastava (2009). "Cardiac Fibroblasts Regulate Myocardial Proliferation through β1 Integrin Signaling." Developmental cell **16**(2): 233-244.

Johansen, S., K. H. Tjessem, K. Fosså, G. Bosse, T. Danielsen, E. Malinen and S. D. Fosså (2013). "Dose Distribution in the Heart and Cardiac Chambers Following 4-field Radiation Therapy of Breast Cancer: a Retrospective Study." Breast Cancer : Basic and Clinical Research **7**: 41-49.

Katz, A. M. (2000). "Cytoskeletal abnormalities in the failing heart: out on a LIM?" Circulation **101**(23): 2672-2673.

Kemp, C. D. and J. V. Conte (2012). "The pathophysiology of heart failure." Cardiovasc Pathol **21**(5): 365-371.

Kempf, S. J., A. Casciati, S. Buratovic, D. Janik, C. von Toerne, M. Ueffing, F. Neff, S. Moertl, B. Stenerlow, A. Saran, M. J. Atkinson, P. Eriksson, S. Pazzaglia and S. Tapio (2014). "The cognitive defects of neonatally irradiated mice are accompanied by changed synaptic plasticity, adult neurogenesis and neuroinflammation." Mol Neurodegener **9**: 57.

Kimura, W., F. Xiao, D. C. Canseco, S. Muralidhar, S. Thet, H. M. Zhang, Y. Abderrahman, R. Chen, J. A. Garcia, J. M. Shelton, J. A. Richardson, A. M. Ashour, A. Asaithamby, H. Liang, C. Xing, Z. Lu, C. C. Zhang and H. A. Sadek (2015). "Hypoxia fate mapping identifies cycling cardiomyocytes in the adult heart." Nature **523**(7559): 226-230.

Klaus, A., Y. Saga, M. M. Taketo, E. Tzahor and W. Birchmeier (2007). "Distinct roles of Wnt/beta-catenin and Bmp signaling during early cardiogenesis." Proc Natl Acad Sci U S A **104**(47): 18531-18536.

Kolkman, A., E. H. Dirksen, M. Slijper and A. J. Heck (2005). "Double standards in quantitative proteomics: direct comparative assessment of difference in gel electrophoresis and metabolic stable isotope labeling." Mol Cell Proteomics **4**(3): 255-266.

Kruse, J. J., C. I. Bart, A. Visser and J. Wondergem (1999). "Changes in transforming growth factor-beta (TGF-beta 1), procollagen types I and II mRNA in the rat heart after irradiation." Int J Radiat Biol **75**(11): 1429-1436.

Kumar, P. P. (1980). "Pericardial Injury from Mediastinal Irradiation." Journal of the National Medical Association **72**(6): 591-594.

Laemmli, U. K. (1970). "Cleavage of structural proteins during the assembly of the head of bacteriophage T4." Nature **227**(5259): 680-685.

Laskey, W. K., L. E. Feinendegen, R. D. Neumann and V. Dilsizian (2010). "Low-level ionizing radiation from noninvasive cardiac imaging: can we extrapolate estimated risks from epidemiologic data to the clinical setting?" JACC Cardiovasc Imaging **3**(5): 517-524.

Lazennec, G., L. Canaple, D. Saugy and W. Wahli (2000). "Activation of peroxisome proliferator-activated receptors (PPARs) by their ligands and protein kinase A activators." Mol Endocrinol **14**(12): 1962-1975.

Lehman, J. J. and D. P. Kelly (2002). "Transcriptional activation of energy metabolic switches in the developing and hypertrophied heart." Clin Exp Pharmacol Physiol **29**(4): 339-345.

Lin, R. and P. Tripuraneni (2011). "Radiation Therapy in Early-Stage Invasive Breast Cancer." Indian journal of surgical oncology **2**(2): 101-111.

Little, M. P. (2003). "Risks associated with ionizing radiation." Br Med Bull **68**: 259-275.

Little, M. P. (2013). "A review of non-cancer effects, especially circulatory and ocular diseases." Radiat Environ Biophys **52**(4): 435-449.

Lorenzo, O., E. Ramirez, B. Picatoste, J. Egido and J. Tunon (2013). "Alteration of energy substrates and ROS production in diabetic cardiomyopathy." Mediators Inflamm **2013**: 461967.

Lottspeich, F. and J. Kellermann (2011). "ICPL labeling strategies for proteome research." Methods Mol Biol **753**: 55-64.

Louch, W. E., K. A. Sheehan and B. M. Wolska (2011). "Methods in Cardiomyocyte Isolation, Culture, and Gene Transfer." Journal of molecular and cellular cardiology **51**(3): 288-298.

Magida, J. A. and L. A. Leinwand (2014). "Metabolic crosstalk between the heart and liver impacts familial hypertrophic cardiomyopathy." EMBO Mol Med **6**(4): 482-495.

Makinde, A. O., P. F. Kantor and G. D. Lopaschuk (1998). "Maturation of fatty acid and carbohydrate metabolism in the newborn heart." Mol Cell Biochem **188**(1-2): 49-56.

Mann, D. L. (2003). "Stress-activated cytokines and the heart: from adaptation to maladaptation." Annu Rev Physiol **65**: 81-101.

Mathias, D., R. E. Mitchel, M. Barclay, H. Wyatt, M. Bugden, N. D. Priest, S. C. Whitman, M. Scholz, G. Hildebrandt, M. Kamprad and A. Glasow (2015). "Low-dose irradiation affects expression of inflammatory markers in the heart of ApoE -/- mice." PLoS One **10**(3): e0119661.

McGale, P., S. C. Darby, P. Hall, J. Adolfsson, N. O. Bengtsson, A. M. Bennet, T. Fornander, B. Gigante, M. B. Jensen, R. Peto, K. Rahimi, C. W. Taylor and M. Ewertz (2011). "Incidence of heart disease in 35,000 women treated with radiotherapy for breast cancer in Denmark and Sweden." Radiother Oncol **100**(2): 167-175.

Merl, J., M. Ueffing, S. M. Hauck and C. von Toerne (2012). "Direct comparison of MS-based label-free and SILAC quantitative proteome profiling strategies in primary retinal Muller cells." Proteomics **12**(12): 1902-1911.

Mi, H., A. Muruganujan and P. D. Thomas (2013). "PANTHER in 2013: modeling the evolution of gene function, and other gene attributes, in the context of phylogenetic trees." Nucleic Acids Res **41**(Database issue): D377-386.

Monceau, V., L. Meziani, C. Strup-Perrot, E. Morel, M. Schmidt, J. Haagen, B. Escoubet, W. Dörr and M.-C. Vozenin (2013). "Enhanced Sensitivity to Low Dose Irradiation of ApoE−/− Mice Mediated by Early Pro-Inflammatory Profile and Delayed Activation of the TGFβ1 Cascade Involved in Fibrogenesis." PLoS ONE **8**(2): e57052.

Moorman, A., S. Webb, N. A. Brown, W. Lamers and R. H. Anderson (2003). "DEVELOPMENT OF THE HEART: (1) FORMATION OF THE CARDIAC CHAMBERS AND ARTERIAL TRUNKS." Heart **89**(7): 806-814.

Nakashima, E., M. Akahoshi, K. Neriishi and S. Fujiwara (2007). "Systolic blood pressure and systolic hypertension in adolescence of atomic bomb survivors exposed in utero." Radiat Res **168**(5): 593-599.

Nau, P. N., T. Van Natta, J. C. Ralphe, C. J. Teneyck, K. A. Bedell, C. A. Caldarone, J. L. Segar and T. D. Scholz (2002). "Metabolic adaptation of the fetal and postnatal ovine heart: regulatory role of hypoxia-inducible factors and nuclear respiratory factor-1." Pediatr Res **52**(2): 269-278.

Ozhan, G. and G. Weidinger (2015). "Wnt/β-catenin signaling in heart regeneration." Cell Regeneration **4**(1): 3.

Panadero, M., E. Herrera and C. Bocos (2000). "Peroxisome proliferator-activated receptor-alpha expression in rat liver during postnatal development." Biochimie **82**(8): 723-726.

Parmley, W. W. (1985). "Pathophysiology of congestive heart failure." Am J Cardiol **56**(2): 7a-11a.

Patterson, A. J. and L. Zhang (2010). "Hypoxia and Fetal Heart Development." Current molecular medicine **10**(7): 653-666.

Peterson, A., L. Hohmann, L. Huang, B. Kim, J. K. Eng and D. B. Martin (2009). "Analysis of RP-HPLC loading conditions for maximizing peptide identifications in shotgun proteomics." Journal of proteome research **8**(8): 4161-4168.

Poirier, Y., V. D. Antonenkov, T. Glumoff and J. K. Hiltunen (2006). "Peroxisomal beta-oxidation--a metabolic pathway with multiple functions." Biochim Biophys Acta **1763**(12): 1413-1426.

Porrello, E. R., A. I. Mahmoud, E. Simpson, J. A. Hill, J. A. Richardson, E. N. Olson and H. A. Sadek (2011). "Transient regenerative potential of the neonatal mouse heart." Science **331**(6020): 1078-1080.

Preston, D. L., Y. Shimizu, D. A. Pierce, A. Suyama and K. Mabuchi (2003). "Studies of mortality of atomic bomb survivors. Report 13: Solid cancer and noncancer disease mortality: 1950-1997." Radiat Res **160**(4): 381-407.

Ream, M., A. M. Ray, R. Chandra and D. M. Chikaraishi (2008). "Early fetal hypoxia leads to growth restriction and myocardial thinning." Am J Physiol Regul Integr Comp Physiol **295**(2): R583-595.

Rodel, F., B. Frey, U. Gaipl, L. Keilholz, C. Fournier, K. Manda, H. Schollnberger, G. Hildebrandt and C. Rodel (2012). "Modulation of inflammatory immune reactions by low-dose ionizing radiation: molecular mechanisms and clinical application." Curr Med Chem **19**(12): 1741-1750.

Rolfe, M., Laura E. McLeod, Phillip F. Pratt and Christopher G. Proud (2005). "Activation of protein synthesis in cardiomyocytes by the hypertrophic agent phenylephrine requires the activation of ERK and involves phosphorylation of tuberous sclerosis complex 2 (TSC2)." Biochemical Journal **388**(Pt 3): 973-984.

Rose, B. A., T. Force and Y. Wang (2010). "Mitogen-activated protein kinase signaling in the heart: angels versus demons in a heart-breaking tale." Physiol Rev **90**(4): 1507-1546.

Rutqvist, L. E., C. Rose and E. Cavallin-Stahl (2003). "A systematic overview of radiation therapy effects in breast cancer." Acta Oncol **42**(5-6): 532-545.

Sander, V., G. Suñe, C. Jopling, C. Morera and J. C. I. Belmonte (2013). "Isolation and in vitro culture of primary cardiomyocytes from adult zebrafish hearts." Nat. Protocols **8**(4): 800-809.

Sanford, L. P., I. Ormsby, A. C. Gittenberger-de Groot, H. Sariola, R. Friedman, G. P. Boivin, E. L. Cardell and T. Doetschman (1997). "TGFβ2 knockout mice have multiple developmental defects that are non-overlapping with other TGFβ knockout phenotypes." Development (Cambridge, England) **124**(13): 2659-2670.

Seemann, I., K. Gabriels, N. L. Visser, S. Hoving, J. A. te Poele, J. F. Pol, M. J. Gijbels, B. J. Janssen, F. W. van Leeuwen, M. J. Daemen, S. Heeneman and F. A. Stewart (2012). "Irradiation induced modest changes in murine cardiac function despite progressive structural damage to the myocardium and microvasculature." Radiother Oncol **103**(2): 143-150.

Semenza, G. L. (2000). "HIF-1: mediator of physiological and pathophysiological responses to hypoxia." J Appl Physiol (1985) **88**(4): 1474-1480.

Semenza, G. L., F. Agani, N. Iyer, B. H. Jiang, S. Leung, C. Wiener and A. Yu (1998). "Hypoxia-inducible factor 1: from molecular biology to cardiopulmonary physiology." Chest **114**(1 Suppl): 40S-45S.

Shapiro, A. L., E. Vinuela and J. V. Maizel, Jr. (1967). "Molecular weight estimation of polypeptide chains by electrophoresis in SDS-polyacrylamide gels." Biochem Biophys Res Commun **28**(5): 815-820.

Shimizu, Y., K. Kodama, N. Nishi, F. Kasagi, A. Suyama, M. Soda, E. J. Grant, H. Sugiyama, R. Sakata, H. Moriwaki, M. Hayashi, M. Konda and R. E. Shore (2010). "Radiation exposure and circulatory disease risk: Hiroshima and Nagasaki atomic bomb survivor data, 1950-2003." BMJ **340**: b5349.

Sim, J. J., J. Shi, R. Al-Moomen, H. Behayaa, K. Kalantar-Zadeh and S. J. Jacobsen (2014). "Plasma renin activity and its association with ischemic heart disease, congestive heart failure, and cerebrovascular disease in a large hypertensive cohort." J Clin Hypertens (Greenwich) **16**(11): 805-813.

Sridharan, V., N. Aykin-Burns, P. Tripathi, K. J. Krager, S. K. Sharma, E. G. Moros, P. M. Corry, G. Nowak, M. Hauer-Jensen and M. Boerma (2014). "Radiation-induced alterations in mitochondria of the rat heart." Radiat Res **181**(3): 324-334.

Srivastava, D. (2006). "Making or breaking the heart: from lineage determination to morphogenesis." Cell **126**(6): 1037-1048.

Staels, B., M. Maes and A. Zambon (2008). "Fibrates and future PPARalpha agonists in the treatment of cardiovascular disease." Nat Clin Pract Cardiovasc Med **5**(9): 542-553.

Stewart, F. A., S. Heeneman, J. Te Poele, J. Kruse, N. S. Russell, M. Gijbels and M. Daemen (2006). "Ionizing radiation accelerates the development of atherosclerotic lesions in ApoE-/- mice and predisposes to an inflammatory plaque phenotype prone to hemorrhage." Am J Pathol **168**(2): 649-658.

Szklarczyk, D., A. Franceschini, S. Wyder, K. Forslund, D. Heller, J. Huerta-Cepas, M. Simonovic, A. Roth, A. Santos, K. P. Tsafou, M. Kuhn, P. Bork, L. J. Jensen and C. von Mering (2015). "STRING v10: protein-protein interaction networks, integrated over the tree of life." Nucleic Acids Res **43**(Database issue): D447-452.

Takeuchi, J. K., X. Lou, J. M. Alexander, H. Sugizaki, P. Delgado-Olguin, A. K. Holloway, A. D. Mori, J. N. Wylie, C. Munson, Y. Zhu, Y.-Q. Zhou, R.-F. Yeh, R. M. Henkelman, R. P. Harvey, D.

Metzger, P. Chambon, D. Y. R. Stainier, K. S. Pollard, I. C. Scott and B. G. Bruneau (2011). "Chromatin remodelling complex dosage modulates transcription factor function in heart development." Nat Commun **2**: 187.

Tatsukawa, Y., E. Nakashima, M. Yamada, S. Funamoto, A. Hida, M. Akahoshi, R. Sakata, N. P. Ross, F. Kasagi, S. Fujiwara and R. E. Shore (2008). "Cardiovascular disease risk among atomic bomb survivors exposed in utero, 1978-2003." Radiat Res **170**(3): 269-274.

Taylor, C. W., J. M. Povall, P. McGale, A. Nisbet, D. Dodwell, J. T. Smith and S. C. Darby (2008). "Cardiac dose from tangential breast cancer radiotherapy in the year 2006." Int J Radiat Oncol Biol Phys **72**(2): 501-507.

Towbin, H., T. Staehelin and J. Gordon (1979). "Electrophoretic transfer of proteins from polyacrylamide gels to nitrocellulose sheets: procedure and some applications." Proc Natl Acad Sci U S A **76**(9): 4350-4354.

Tukenova, M., C. Guibout, O. Oberlin, F. Doyon, A. Mousannif, N. Haddy, S. Guerin, H. Pacquement, A. Aouba, M. Hawkins, D. Winter, J. Bourhis, D. Lefkopoulos, I. Diallo and F. de Vathaire (2010). "Role of cancer treatment in long-term overall and cardiovascular mortality after childhood cancer." J Clin Oncol **28**(8): 1308-1315.

Ueda, P., S. Cnattingius, O. Stephansson, E. Ingelsson, J. F. Ludvigsson and A. K. Bonamy (2014). "Cerebrovascular and ischemic heart disease in young adults born preterm: a population-based Swedish cohort study." Eur J Epidemiol **29**(4): 253-260.

UNSCEAR (2000). "Sources and Effects of Ionizing Radiation. UNSCEAR 2000 Report to the General Assembly, with Scientific Annexes. ." **I**.

Vakili, B. A., P. M. Okin and R. B. Devereux (2001). "Prognostic implications of left ventricular hypertrophy." Am Heart J **141**(3): 334-341.

Vallaster, M., C. D. Vallaster and S. M. Wu (2012). "Epigenetic mechanisms in cardiac development and disease." Acta Biochim Biophys Sin (Shanghai) **44**(1): 92-102.

Van der Meeren, A., M. A. Mouthon, M. Vandamme, C. Squiban and J. Aigueperse (2004). "Combinations of cytokines promote survival of mice and limit acute radiation damage in concert with amelioration of vascular damage." Radiat Res **161**(5): 549-559.

van Weerd, J. H., K. Koshiba-Takeuchi, C. Kwon and J. K. Takeuchi (2011). "Epigenetic factors and cardiac development." Cardiovascular Research **91**(2): 203-211.

Vanden Heuvel, J. P., D. Kreder, B. Belda, D. B. Hannon, C. A. Nugent, K. A. Burns and M. J. Taylor (2003). "Comprehensive analysis of gene expression in rat and human hepatoma cells exposed to the peroxisome proliferator WY14,643." Toxicol Appl Pharmacol **188**(3): 185-198.

Ventura-Clapier, R., A. Garnier and V. Veksler (2004). "Energy metabolism in heart failure." J Physiol **555**(Pt 1): 1-13.

Vrijheid, M., E. Cardis, P. Ashmore, A. Auvinen, J. M. Bae, H. Engels, E. Gilbert, G. Gulis, R. Habib, G. Howe, J. Kurtinaitis, H. Malker, C. Muirhead, D. Richardson, F. Rodriguez-Artalejo, A. Rogel, M. Schubauer-Berigan, H. Tardy, M. Telle-Lamberton, M. Usel and K. Veress (2007). "Mortality from diseases other than cancer following low doses of ionizing radiation: results from the 15-Country Study of nuclear industry workers." Int J Epidemiol **36**(5): 1126-1135.

Weber, C. and H. Noels (2011). "Atherosclerosis: current pathogenesis and therapeutic options." Nat Med **17**(11): 1410-1422.

Weber, K. and M. Osborn (1969). "The reliability of molecular weight determinations by dodecyl sulfate-polyacrylamide gel electrophoresis." J Biol Chem **244**(16): 4406-4412.

Weischer, M., K. Juul, J. Zacho, G. B. Jensen, R. Steffensen, T. V. Schroeder, A. Tybjaerg-Hansen and B. G. Nordestgaard (2010). "Prothrombin and risk of venous thromboembolism, ischemic heart disease and ischemic cerebrovascular disease in the general population." Atherosclerosis **208**(2): 480-483.

Wessels, A. and D. Sedmera (2003). "Developmental anatomy of the heart: a tale of mice and man." Physiol Genomics **15**(3): 165-176.

Wierzbicki, M., A. Chabowski, M. Zendzian-Piotrowska, E. Harasim and J. Gorski (2009). "Chronic, in vivo, PPARalpha activation prevents lipid overload in rat liver induced by high fat feeding." Adv Med Sci **54**(1): 59-65.

Wilkins, M. (2009). "Proteomics data mining." Expert Rev Proteomics **6**(6): 599-603.

Wilson, P. W., R. B. D'Agostino, D. Levy, A. M. Belanger, H. Silbershatz and W. B. Kannel (1998). "Prediction of coronary heart disease using risk factor categories." Circulation **97**(18): 1837-1847.

Wondergem, J., M. Boerma, K. Kodama, F. A. Stewart and K. R. Trott (2013). "Cardiovascular effects after low-dose exposure and radiotherapy: what research is needed?" Radiat Environ Biophys **52**(4): 425-434.

Wondergem, J., L. E. Wedekind, C. I. Bart, A. Chin, A. van der Laarse and H. Beekhuizen (2004). "Irradiation of mechanically-injured human arterial endothelial cells leads to increased gene expression and secretion of inflammatory and growth promoting cytokines." Atherosclerosis **175**(1): 59-67.

Wong, F. L., S. Bhatia, W. Landier, L. Francisco, W. Leisenring, M. M. Hudson, G. T. Armstrong, A. Mertens, M. Stovall, L. L. Robison, G. H. Lyman, S. E. Lipshultz and S. H. Armenian (2014). "Efficacy and Cost-effectiveness of the Children's Oncology Group Long-Term Follow-Up Screening Guidelines for Childhood Cancer Survivors at Risk of Treatment-related Heart Failure." Annals of internal medicine **160**(10): 672-683.

Wong, N. D. (2014). "Epidemiological studies of CHD and the evolution of preventive cardiology." Nat Rev Cardiol **11**(5): 276-289.

Xin, M., E. N. Olson and R. Bassel-Duby (2013). "Mending broken hearts: cardiac development as a basis for adult heart regeneration and repair." Nat Rev Mol Cell Biol **14**(8): 529-541.

Yalow, R. S. and S. A. Berson (1960). "Immunoassay of endogenous plasma insulin in man." J Clin Invest **39**: 1157-1175.

Yang, K. C., M. G. Bonini and S. C. Dudley, Jr. (2014). "Mitochondria and arrhythmias." Free Radic Biol Med **71**: 351-361.

Yentrapalli, R., O. Azimzadeh, Z. Barjaktarovic, H. Sarioglu, A. Wojcik, M. Harms-Ringdahl, M. J. Atkinson, S. Haghdoost and S. Tapio (2013). "Quantitative proteomic analysis reveals induction of premature senescence in human umbilical vein endothelial cells exposed to chronic low-dose rate gamma radiation." Proteomics **13**(7): 1096-1107.

Yentrapalli, R., O. Azimzadeh, A. Sriharshan, K. Malinowsky, J. Merl, A. Wojcik, M. Harms-Ringdahl, M. J. Atkinson, K. F. Becker, S. Haghdoost and S. Tapio (2013). "The PI3K/Akt/mTOR pathway is implicated in the premature senescence of primary human endothelial cells exposed to chronic radiation." PLoS One **8**(8): e70024.

Yeoh, K. W. and N. G. Mikhaeel (2011). "Role of Radiotherapy in Modern Treatment of Hodgkin's Lymphoma." Adv Hematol **2011**: 258797.

Zeisberg, E. M. and R. Kalluri (2010). "Origins of cardiac fibroblasts." Circ Res **107**(11): 1304-1312.

Acknowledgments

First of all I would like to thank to the director of the Inst. of radiation biology (ISB) and my primary doctoral adviser, Prof. Dr. Michael J. Atkinson for giving me a great opportunity to do my PhD thesis in his department and supporting me throughout the entire PhD life. Under Mike´s precious supervision, I have learned the technical aspects of radiation biology and social features of the scientific world.

I would like to extend my great thanks to PD Dr. Soile Tapio for giving me chance to work in her group for my PhD thesis. Under Soile´s mentorship, I have learned the skill of effective writing of the scientific results and presentation of the data.

I would like to thank to Prof. Dr. Gabriele Multhoff of TUM for being the second supervisor for my doctoral work and for her great advice during the thesis committee meetings.

I am also very thankful to Prof. Dr. Jacek Wisniewski of the Max-Planck-Inst of Biochemistry for being the external supervisor for my doctoral thesis and providing me a unique opportunity to work in his state-of-the-art proteomics lab.

My special thanks go to Dr. Omid Azimzadeh, without Omid´s great support in the field of proteomics it would have been hard to accomplish this thesis work.

I would like to thank Dr. Zarko Barjaktarovic for his great help in the lab work and in the scientific discussions.

I am also very thankful to Dr. Julianne Merl-Pham from the core-facility proteomics at HMGU, Dr. Sonja Buratovic and Prof. Per Eriksson from the Uppsala University and Dr. Tine Verreet and Dr. Benotmane from the SCK-CEN Belgium for the great collaborative efforts.

I would like to thank proteomics team of ISB: Ramesh, Stefan, Vikram, and Steffi for the abundant technical help and for the great social life we shared in office and privately.

Thanks to all members of Institute of Radiation Biology (ISB) for their co-operation and help. Thanks to Theresa and Sabine for helping me with the German translations. Thanks to Bahar for maintaining cheerful atmosphere in the office.

Special thanks to Maja Miloradovic Van Doorn for a lot of support in every situation and all the time spent together during last three years. Thanks a lot to Shrihari, Vanja, and Arjen, for spending extraordinary social time with me during last years.

Last but not least, I would like to thanks my parents for lots of love and great support during my PhD thesis. Thank you so much!